



University of Natural Resources and Life Sciences, Vienna

Department of Food Science and Technology

Institute of Food Technology

**The effects of different dextrose equivalent (DE) corn syrups on crystallization kinetics of amorphous sucrose matrices**

by

Lukas Leutgöb

**Master Thesis**

submitted in partial fulfillment of the requirements for the degree of

Master of Science  
(Food Science and Technology)

Research conducted at the

**University of Wisconsin-Madison**

Supervisor: Univ.Prof. Dipl.-Ing. Dr.techn. Dietmar Haltrich

Co-Supervisor: Prof. Dr. Richard W. Hartel (University of Wisconsin-Madison)

Vienna, November 2015

# Table of Contents

Abstract - short.....	v
Kurzfassung .....	v
Abstract .....	vi
Acknowledgements .....	ix
List of Tables .....	x
List of Figures.....	xi
1. Introduction.....	1
2. Literature review .....	3
2.1 The Glassy State .....	3
2.2 Glass Transition .....	4
2.2.1 Differential Scanning Calorimetry (DSC).....	5
2.2.2 Factors Influencing Glass Transition Temperature.....	6
2.2.2.1 Molecular Weight.....	6
2.2.2.2 Moisture content.....	7
2.2.2.3 Additives .....	7
2.2.2.3.1 Corn Syrup .....	8
2.4 Crystallization of Sucrose .....	9
2.4.1 Sucrose Solubility .....	10
2.4.2 Supersaturation .....	11
2.4.3 Nucleation .....	13
2.4.3.1 Primary Homogenous Nucleation .....	13
2.4.3.2 Primary Heterogeneous Nucleation .....	16
2.4.3.3 Secondary Nucleation .....	18
2.4.3.4 Effects of Additives on Sucrose Nucleation.....	18
2. 4.4 Crystal Growth.....	19
2.4.4.1 Mass Transfer Theory .....	21
2.4.4.2 Surface Incorporation Theory .....	24
2.4.4.3 Sucrose Crystal Growth Parameters.....	27
2.4.4.3.1 Supersaturation.....	27
2.4.4.3.2 Temperature.....	27
2.4.4.3.3 Additives and Impurities.....	30
2.4.4.3.4 Viscosity / Molecular Mobility.....	32

2.4.5 Arrhenius Equation.....	32
2.4.6 William-Landel-Ferry Equation.....	34
2.4.6.1 WLF Coefficients.....	36
2.4.7 Hoffmann-Lauritzen Growth Equation.....	36
3. Materials and Methods .....	40
3.1 Experimental Formulations .....	40
3.2 Cooking Procedure of Sugar Syrup .....	41
3.3 Sugar Glass Preparation .....	42
3.4 Moisture Content .....	43
3.5 Non-isothermal Determination of Glass Transition Temperature $T_g$ , Crystallization Temperature $T_c$ and Solubility Temperature $T_m$ .....	45
3.6 Isothermal Determination of Crystallization Characteristics .....	47
3.7 Data Analysis .....	50
4. Results and discussion.....	51
4.1 Moisture content.....	51
4.2 Non-isothermal DSC .....	55
4.2.1 Glass Transition Temperature .....	55
4.2.1.1 Effect of Moisture Content.....	56
4.2.1.2 Effect of Composition .....	58
4.2.2 Crystallization Temperature .....	61
4.2.2.1 Effect of Moisture Content.....	61
4.2.2.2 Effect of Composition .....	63
4.2.3 Solubility Temperature .....	65
4.2.3.1 Effect of Moisture Content.....	65
4.2.3.2 Effects of Composition .....	65
4.2.4 Relationship between Temperature of Maximum Crystallization Rate $T_c$ , Glass Transition Temperature $T_g$ and Solubility Temperature $T_m$ .....	67
4.3 Isothermal DSC .....	69
4.3.1 Crystallization from the Amorphous State .....	70
4.3.2 Parameters of Isothermal Crystallization .....	71
4.3.2 Experimental Difficulties .....	72
4.3.3 Crystallization Kinetics (Crystallization Half Times).....	74
4.3.3.1 Effect of Crystallization Temperature .....	76
4.3.3.2 Effect of Moisture Content.....	79

4.3.3.3 Effect of Composition .....	80
4.4 Factors on Crystallization Deviations between Syrups .....	85
4.3.1 Arrhenius Equation.....	87
4.4.2 Williams-Landel-Ferry (WLF) Kinetics.....	89
4.4.2 Hoffman-Lauritzen Kinetics .....	93
5. Conclusion and Recommendation.....	97
5.1 Conclusion .....	97
5.2 Recommendations for Future Work.....	104
6.References.....	105
Appendix.....	109

## Abstract - short

The effect of corn syrups of different dextrose equivalents (DE) on the crystallization rate, glass transition temperature ( $T_g$ ), crystallization temperature ( $T_c$ ) and solubility temperature ( $T_m$ ) of amorphous sucrose were studied using isothermal and non-isothermal DSC.  $T_g$ ,  $T_c$  and  $T_m$  of the sucrose corn syrup mixes depended on DE and level of syrup. Isothermal crystallization of sucrose was affected by both, the type and ratio of syrup (26DE>24DE>62DE). Arrhenius and Williams-Landel-Ferry equations were used to model the crystallization data and a Lauritzen-Hoffman like expression was used to fit the derived rate of crystallization over the temperature range  $T_g < T < T_m$ . Crystallization of sucrose depended mainly on  $T_g$  but was assumed to be influenced by specific interactions between molecules as well.

## Kurzfassung

Der Effekt von verschiedenen Maissirupen mit variierenden Dextrose-Äquivalenten (DE) auf die Kristallisationsrate, Glasübergangstemperatur ( $T_g$ ), Temperatur der schnellsten Kristallisation ( $T_c$ ) und der Löslichkeitstemperatur ( $T_m$ ) von amorpher Saccharose wurde anhand von dynamischer Differenzkalorimetrie (DSC) untersucht. Thermisch graduelle sowie isotherme Experimente zeigten eine Beeinflussung von  $T_g$ ,  $T_c$  und  $T_m$  durch Dextrose-Äquivalent und Konzentration des verwendeten Sirups. Die isotherme Kristallisationsrate von Saccharose, ein wichtiger Prozessfaktor, wies eine ähnliche Beeinflussung durch die Konzentration und das DE des Sirups auf und stieg in folgender Reihung 26DE<42DE<62DE. Die ermittelten Kristallisationsdaten und das daraus erhaltene Kristallisationsverhalten wurden auf mathematische Modelle nach Arrhenius und Williams-Landel-Ferry übertragen. Im Weiteren wurden die Kristallisationskinetik durch ein Hoffmann-Lauritzen Modell angenähert und über den Temperaturbereich  $T_g < T < T_m$  untersucht. Die Ergebnisse zeigen, dass das Kristallisationsverhalten von amorpher Saccharose, neben spezifischen molekularen Interaktionen, hauptsächlich durch die Glasübergangstemperatur ( $T_g$ ) des Systems beeinflusst wird.

## Abstract

The crystallization of sucrose systems shows importance in different areas of food systems.

Crystallization can be undesired and should be avoided for example in amorphous sucrose systems such as hard candy. Crystallization within the product changes both texture and appearance and limits the shelf life of the product. Other products such as extruded cereals favor a strong crystallization of sucrose systems in respect to the coating of these products. A fully crystallized sucrose coating around a cereal prevents the cereals from sticking and increases bowl-life of the product, thus the cereal stays crunchy for a longer time when exposed to fluids like milk. Sucrose systems often include corn syrup, which influences the crystallization behavior of the system to a different extent. The objectives of this work were to determine the influence of corn syrups with different dextrose equivalent (DE) on the crystallization behavior of an amorphous sucrose system and to determine whether crystallization of the sucrose system correlates with the dextrose equivalent of the syrups.

The crystallization of amorphous sucrose systems is influenced by a variety of factors, such as the amount of water in the system as well as the temperature at which crystallization is performed. For this reason the effects of varying dextrose equivalents (DE) corn syrups on glass transition, and crystal growth of amorphous sugar glasses were studied at different moisture contents (3.8%, 4.3%, 5.1%, 5.9%) and isothermal holding temperatures. Two ratios of sucrose to corn syrup were used (14/86 and 22/78 w/w dry basis) with three different types of corn syrup (26DE, 42DE, and 62 DE). The glass transition temperature ( $T_g$ ), temperature of maximum crystallization ( $T_c$ ), and the solubility temperature ( $T_s$ ) of each formulation were determined using non-isothermal differential scanning calorimetry (DSC). The crystallization process was investigated focusing on crystallization halftimes and corresponding crystallization rates. For isothermal crystallization the glasses were held at 80, 85, 90, 100 and 110°C using a differential scanning calorimeter (DSC) to observe onset time, degree of crystallinity and growth rate in respect to time.

The  $T_g$  of the sugar glasses was directly related to moisture content and corn syrup ratio of the samples and inversely related to the DE used, from 19.58°C for 62DE samples with 5.8% moisture to 38.13°C for 26DE samples with 3.8% moisture content. The crystallization temperature showed the same relationship to DE, moisture content and ratio of corn syrup, although in a non linear manner to the values of  $T_g$ . The solubility temperature decreased with both the DE of syrup and the ratio of syrup due to the increase in saccharides derived from the added corn syrup competing with sucrose for water hydrogen bonding sites.

The isothermal crystallization rates were directly related to the holding temperatures and inversely related to the moisture content of the sample. The DE of the syrup showed an inverse relationship to crystallization rates. The crystallization rate increased in the sequence 62DE > 42DE > 26DE and crystallization halftimes decreased vice versa. The differences in crystallization rates between the types of syrup decreased at higher holding temperatures and higher moisture contents. Crystallization rates and crystallization halftimes were both fit to the Arrhenius and William-Landel Ferry equations. The Arrhenius equation used under the assumption of higher and approximate constant supersaturation fit the crystallization rates well. Calculated values of the activation energy for crystal growth were inversely related to the DE used, suggesting that the kinetic barrier to diffusion in the experimental crystallization process is related to the DE of corn syrup used. The WLF equation used with variable constants fit the experimental data very well. The crystallization rates increased exponentially as temperature increased from 80 to 110°C. The type of corn syrup used caused no significant difference of the WLF constants at any moisture or syrup level. As WLF explains  $T - T_g$  as the driving force for crystallization above  $T_g$  in respect to greater molecular mobility and decreasing relaxation times, it is assumed that the bigger part of differences in crystallization rates between the syrups can be explained by alterations of  $T_g$  due to the different types of syrup, which in return is due to different molecular weights of the glasses. Crystallization rate data was also fit to the Hoffmann-Lauritzen like expression in order to predict maximum crystallization temperature and rates above the experimental temperature range ( $>110^\circ\text{C}$ ).

Differences in maximum crystallization rates (62DE>42DE>26DE) were approximated as a function of  $T_g$  and  $T_m$ . These differences, independent from  $T_g$  were explained by specific interactions between molecules.

The results suggest that isothermal crystallization rates for the most part relate to  $T_g$  of the glasses and the relative molecular mobility in respect to  $(T-T_g)$  for the crystallization above the glass transition temperature. Differences in crystallization rates that could not be explained by the variation of  $T_g$  were assumed to be caused by specific interactions between molecules.



## Acknowledgements

I would like to thank many people who contributed in one way or another to my thesis. First I would like to thank Prof. Richard W. Hartel for inviting me to his research group, for the open and productive conversations we had and for his support and guidance during my master's project.

I would also like to thank Prof. Dietmar Haltrich for supporting my master's project abroad. I appreciate his understanding for difficulties that might come up during such a project and his far-reaching support and encouragement.

I am grateful for support from my Mom and sister Valerie, helping me through intense times and being family. I am also very grateful for the love and empathy from my wife Kalie who was always supportive and a true partner.

I would like to thank my close friends for their advice and company within the last 9 months (Katharina Payk, Zeyad El Omari, Alvaro Linares Fuster, Daniel Richter, Veronika "Lonny" Mutschlechner, Sophia Hütter and many more). You made my life more colorful!

I would also like to thank my labmates, I had many pleasant conversations with them, especially Vikas Malik for the great subject-specific discussions and shared knowledge, and Margaret Geary for the numerous funny late-night sessions in the lab.

Finally I would like to thank the University of Natural Resources and Life Sciences, Vienna for the financial support which enabled this great research project together with the University of Wisconsin-Madison.

## List of Tables

Table 3.1: Analysis of sugar used in all experiments, all % data on a w/w dry basis. ....	40
Table 3.2: Technical data of corn syrup used in all formulations, % data on a w/w dry basis. ....	41
Table 3.3 : Formulation of sugar glasses on a w/w dry basis before cooking. Each formulation contains sucrose and one type of corn syrup. ....	41
Table 3.4 Matrix plan of isothermal differential scanning calorimeter (DSC) experiments using three different types of syrup with varying dextrose equivalent (DE) cooked to 4 different temperatures. ....	48
Table 4.1 Average molecular weight (dry) of experimental formulations with 14% and 22% corn syrup w/w on a dry basis. ....	58
Table 4.2 Activation energy for crystal growth of amorphous sugar matrices composed of either 14% or 22% corn syrup (26DE, 42DE, 62DE) at different moisture levels. ....	88
Table 4.3 WLF values for constants $C_1$ and $C_2$ for crystallization halftimes of amorphous sugar matrices composed of 14% / 22% corn syrup with different DE using crystallization temperatures T of 80, 85, 90, 100, 110°C and $T_g$ of each formulation. ....	91

## List of Figures

Figure 2.1 Phase equilibrium diagram sucrose-water (Mathlouthi & Reiser, 2012). .....	11
Figure 2.2: Solubility- supersolubility curve showing equilibrium solubility, supersaturation and metastable limit. The width of metastable zone depends on the nature of solute and condition of crystallization (Pantaraks, 2004). .....	12
Figure 2.3 The free energy of embryo development ( $\Delta G$ ) shown as a combination of the free energy of surface formation ( $\Delta G_s$ ) and the free volume formation ( $\Delta G_v$ ). The relationship of the critical radius size ( $r_c$ ) and the critical free energy of nuclei formation ( $\Delta G_c$ ) are also shown (Hartel, 2001). .....	14
Figure 2.4 Important diffusional processes (volume and surface) affecting crystal growth (Myerson, 1993). .....	20
Figure 2.5 Model of the concentration driving force near crystal surface (Pantaraks, 2004). .....	21
Figure 2.6 Schematic model of crystal lattice and incorporation sites based on simple cubic units: a, b, c, and d represent different potential sites for molecular incorporation into the crystal lattice (Hartel, 2001). .....	24
Figure 2.7 Schematic illustration of the temperature dependence of nucleation rate ( $I$ ) and crystal growth rate ( $G$ ). $T_c(I)$ and $T_c(G)$ are the temperatures at which $I$ and $G$ are maxima, respectively (Okui, 1990). .....	28
Figure 2.8 Hoffman Lauritzen like fit of crystallization rate of lactose and sucrose as a function of crystallization temperature, $T_g$ and $T_m$ obtained from a range of isothermal holding temperatures (Kedward et al., 1998). .....	29
Figure 2.9 Application of the Arrhenius and Williams-Landel-Ferry (WLF) kinetics in different physical states. The glass transition temperature ( $T_g$ ) and melting temperature ( $T_m$ ) are showed on the graph. The diagram represents viscosity ( $\eta$ ) as a function of reduced temperature ( $T_m/T$ ). (Levine & Slade, 1988). .....	35
Figure 2.10 Classification of growth kinetics according to Hoffman and Lauritzen (Ohneiser, 2011). ....	37
Figure 2.11 Growth rate as a function of temperature according to the Hoffman-Lauritzen equation. ...	38
Figure 3.1 Schematic representation of a differential scanning calorimeter (DSC) thermogram for amorphous sugar glass cooked to 150°C, 14% w/w 42DE syrup dry basis. ....	46

Figure 3.2 Pyris (v. 11) analysis of isothermal crystallization curve (42DE, 22% syrup, 3.8% moisture, 90°C) for the determination of onset, peak height, time until peak, time until end of crystallization and peak area. ....	48
Figure 4.1 Moisture content (%) of sugar glasses made with sucrose and 14 & 22 % w/w corn syrup on a dry basis (26DE, 42DE, 62DE). Solid symbols represent samples containing 14% corn syrup, outlined symbols represent samples containing 22% corn syrup. ....	54
Figure 4.2 Glass transition temperature ( $T_g$ ) for amorphous sugar matrices composed of 14% corn syrup (26DE, 42DE, or 62DE). ....	56
Figure 4.3 Glass transition temperature ( $T_g$ ) for amorphous sugar matrices composed of 22% corn syrup (26DE, 42DE, or 62DE) as a function of moisture content. ....	57
Figure 4.4 Glass transition temperature of sugar glasses with 22% (w/w on a dry basis) corn syrup (CS) (26DE, 42DE, 62DE) at ~3.8% moisture content. Data for pure sucrose obtained from Sun et al. (3.66% moisture content) (1996). ....	59
Figure 4.5 Glass transition temperature ( $T_g$ ) for amorphous sugar matrices as a function of moisture content for formulations containing 14 and 22% (w/w dry basis) corn syrup (CS) (26DE, 42DE). ....	60
Figure 4.6 Temperature of maximum crystallization rate ( $T_c$ ) of sugar glasses composed of 14%/22% corn syrup (CS) (26DE, 42DE, 62DE) as a function of moisture content. ....	62
Figure 4.7 Solubility temperature ( $T_m$ ) as a function of moisture content for sucrose glasses composed of 14% and 22% (w/w on dry basis) corn syrup (CS) (26DE, 42DE, 62DE). ....	66
Figure 4.8 Ratio of temperature of maximum crystal growth $T_c$ vs. ( $T_m/T_g$ ) as function of moisture content [%] at either 14%/22% (w/w on dry basis) corn syrup (CS) level. Solid symbols represent samples containing 14% corn syrup, outlined symbols represent samples containing 22% corn syrup. ....	68
Figure 4.9: Combined scans of 42DE samples with the same moisture content (4.3 %) crystallized at 3 different crystallization temperatures (110°, 100°, 90°C). ....	72
Figure 4.10: Isothermal DSC trace of amorphous sugar glass containing 26DE syrup and 3.8% moisture at 90°C over 20 minutes. The indistinct onset can be seen between min. 1 and min. 8 (dotted rectangle). ....	73
Figure 4.11 Isothermal DSC trace for amorphous sugar glass containing 42DE corn syrup (CS) and 3.8% moisture, crystallized at 100°C (solid line). The integrated isothermal DSC trace is shown by the dotted line. ....	74
Figure 4.12 Crystallization half times as a function of crystallization temperature for samples containing 14% w/w corn syrup (26DE, 42DE, 62DE)(a-c) at different moisture levels (%). ....	77
Figure 4.13 Crystallization half times as a function of crystallization temperature for samples containing 22% w/w corn syrup (26DE, 42DE, 62DE)(a-c) at different moisture levels (%). ....	78

Figure 4.14 Crystallization halftimes as a function of crystallization temperature in order to compare the effect of DE at different crystallization temperatures [°C] and moisture levels [%] for samples containing 14% corn syrup. Solid lines represent crystallization halftimes, dotted lines represent crystallization rates [min <sup>-1</sup> ].	82
Figure 4.15 Crystallization halftimes and rates as a function of crystallization temperatures [°C] at different moisture levels[%] for samples consisting of 22% corn syrup. Solid lines represent crystallization halftimes, dotted lines represent crystallization rates [min <sup>-1</sup> ].	84
Figure 4.16 Crystallization halftime values and rates plotted as a function of T-T <sub>g</sub> for samples of 4.3% moisture and 14% (w/w dry basis) corn syrup.	86
Figure 4.17 Arrhenius equation fit to crystallization rate data for amorphous sugar matrices with 14% corn syrup (w/w dry basis) at a 4.3% moisture level.	88
Figure 4.18 Williams-Landel Ferry (WLF) fit to crystallization halftime data for amorphous sugar matrices composed of 14% / 22% corn syrup with different DE at different moisture levels. WLF fit represented for: 26DE as solid line, 42DE as dotted line, 62DE as dot-dashed line.	92
Figure 4.19 Experimental crystallization rate and Hoffman-Lauritzen like fit as a function of crystallization temperature for amorphous sugar glasses made with 14% (w/w dry basis) corn syrups (26DE, 42DE,62DE) at a moisture level of 4.3%.	94
Figure 4.20 Experimental crystallization rate and Hoffman-Lauritzen like fit as a function of T-T <sub>g</sub> /T <sub>m</sub> -T <sub>g</sub> for amorphous sugar glasses made with 14% (w/w dry basis) corn syrups (26DE, 42DE,62DE) at a moisture level of 4.3%.	95

## 1. Introduction

Many sucrose based food systems are influenced by the crystallization of this ingredient. Crystallization of sucrose can be desired or unwanted based on the product and the favored product properties. In hard candy, crystallization and the resulting crystals are shelf life limiting and undesirable. The crystals change the texture of the product (grainy) and cause a defect in the appearance of the product. In extruded cereals, though, the crystallization of a sucrose-slurry is desired. These products are coated with a thin multi component sucrose layer which, if crystallized, prevents the cereals from sticking to each other and extends the bowl-life of the cereals. Here, fully crystallized sucrose provides the desired properties for this product.

Crystallization of an amorphous sugar matrix, as used in this work, is influenced by a variety of parameters, which sometimes interfere or superimpose each other. Most important is crystallization affected by the water content, additives, and environmental conditions such as temperature or humidity. Additives and water can both affect the glass transition temperature ( $T_g$ ) of a product by, among others, increasing or decreasing the molecular mobility of the sucrose molecules thus being a crucial parameter for the crystallization within a system. The glass transition temperature  $T_g$  is the temperature of a polymer or polymer mixture at which the polymer softens from a solid-like to a rubber-like state and begins to flow. Below  $T_g$ , the system is in a glassy state, molecular mobility is minimal to none and the system is stable to most physical and chemical reactions (Hartel, 2001). Above  $T_g$ , the molecular mobility increases with temperature allowing the components of the system to interact, enabling chemical and physical reactions. To initiate crystallization, the system needs to overcome the glass transition temperature to provide physical properties that enable the diffusion of molecules within the matrix.

Therefore, it is necessary to control and understand the effects of formulation, water content, inhibitory impurities,  $T_g$  and external conditions in order to obtain conditions favoring or preventing the crystallization of a sucrose-polymer system.

Both level and type of additives in an amorphous sugar matrix affect the  $T_g$  and the tendency of the systems to crystallize. In sucrose systems, the addition of corn syrup to the sucrose system is known to inhibit nucleation, to decrease crystal growth and to increase induction time of nuclei formation (Hartel, 2001). The inhibitory effect on the crystallization of sucrose systems due to corn syrup is based on both the ratio of corn syrup and the degree of polymerization of the additives from the syrup (Gabarra & Hartel, 1998; Saleki-Gerhardt & Zografi, 1994).

The primary goal of this work was to study the effect of different corn syrups on the crystallization of amorphous sucrose systems or glasses. The emphasis was put on the dextrose equivalent of the different syrups, which in return provides information about the degree of polymerization and molecular mass of the polysaccharide fractions contained in the particular syrups. Parameters studied in this work include glass transition temperature, temperature of highest crystallization and solubility temperature when the systems were exposed to a temperature gradient (non-isothermal). Subsequently, crystallization rate and degree of crystallization were studied under isothermal conditions to clarify potential inhibitory effects on the sucrose crystallization at different holding temperatures.

## 2. Literature review

### 2.1 The Glassy State

Glass is an amorphous solid, consisting of a liquid of very high viscosity ( $>10^{12}$  Pa\*s) that exists in a metastable state (Roos, 1995). Typical properties of glassy materials are brittleness and transparency. Their molecular motions are restricted to vibrations and short-range rotational motions (Sperling, 1986), and changes that occur in the glassy state are extremely slow and are often referred to as physical aging. Even though glasses show mechanical properties of those of solid materials, the molecules in glasses have no definite order such as solids that exist in the equilibrium, crystalline state. The glassy state is spatially homogenous, but has no long-range lattice order over a practical time range. Quenching of a liquid to the form of a glass is the most common method of producing amorphous super cooled materials and glasses, and involves rapid evaporation of the solvent molecules followed by a rapid cooling to avoid the formation of the equilibrium crystalline state. A common feature of amorphous materials is that they contain excess free energy and entropy in comparison to their crystalline counterparts at the same temperature and pressure conditions (Roos, 1995). Although the driving force for crystallization is very high, the high viscosity and low molecular mobility inhibit crystallization (Hartel, 2001).



## 2.2 Glass Transition

The glass transition temperature of polymers is defined to be the temperature at which the material softens due to the onset of long-range coordinated molecular motion (Sperling, 2005). Also the temperature at which the material changes from a solid-like to a liquid- or rubber-like state is known as glass transition temperature ( $T_g$ ). The heat transfer can be reversed and  $T_g$  also represents the temperature at which highly supersaturated, viscous amorphous fluid becomes a solid-like glass when rapidly cooled. Typically,  $T_g$  is noted where either a sharp change in heat capacity or thermal expansion coefficient occurs, and since both of these values are second order derivatives of Gibbs free energy,  $T_g$  is considered to be a second order phase transition (Roos & Drusch, 2015). A general rule for polymers is that cross-linked amorphous polymers exhibit rubber elasticity and linear amorphous polymers exhibit flow at temperatures above  $T_g$  (Sperling, 2005)

The structure of amorphous materials often “stabilizes” as a function of time when they are annealed at a temperature below  $T_g$ . Because of the metastability of the amorphous state such materials tend to crystallize when sufficient time is allowed at temperatures above  $T_g$ .

The importance of the  $T_g$  of amorphous food materials to the processability and storage stability is high and  $T_g$  has become an essential concept in food processing as many food products, like sugars, starches, proteins, and water, exhibit this behavior. Various techniques have been used to measure  $T_g$ . One of the most common techniques is differential scanning calorimetry (DSC).

### 2.2.1 Differential Scanning Calorimetry (DSC)

Differential scanning calorimetry (DSC) is a technique used to detect chemical or physical changes that occur in a material as a function of temperature. A DSC measures the change of a property – namely of heat flow rate difference – which normally is released due to an alteration of the sample temperature (Höhne, Hemminger, & Flammersheim, 2003). In other words a DSC monitors exothermic or endothermic changes that occur with a change in temperature or time.

During a typical scan a DSC alters the temperature of both, the sample pan and reference pan at the same time either by cooling or heating. The energy uptake or release by the sample is detected and recorded providing conclusions about the physical changes of the sample. The subsequent scan can be plotted as a function of temperature or time.

During isothermal scans, the temperature of sample and reference pan is ramped up to a target holding temperature where both are held over a certain amount of time without any alteration. Some processes like crystallization of sucrose systems are temperature dependent and provide different information about internal processes when scanned under constant conditions. Here, energy uptake or release is monitored and recorded over time.

Phase transitions are often categorized according to first-order, second-order, or higher order transitions (Roos, 1995). A first-order transition (melting, crystallization) is expressed as a peak in the heat flow curve of the sample due to the change of enthalpy,  $H$ , of the material. Glass transition is a second order transition, thus only heat capacity  $C_p$  changes, which can be seen as a shift in the trace of the heat flow in a DSC.

## 2.2.2 Factors Influencing Glass Transition Temperature

The glass transition temperature of amorphous sugar glasses is related to the composition of the glass, including average molecular weight, moisture content, and any additional ingredients that have been added. Additional factors are thermal history of the glass as well as aging of the amorphous glass matrix (Roos, 1995).

### 2.2.2.1 Molecular Weight

The molecular weight of a compound or material is an important factor determining the  $T_g$ . Molecular weight has been found to have an effect on both first and second-order-phase transition temperatures, thus affecting the glass transition temperature (Roos 1995). In general, the  $T_g$  is directly linked to the molecular weight of a compound. As the molecular weight increases, the  $T_g$  increases, but only up to a limiting point, after which the  $T_g$  remains fairly constant (Fennema, 1996). At not very low MW, the molecular weight dependence of  $T_g$  is usually described reasonably well by the empirical Fox – Flory equation:

$$T_g = T_g(\infty) - \frac{K_g}{M} \quad (2.1)$$

where  $M$  is the molecular weight,  $K_g$  is a constant, and  $T_g(\infty)$  is the limiting  $T_g$  at high molecular weight (Fox & Flory, 1950). This dependence has been explained in the framework of the Gibbs-Di Marzio theory (Greenberg & Kusy, 1984). In all of these cases,  $T_g$  is assumed to be a smooth function of MW. However it has been suggested that the  $T_g$  (MW) may have three different regions: (i) at very low MW  $T_g$  varies nearly linear with  $\log(M_n)$  up to some  $MW_1$ ; (ii) above  $MW_1$  the  $T_g$  exhibits a much weaker but still linear variation of  $T_g$  with  $\log(M_n)$  up to some  $MW_2$ ; and (iii)  $T_g$  is independent of molecular weight when  $MW > MW_2$  (Cown, 1975). The nature of the weight (MW) dependence of the glass transition temperature in polymers still remains a subject of discussion.

### 2.2.2.2 Moisture content

Water acts as a plasticizer in many food systems, such as starches, proteins and sugars (Hartel, 2001), which leads to increased free volume, decreased viscosity, and increased molecular mobility (Slade, Levine, Ievolella, & Wang, 1993). Increasing presence of water causes significant decrease of the glass transition temperature (Hartel, 2001), where a relatively small increase in water content can decrease the  $T_g$ , and as a result bring it below room temperature. As a consequence, even small alterations in the water content can have large effects on storage stability and crystallization of amorphous sugar glasses. According to Herrington & Branfield (1984) sugar glasses containing 14-30% DE corn syrup showed negligible differences in glass transition temperatures between samples, compared with a small change in water content. They stated that in amorphous sugar glasses the percentage of water is the more important parameter determining  $T_g$ , in comparison to the amount of corn syrup added. Various other authors have found similar results when investigating the effect of water on the  $T_g$  (Nowakowski & Hartel, 2002).

### 2.2.2.3 Additives

Pure systems in terms of molecular composition, such as sugars, protein blends and other carbohydrates rarely exist in food. The  $T_g$  of mixtures based on the composition is often given by the Gordon and Taylor equation for a binary system:

$$T_g = \frac{x_1 T_{g1} + k_{x2} T_{g2}}{x_1 + k_{x2}} \quad (2.2)$$

where,  $k$  is the ratio of heat capacities of component 2 to 1,  $x_1$  and  $x_2$  are mole fractions and  $T_{g1}$  and  $T_{g2}$  are glass transition temperatures of components 1 and 2, respectively (Roos, 1995). As mentioned previously, the addition of a higher molecular weight component and subsequent increase of MW of the system would cause an increase in  $T_g$ . Gabarra & Hartel (1998) found that the  $T_g$  of a freeze dried corn

syrup – sucrose mixture directly relates to the average-number molecular weight of the corn syrup saccharides in the mixture .

### **2.2.2.3.1 Corn Syrup**

Corn syrup is made from the starch of corn and contains various amounts of glucose, maltose and higher oligosaccharides. The dextrose equivalent (DE) as mentioned throughout this work is a measure of reducing sugars present in a product, relative to dextrose (glucose) and is expressed as a percentage on a dry basis. The reducing power of dextrose is set to the value 100, and the DE gives an indication of the average degree of polymerization (DP) for starch sugars. High-dextrose equivalent (DE) corn syrups contain many low molecular weight sugars, whereas low-DE corn syrups contain higher molecular weight sugars. The rule of thumb between DE and DP is  $DE \times DP = 120$  (Dziedzic & Kearsley, 2012). However, the ratio of oligosaccharides of different DP can also vary between different syrups of the same DE.

Corn syrup is commonly added in hard candies to inhibit crystallization, allowing formation and maintenance of the glassy state and enhancing stability during storage. In cereal coatings, corn syrups are added to replace sucrose and furthermore to lower the amount of sucrose in the product. Unlike in hard candy, the inhibitory effect on crystallization of the added corn syrup is not desired in cereal coatings and added corn syrup causes partially crystallized sucrose in the cereal coating. As a result, stickiness of cereals increases and a decrease in the opaqueness of the coating is observed. The type of corn syrup as well as the amount of syrup is crucial for sucrose crystallization (Gabarra & Hartel, 1998) .

As mentioned previously, according to equation of Gordon & Taylor (Equation 2.2),  $T_g$  is directly related to molecular weight, and a mixture of two components should show an intermediate  $T_g$ ; therefore, a lower DE corn syrup should result in a higher  $T_g$ . The magnitude of the effect on the  $T_g$  depends on the composition of the syrup as well as the ratio and can possibly determine the likelihood of crystallization

(Hartel, 2001). Various mechanisms on a molecular level may affect crystallization. The high DP and therefore larger size of oligosaccharides in the low DE syrups could increase viscosity, decrease mobility and therefore inhibit crystallization.

Bamberger et al. (1980) and Dziedzic & Kearsley (1984) found that the DE of corn syrup used had a direct relationship with the moisture content retained in the product. This correlates well with principles of boiling point elevation and has an effect on the final product. A product or glass containing a syrup with higher DE has a higher moisture content when cooked to the same boiling point than a product with a lower DE corn syrup. It follows that the addition of higher DE corn syrups results in higher moisture contents, thus lower  $T_g$  when cooked to the same temperature. Lower  $T_g$ , in turn, would cause an increased driving force for crystallization. To compare different DE on their effect on crystallization solely focusing on molecular effects, the influence of moisture content on the crystallization must be minimized, and a variation in the boiling procedure is necessary.

## **2.4 Crystallization of Sucrose**

The crystallization of sucrose is important in many food and pharmaceutical applications. Sucrose crystallization in food products includes confections, snack foods and cereals. Crystallization of sucrose is desired in frosted products such as coated cereals but undesired in many types of hard candy as it causes defects in texture and appearance.

The degree of supersaturation is the driving force for sucrose crystallization in an aqueous system.

Supersaturation is achieved when the saturation concentration of sucrose in the system is exceeded and crystalline as well as solution phase are not in a thermodynamic equilibrium. As crystallization proceeds, the concentration of the remaining solution decreases until the solubility concentration is reached and phase equilibrium state is achieved. Crystallization ceases at this point until the system leaves the equilibrium state again.

### 2.4.1 Sucrose Solubility

Sucrose has a high solubility in water (203,6 g/100mL at 20°C) and dissolves quite rapidly (Browne, 1912). The rate of sucrose dissolution decreases with increasing concentration of sucrose in a solution. The rate of dissolution becomes zero when the concentration of sucrose reached the saturation concentration of the solution at a given temperature. At this point, no more sucrose can be dissolved in the solution, the solution is in a chemical equilibrium and additional solid sucrose added to a saturated solution remains undissolved.

Both dissolution and crystallization of sucrose are phase changes, with the difference in Gibbs free energy,  $\Delta G$ , expressed as:

$$\Delta G = (\mu_2 - \mu_1) \quad (2.3)$$

where  $\mu_1$  and  $\mu_2$  are the chemical potentials of phase 1 and 2, respectively. Equation 2.3 applies at constant pressure and temperature (Dirksen & Ring, 1991). Solubility concentration is reached when the potential of the crystalline phase equals the chemical potential of the solution phase, at this point both phases are in a thermodynamic equilibrium.

If the solution is not saturated, the chemical potential of sucrose in solution is less than the chemical potential of crystals, and thus, crystals dissolve in aqueous solution. Likewise if the chemical potential of crystalline state is less than the chemical potential of the solution phase, ergo the difference in Gibbs free energy is negative, crystals grow. This will occur in supersaturated solutions. In a binary system of sucrose and water, the solubility of sucrose increases with the temperature of the solvent (Fig 2.1 )

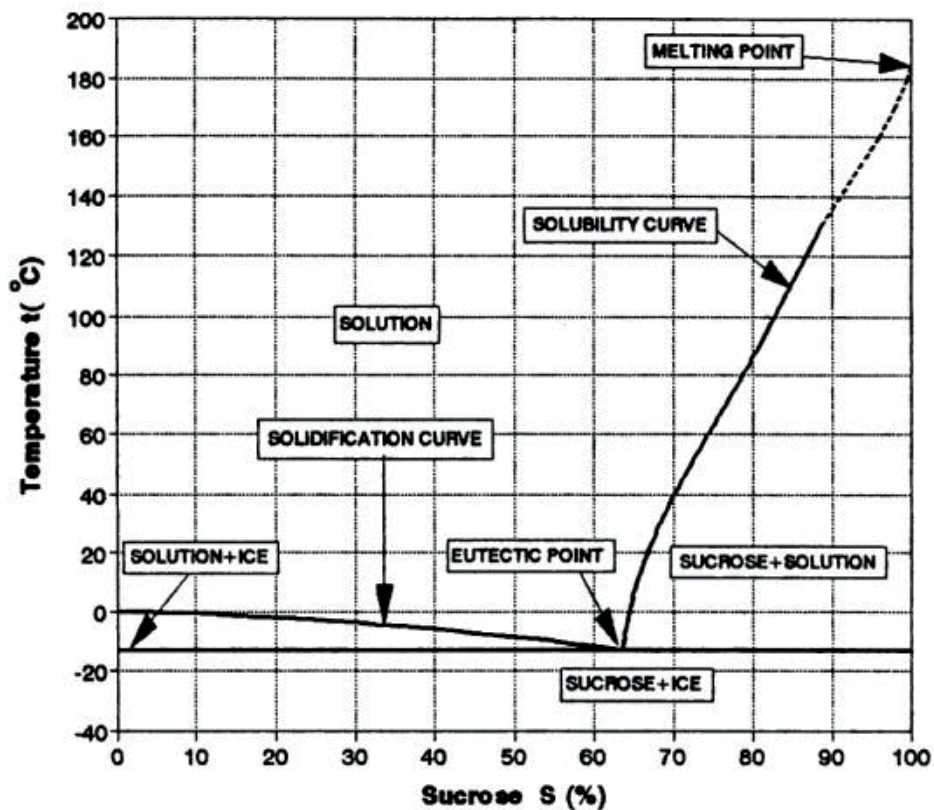


Figure 2.1 Phase equilibrium diagram sucrose-water (Mathlouthi & Reiser, 2012).

## 2.4.2 Supersaturation

A solution that contains more dissolved solids than represented by the solubility concentration as well as the chemical phase equilibrium is called supersaturated (Mullin, 2001). Supersaturated solutions are required for nucleation and crystal growth. The supersaturation ratio,  $S$ , defined as the ratio of the actual amount of solute in solution to the amount in a saturated solution at the same temperature (Hartel, 2001), is the driving factor in predicting the extent of crystallization in sugar-based systems (Hartel & Shastry, 1991). In general, as supersaturation increases, the nucleation rate increases with the increasing difference in Gibbs free energy. The increase in the nucleation rate stops when the supersaturation ratio reaches a system dependent threshold. At this point, the viscosity increases due to the high concentration of the solute and the decreased molecular mobility counteracts the nucleation. If the



supersaturation ratio is further increased, nucleation ceases and an amorphous glass is formed.

Nucleation is also dependent on temperature due to the temperature dependency of the molecular mobility in an aqueous system. Crystallization increases with temperature until the solubility of the solute increases due to the increased temperature to an extent when the thermodynamic equilibrium is achieved again (Hartel, 2013).

Areas above the solubility curve can be defined in different zones, where different regions of supersaturation cause different manners of crystallization. Labile and metastable regions were first introduced to classify supersaturated solutions in which spontaneous nucleation would or would not occur. These regions are shown in the solubility-supersolubility diagram in Figure 2.2 :

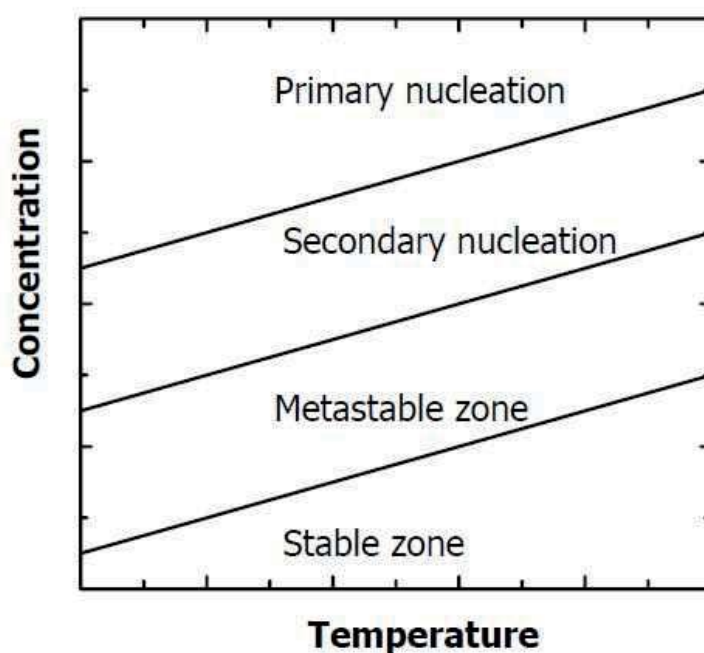


Figure 2.2: Solubility- supersolubility curve showing equilibrium solubility, supersaturation and metastable limit. The width of metastable zone depends on the nature of solute and condition of crystallization (Pantaraks, 2004).

Solutions are supersaturated beyond the equilibrium line (first solid line in Fig 2.2). In this metastable region of  $S = 1-1.2$  (g sucrose/ 100g water), crystal growth occurs from existing seeds but new crystals are not formed. The driving energy or free Gibbs energy at low supersaturation levels is not sufficient to overcome the energy barriers of nucleation. With increasing supersaturation from  $1.2 < S < 1.3$ , the system is in the intermediate region. Crystals will grow in the presence of existing seeds and secondary nucleation occurs due to impact of seeds against impeller blades or vessel walls or the agitation of seed crystals.

With  $S > 1.3$  the system is in a labile zone. Nucleation formation can occur spontaneously without the presence of existing crystals / seeds (van Hook, 1961).

### **2.4.3 Nucleation**

Nucleation is classified into primary and secondary nucleation. Primary nucleation does not require the presence of seed crystals, whereas secondary nucleation does not occur unless seed nuclei are present to provide nucleation sides. The primary nucleation can be divided into homogenous and heterogeneous nucleation. Homogenous nucleation occurs spontaneously, whereas heterogeneous nucleation occurs with the aid of foreign particles (Mullin, 2001).

#### **2.4.3.1 Primary Homogenous Nucleation**

The classic theory of nucleation describes primary homogenous nucleation. In this theory, spontaneous motion brings molecules together in solution to form clusters of molecules. For nucleation to occur, these clusters must resist the tendency to redissolve and must orient into an ordered lattice. Both molecular mobility and supersaturation must be sufficient in order to form a stable crystal.

The initial cluster of molecules is described as embryos. When these initial clusters or embryos are smaller than a critical size,  $r_c$ , they are likely to redissolve. The embryos must grow larger than this critical size to form a stable nucleus.

Based on the formation of a spherical nucleus, the net free energy change of the embryo development ( $\Delta G$ ) is a combination of the positive free energy change of formation of an interfacial tension ( $\Delta G_s$ ) and the negative free energy change of formation of a bulk crystal ( $\Delta G_v$ ). The energy due to the interfacial tension represents the formation of the crystal surface and is proportional to the surface area. The energy released as latent heat of fusion from the phase change is proportional to the volume. Based on these energy considerations, there is a critical radius size,  $r_c$ , to which an embryo must grow in order to form a stable nucleus. The relationship can be seen in Figure 2.3.

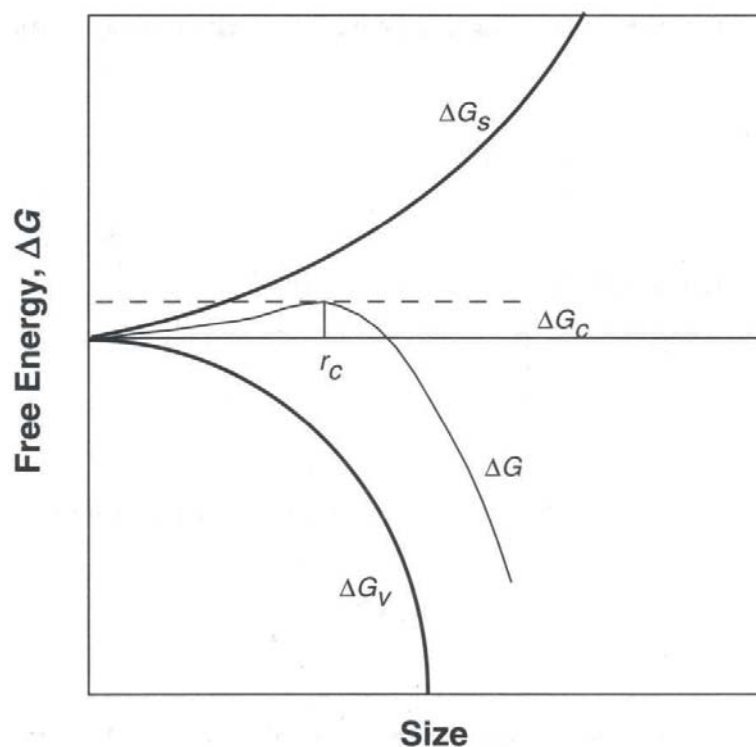


Figure 2.3 The free energy of embryo development ( $\Delta G$ ) shown as a combination of the free energy of surface formation ( $\Delta G_s$ ) and the free volume formation ( $\Delta G_v$ ). The relationship of the critical radius size ( $r_c$ ) and the critical free energy of nuclei formation ( $\Delta G_c$ ) are also shown (Hartel, 2001)

The critical size  $r_c$  is reached at some point where the rate of molecular association is greater than the rate of dissociation and the cluster is likely to grow into a stable crystal. According to the classical nucleation theory, the critical radius size is defined as (Hartel, 2001) :

$$r_c = \frac{2\sigma_s \nu}{kT \ln(S)} \quad (2.4)$$

Where,  $\sigma_s$  is the interfacial tension ( $\text{J/m}^3$ ),  $\nu$  is the molecular volume ( $\text{m}^3$ ),  $k$  is the Boltzman's constant ( $\text{J/K}$ ),  $T$  is absolute temperature ( $\text{K}$ ) and  $S$  is supersaturation ratio.

The critical radius size corresponds to a maximum in the net free energy, indicating that an energy barrier must be overcome for spontaneous nuclei formation (Hartel, 2001). According to the classical homogenous nucleation model, the critical free energy for nuclei formation is given as:

$$\Delta G = \frac{16\pi\sigma_s^3 \nu^2}{3k^2 T^2 \ln^2(S)} \quad (2.5)$$

Where,  $\sigma_s$  is the interfacial tension ( $\text{J/m}^3$ ),  $\nu$  is the molecular volume ( $\text{m}^3$ ),  $k$  is the Boltzman's constant ( $\text{J/K}$ ),  $T$  is absolute temperature ( $\text{K}$ ) and  $S$  is supersaturation ratio.

The rate of nucleation,  $J$ , is defined as the number of crystals formed per unit time per unit volume.

Using the equation for the critical free energy along with the rate of nucleation, the classical nucleation rate equation for a glass-former can be written in the form of an Arrhenius equation as (Hartel, 2001):

$$J = A \exp \left\{ -\frac{\Delta G_c}{kT} + \frac{\Delta G'_v}{kT} \right\} = A \exp \left\{ -\frac{16\pi\sigma_s^3 \nu^2}{3k^2 T^2 \ln^2(S)} + \frac{\Delta G'_v}{kT} \right\} \quad (2.6)$$

Where,  $J$  is nucleation rate,  $A$  is the Arrhenius pre-exponential factor,  $\Delta G_c$  is the excess free energy required to form a critical nucleus, and  $\Delta G'_v$  is the activation energy for molecular diffusion. The term  $\Delta G_c/kT$  is the thermodynamic kinetic term and accounts for the supersaturation effects, whereas the

$\Delta G'_v/kT$  is the molecular diffusion term, which accounts for the temperature-based viscosity effects.  $\Delta G_c/kT$  determines the nucleation rate when the molecular diffusivity is high, so that nucleation rate depends only on the kinetic term caused by the supersaturation. At high viscosities (low diffusivity) the term  $\Delta G'_v/kT$  defines and controls the nucleation rate overruling the driving force due to supersaturation. Here, the rate of nuclei formation depends strongly on the molecular diffusion rate within the sucrose matrix. When the system becomes highly viscous, the term  $\Delta G'_v/kT$  dominates the equation and any increase in supersaturation decreases the nucleation rate due to decreasing diffusivity. This situation is given in the glassy state, when supersaturation is high and the molecular mobility is low due to the high viscosity of the system ( $>10^{12}$  Pa\*s). Even when the glass is heated above  $T_g$  viscosity might be so high that nucleation is minimal.

#### **2.4.3.2 Primary Heterogeneous Nucleation**

True homogenous nucleation rarely occurs, because in most practical situations, heterogeneous nucleation is most likely to occur. Here, crystallization occurs around foreign impurities, such as dirt, dust, vessel walls, or other surfaces. Nucleation at foreign particles or surfaces requires a lower supersaturation level and temperatures than for homogenous crystallization. The reason for this is seen in the assistance of the foreign impurities in the orientation of the molecules toward a crystal lattice and occurs by reducing the energy barrier as well as number of molecules needed to form a stable nucleus (Hartel, 2001).

When the lattice structure of both the solute as well as the impurity match well, the formation of new crystals on the heterogenous nucleation site is favored. If the lattices do not match, then compression and decompression effects occur to the respective lattices and the formation of crystals is unfavorable (Kelton & Greer, 2010).

The free energy change of nuclei formation for heterogeneous nucleation ( $\Delta G'_c$ ) is less than the  $\Delta G_c$  for homogeneous nucleation. The rate equation for heterogeneous nucleation is represented as:

$$J = A \exp \left\{ -\frac{\Delta G'_c}{kT} \right\} \quad (2.7)$$

Where  $\Delta G'_c$  is given as:

$$\Delta G'_c = \phi \Delta G_c \quad (2.8)$$

The kinetic term of Equation 2.6 is multiplied by an interrelation term ( $\phi$ ) between the foreign particle, crystal lattice and the solution since the nucleation process depends on the surface characteristics of the nucleation sites.  $\phi$  is given as (Hartel, 2001):

$$\phi = \frac{1}{4} (2 + \cos \theta) (1 - \cos^2 \theta) \quad (2.9)$$

Where,  $\theta$  is the wetting angle between the crystal and the surface of the nucleation solid. When  $\theta$  is zero, the kinetic term in Equation 2.9 is zero, the crystal is fully wetting with the surface. In this case, there is no barrier for nucleation at the surface, and thus, nucleation occurs readily. On the other hand, when  $\theta$  is  $180^\circ$ ,  $\phi$  becomes 1, with the result that there is no wetting of the surface and, hence no catalysis by the surface, making this a homogeneous nucleation (Hartel, 2001).

### **2.4.3.3 Secondary Nucleation**

Secondary nucleation occurs with the aid of existing solute crystals. Contact of an existing crystal with another existing crystal, the vessel wall or a stirrer can generate new nuclei to form where the conditions may not have been sufficient otherwise. Secondary nucleation is unlikely to occur from a stagnant amorphous matrix; however, it often occurs in industrial crystallization processes where an agitated suspension of crystals exist.

### **2.4.3.4 Effects of Additives on Sucrose Nucleation**

Various ingredients and additives can affect crystallization and crystallization tendencies. Such additives are sugars, corn syrups, gums and others. Additives may act on both nucleation and crystal growth.

Mechanisms behind the inhibitory effects are : variation of solubility, decrease of molecular mobility and increase in  $T_g$ , or direct interactions between the additive and the sucrose molecules are possible. In many cases, the addition of additives significantly affects the solubility of sucrose by competing with sucrose molecules for hydrogen bonding sites with water (Mullin, 2001). The presence of additives often has negative effects on the equilibrium concentration of sugars, and in particular, the addition of corn syrup, invert sugar, gelatin, proteins, and starches decrease the saturation concentration in sucrose. The decrease in solubility, however, does not lead to higher crystallization rates as the additives also serve to inhibit crystallization by other means, and molecular mobility directly affects the nucleation rate (Equation 2.5 and 2.6). These additives may decrease the total molecular mobility and often interfere with mass transport due to their larger molecule size.

The effect of additives on sucrose molecule mobility has been explained by different authors. Saleki-Gerhardt & Zografi (1994) investigated the effect of disaccharides (lactose, trehalose) and trisaccharides (raffinose) on their inhibitory effect on sucrose crystallization. Although all additives showed the same  $T_g$  when mixed with sucrose, the trisaccharide raffinose (highest MW) showed a significantly greater

inhibitory effect when compared on an equimolar basis. They concluded a correlation between molecular mass and inhibitory effect is a combination of steric effects and a possible adsorption on the particle surface of impurities, both inhibiting the mass transport to the nucleation site. It cannot be ruled out, that both nucleation and growth are affected by specific interactions between sucrose and additives, thus inhibition of crystallization might be a result of the combination of both specific interaction mechanisms.

## **2. 4.4 Crystal Growth**

From the moment on when nuclei have reached a critical size in a supersaturated solution, their growth rate depends on a series of steps depending on conditions in their surrounding environment (Mullin, 2001) Following steps are necessary for a crystal to grow by molecular incorporation (Hartel & Shastry, 1991):

1. Molecules of the crystallizing species must diffuse from bulk solution to the crystal surface.
2. Formation of the appropriate molecular conformation must occur (e.g., mutarotation of lactose molecules)
3. Any non-crystallizing species must counter-diffuse from the crystal surface.
4. The crystallizing species must orient into the appropriate growth unit at the crystal surface.
5. Growth units must diffuse along the surface to the lattice site of incorporation
6. Growth units are incorporated into the lattice
7. Latent heat generated due to phase change must be removed.

For sucrose crystallization, different steps have been described to be rate-limiting: (i) In pure sucrose solutions, diffusion from the bulk solution to crystal surface and integration of the sucrose molecule into the lattice structure are the typical rate limiting steps (Hartel, 2013b; van Hook, 1981).



(ii) At a certain supersaturation level, bulk diffusion becomes less important, but surface diffusion at the crystal lattice and the incorporation of growth units may be inhibited. This is caused by potential non-crystallizing species such as corn syrup saccharides, which slowly counter diffuse from the crystallizing surface, and thus inhibit the incorporation of growth units into the lattice. (Gabarra & Hartel, 1998; Saleki-Gerhardt & Zografi, 1994).

The two diffusional steps mentioned previously are shown in Figure 2.4

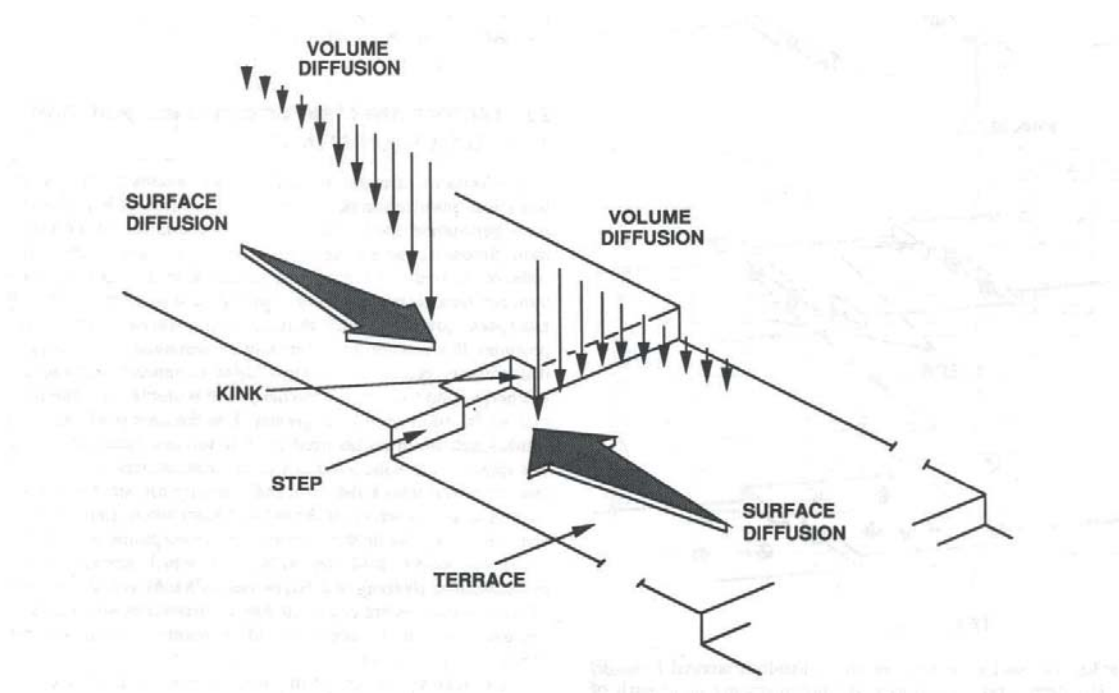


Figure 2.4 Important diffusional processes (volume and surface) affecting crystal growth (Myerson, 1993)

#### 2.4.4.1 Mass Transfer Theory

The driving factor for crystal growth in this theory is the concentration gradient of different layers between the bulk and the crystal surface. Here, concentration of the bulk solution  $C$  is considered to be supersaturated. The concentration at the crystal surface however, is considered to be at equilibrium concentration  $C^\circ$ , the interface or volume between the solution and the absorbed layer is defined as  $C'$ .

The different zones of concentration are shown in Figure 2.5, driving forces will rarely be of equal magnitude, and the concentration drop across the stagnant film is not necessarily linear.

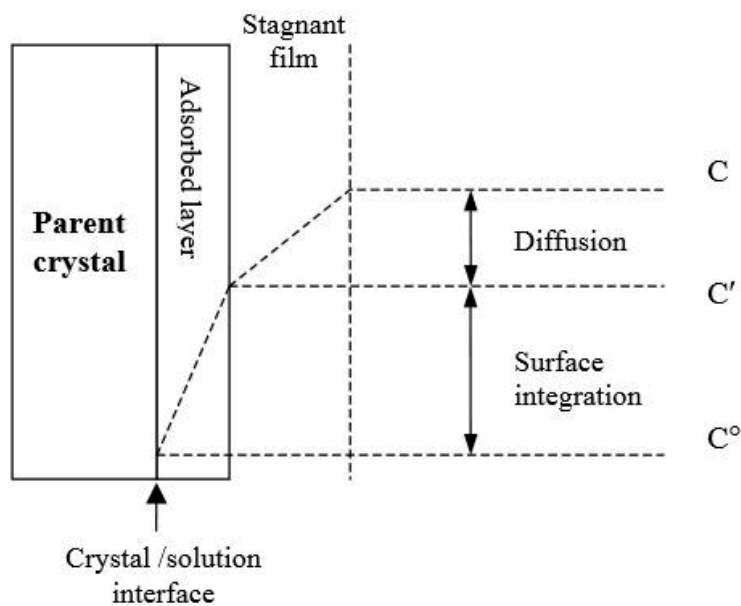


Figure 2.5 Model of the concentration driving force near crystal surface (Pantaraks, 2004).

Two steps in the mass deposition or diffusion were postulated; first molecules are transported from the bulk of the fluid phase to the solid surface, followed by a first-order reaction when the solute molecules arrange themselves into the crystal lattice. These two stages, occurring under the influence of different concentration driving forces, can be represented by the equations (Mullin, 2001)

$$\frac{dm}{dt} = k_d A (C - C') \quad (\text{diffusion}) \quad (2.10)$$

and

$$\frac{dm}{dt} = k_r A (C' - C^\circ) \quad (\text{reaction}) \quad (2.11)$$

where  $\frac{dm}{dt}$  is the rate of mass transfer across the boundary layer ( $\text{kg}/\text{m}^2\text{s}$ ),  $A$  is the surface area normal to flux ( $\text{m}^2$ ),  $k_d$  = a coefficient of mass transfer by diffusion;  $k_r$  is a rate constant for the surface reaction (integration) process,  $C'$  is the solute concentration in the solution at the crystal-solution interface (Mullin, 2001).

Equations 2.10 and 2.11 are not easy to apply in practice because they involve interfacial concentrations that are difficult to measure. It is usually more convenient to eliminate the term  $C'$  by considering an overall concentration driving force,  $C - C^\circ$ , which is quite easily measured. A general equation for crystallization is based on this overall driving force and can be written as:

$$\frac{dm}{dt} = K_G A (C - C^\circ)^n \quad (2.12)$$

where  $K_G$  is the overall crystal growth coefficient. The exponent  $n$  is usually referred to as the “order” of the overall crystal growth process and is in a range of 1 to 2.

However, at a growing crystal surface, a boundary layer exists where the concentration varies from the bulk solution to that of the surface crystal. Diffusion theory predicts the rate of mass transfer across the hydrodynamic boundary layer based on the concentration driving forces between the bulk and the interfacial concentrations (Hartel, 2001).

This is given as

$$\dot{m} = k_d (C - C^\circ) \quad (2.13)$$

where  $\dot{m}$  is the mass flux of solute crossing the boundary layer ( $\text{kg}/\text{m}^2\text{-sec}$ ), and  $k_d$  is a mass transfer coefficient ( $\text{m}^2/\text{sec}$ ). Subsequently the linear growth rate (in  $\mu\text{m}/\text{min}$ ) can be expressed as

$$G = k_d k_1 (C - C^\circ) \quad (2.14)$$

where  $k_1$  is a conversion constant from crystal mass to crystal size.

The mass transfer coefficient,  $k_d$ , combines the effects of convective transport and diffusion (Hartel, 2001). The temperature dependence of the mass transfer coefficient can be written as the Arrhenius relationship:

$$k_d = k_{d0} \exp\left(\frac{-E_a}{kT}\right) \quad (2.15)$$

Where  $k_d$  is the diffusion coefficient,  $k_{d0}$  is the maximum diffusion coefficient (at infinite temperature;  $\text{m}^2/\text{s}$ ),  $E_a$  is the activation energy for diffusion in dimensions of ( $\text{J molecule}^{-1}$ ),  $T$  is the absolute temperature and  $k$  is the Boltzmann constant.

#### 2.4.4.2 Surface Incorporation Theory

The theory of surface incorporation or adsorption involves the movement of sucrose molecules along the crystal surface and the integration into the lattice. The migration of the molecule along the surface until a favorable site is found is called surface diffusion. Subsequently, surface integration is the step where the molecule joins the lattice structure (van Hook, 1961).

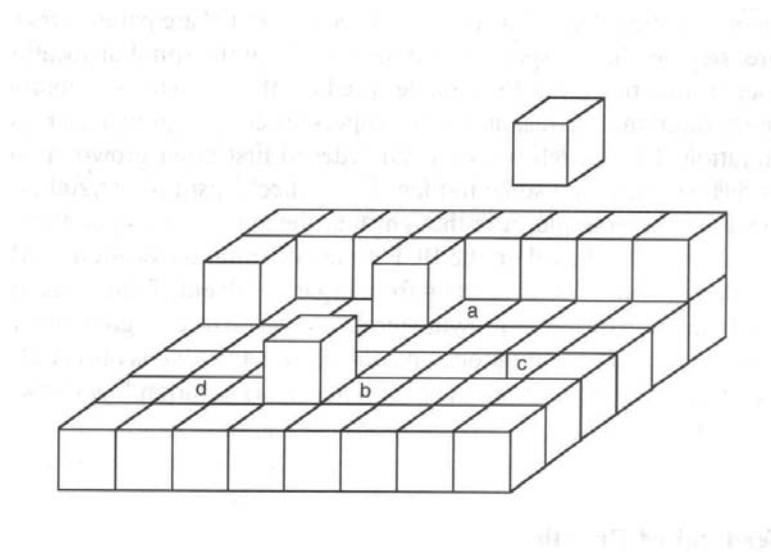


Figure 2.6 Schematic model of crystal lattice and incorporation sites based on simple cubic units: a, b, c, and d represent different potential sites for molecular incorporation into the crystal lattice (Hartel, 2001).

Figure 2.6 shows a schematic model of crystal lattice and incorporation sites in a simplified cubic form. Depending on the growth conditions, different incorporation sites might be chosen. The most energetically favorable site for incorporation is chosen when the growth rate is low. These favorable sites are the ones where attractive forces are the greatest, such as those sites where the growth units are bonded on several sites (sites, a, b, and c in Figure 2.6). However if the rate of crystal growth is high due to higher driving forces, the growth units fit into less energetically favorable sites and the crystal grows more imperfectly (Hartel, 2001). Growth unit incorporation on the surface of the crystal also depends on the surface structure. The solute molecule or growth unit must integrate in a plane type if

the surface of the crystal is very smooth; on the other hand, on a very rough crystal surface with many imperfections, numerous kink sites can be found for incorporation and surface integration may not be rate limiting. Thus it has been noted that crystal surface is an important factor in a crystal growth process (Mullin, 2001).

Equation 2.11 as previously described, represents the reaction or incorporation step:

$$\frac{dm}{dt} = k_r A (C' - C^\circ) \quad (\text{reaction}) \quad (2.11)$$

The overall driving force was expressed as :

$$G = K_g A (C - C^\circ)^n \quad (2.12)$$

In the simplest case, when  $n = 1$ , the term  $C'$  (the interfacial concentration) can be eliminated in order to obtain the following expression :

$$K_g = \frac{k_d k_r}{k_d + k_r} \quad (2.16)$$

and subsequently:

$$R_g = \frac{k_d k_r}{k_d + k_r} (C - C^\circ) \quad (2.17)$$

where,  $k_d$  is the coefficient of mass transfer by diffusion and  $k_r$  is the surface integration rate constant. For cases of extremely rapid reaction, i.e. large  $k_r$ ,  $K_g \approx k_d$  and the crystallization process is controlled by diffusion. Similarly, if the value of  $k_d$  is large, i.e. diffusional resistance is low,  $K_g \approx k_r$ , and the process is controlled by the surface integration.  $K_g$  could be defined as a function of the external

processing conditions such as temperature, agitation rate, and the presence of additives or impurities (Hartel, 2001).

Three mechanisms were discussed for surface diffusion (Mullin, 2001):

1. Gibbs-Volmer Theory: two-dimensional nucleation theory
2. Surface nucleation on dislocations: layer by layer growth
3. Burton, Cabrera, and Frank (BCF) model growth: screw dislocations

The migration in two dimensions along the crystal surface with a subsequent integration in the surface at a point where critical mass is reached is postulated by the Gibbs -Volmer theory. This model is proposed for the system with smooth crystal surface. In the case of rough surfaces, any molecules diffusing to the surface of the crystal are incorporated immediately. The layer by layer growth model assumes that the growth units can integrate continuously at the dislocations (Kinks, steps, etc) in a way where they have the lowest energy for incorporation due to multiple bonding sites. The third model, the Burton-Caberra-Frank (BCF) model describes how an otherwise flat crystal surface grows by addition of growth units to kink sites in an infinite spiral (Pantaraks, 2004). Not only are the growth units added at kink sites provided by a screw dislocation but also creating another kink site, which is favorable for growth.

### **2.4.4.3 Sucrose Crystal Growth Parameters**

#### **2.4.4.3.1 Supersaturation**

Supersaturation is the driving force for crystallization and plays an important role in controlling the rate of crystal growth. Higher driving forces usually result in faster crystal growth, but only up to the point where the growth rate reaches a maximum based on the balance between the thermodynamic driving force for crystallization and the diffusional limitation to molecular mobility. Very high supersaturations and/or low temperatures, reduce the molecular mobility that crystal growth rates decrease rapidly. When concentration is sufficiently high or moisture content low, the glassy state is reached, where the molecular mobility is adequately decreased and the growth of sugar crystals ceases.

#### **2.4.4.3.2 Temperature**

The driving force of crystallization is intimately linked to the temperature. In melt systems, the temperature difference between the actual temperature and the melting point provides the driving force for growth or dissolution. When a solution of given concentration is cooled below the solubility temperature, supersaturation increases at a rate dependent on the change in solubility with temperature. Growth rate initially increases as temperature decreases from the solubility point. However, as temperature decreases to the point where molecular mobility becomes limiting, the growth rate begins to decrease. At the temperature where glass transition is reached, growth rate ceases. Temperature has been shown to affect the rate limiting steps for sucrose crystal growth. At low temperatures, the surface reaction step dominates, while at higher temperature (above 40°C), mass transfer effects or diffusion provide greater limitation (Hartel, 2001).

The temperature at which the crystal growth rate ( $G$ ) of a system is the highest is defined as  $T_{Gc}$  or  $T_{cGmax}$ . This temperature could be expressed in a ratio to  $T_m$ , the melting temperature of the crystals.



The ratio of  $T_c(G)/T_m$  for polymer crystal growth is very stable and usually ca. 0.8 to 0.9. According to the classical crystallization theory for the temperature dependence of the crystal growth rate from the melt, growth rate  $G$  is generally described as (Okui, 1990):

$$G = G_0 \exp \left( -\frac{\Delta E}{RT} - \frac{K_1 T_m}{RT \Delta T} \right) \quad (2.18)$$

And nucleation rate  $I$  as

$$I = I_0 \exp \left( -\frac{\Delta E}{RT} - \frac{K_2 T_m^2}{RT (\Delta T)^2} \right) \quad (2.19)$$

Where  $\Delta E$  is the activation energy for migration through the nucleus-melt interface,  $K_1$  and  $K_2$  is a nucleation parameter and  $\Delta T$  is the degree of supercooling ( $T_m - T$ ),  $T$  is the crystallization temperature,  $G_0$  and  $I_0$  are constants and  $R$  is the universal gas constant. The temperature  $T_c$  at which  $G$  is maximum can be obtained by equating to zero the derivate of Equation 2.18 with respect to temperature. The maximum temperature of crystallization and nucleation in relation to  $T_g$  and  $T_m$  are shown in Figure 2.7

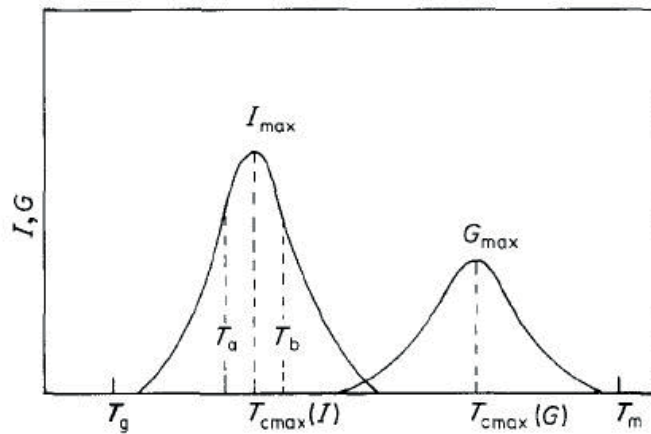


Figure 2.7 Schematic illustration of the temperature dependence of nucleation rate ( $I$ ) and crystal growth rate ( $G$ ).  $T_c(I)$  and  $T_c(G)$  are the temperatures at which  $I$  and  $G$  are maxima, respectively (Okui, 1990).

The temperature at which overall crystallization rate, as a product of nucleation and growth, is the highest is defined as  $T_c$ . The location of the maximum crystallization rate  $T_c$  between glass transition temperature  $T_g$  and solubility temperature  $T_m$  can be expressed as the ratio  $R_{Tc}$ :

$$R_{Tc} = \frac{T_{(c)} - T_g}{T_m - T_g} \quad (2.19)$$

Saleki-Gerhardt and Zografi (1994) found  $T_c$  to be exactly at the midpoint between  $T_g$  and  $T_m$  (ratio = 0.5) for amorphous sucrose solutions with a moisture content from 0-3.3%.

Kedward et al. (1998) used isothermal DSC experiments on freeze dried amorphous sucrose and lactose at moisture levels of 3,2% for lactose and 0,94% for sucrose, respectively.  $T_c$  values obtained from these experiments ranged slightly above the midpoint between  $T_g$  and  $T_m$  ( $\sim 0.55$ ).

Values for crystallization rate as a function of  $R_{Tc}$  of amorphous sucrose and lactose in a Hoffman-Lauritzen like fit are shown in Figure 2.8:

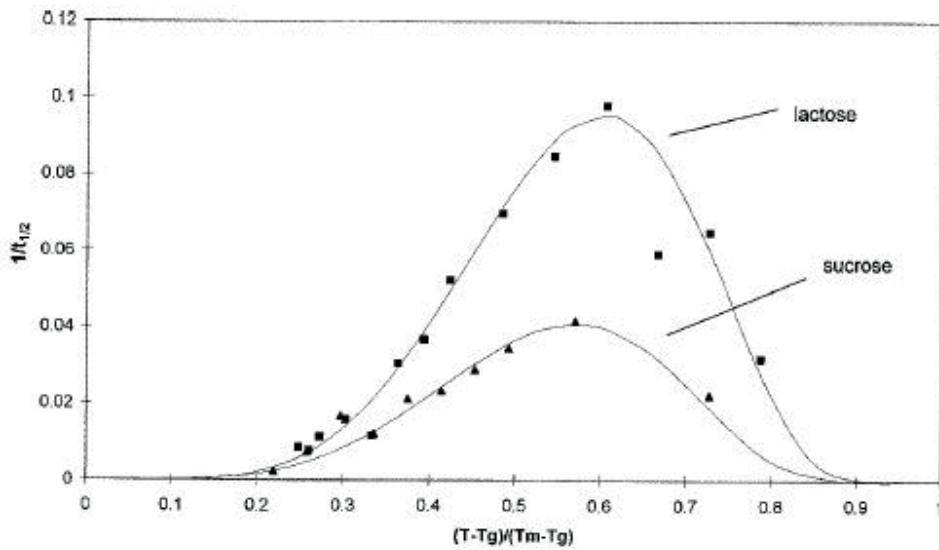


Figure 2.8 Hoffman Lauritzen like fit of crystallization rate of lactose and sucrose as a function of crystallization temperature,  $T_g$  and  $T_m$  obtained from a range of isothermal holding temperatures (Kedward et al., 1998).

Saleki-Gerhardt and Zografi (1994) considered two factors important in the crystallization mechanism of amorphous sucrose: (i) the rate of nuclei formation, and (ii) diffusion of molecules to the crystallization site. Based on these competing mechanisms, the overall rate of crystallization was predicted to be highest at a temperature midway between  $T_g$  and  $T_m$ . Thus, in DSC experiments,  $T_c$  should fall at this midpoint temperature (Gabarra & Hartel, 1998). Literature values for  $T_c$  confirmed this prediction (Kedward, MacNaughtan, & Mitchell, 2000; Saleki-Gerhardt & Zografi, 1994) indicating that crystallization of sucrose was a nucleation controlled process, where rates of nuclei formation and molecular mobility contribute equally to the overall crystallization.

#### **2.4.4.3.3 Additives and Impurities**

Additives and impurities can influence crystal growth either due to a change in the thermodynamic driving force, which means affecting the solubility concentration, or due to specific growth inhibition effects of the individual molecules (Mullin, 2001). Foreign molecules may inhibit growth in three ways: (A) foreign molecules may impede diffusion of sucrose molecules to the crystal surface and thereby slow growth, (B) the foreign molecules may adsorb to the crystal surface (most likely by hydrogen bonding) and inhibit the ability of molecules to incorporate into the lattice, and (C) the foreign molecules may adsorb so strongly that they actually become incorporated into the lattice, where they prevent the addition of new sucrose molecules to the lattice.

As corn syrup is commonly used in various food products to impede the crystallization of sucrose, interactions and inhibitory mechanisms in these systems were discussed and postulated. Similarly to the basic inhibitory principles (A-C), the inhibitory effect of corn syrup on the sucrose crystallization can be explained by different approaches: (i) corn syrup saccharides ( monosaccharides, glucose, fructose, and glucose polymers) adsorb onto the crystal lattice structure. This mechanism was proposed for

crystallization of sucrose in solutions (Bamberger et al., 1980; Gabarra & Hartel, 1998; Hartel, 2001; Saleki-Gerhardt & Zografi, 1994). (ii) The addition of corn syrup may increase the viscosity of the system, lowering the mobility of the molecules and thus increasing the energy required for crystallization (Levenson & Hartel, 2005) (iii) Corn syrup polysaccharides may also interact with sucrose molecules by hydrogen bonding, thereby affecting both translational and rotational diffusion. More energy would be needed for the sucrose molecules to diffuse through bulk solution for nucleation and growth to occur (Levenson & Hartel, 2005). As corn syrups offer a specific profile of polysaccharides with varying degree of polymerization and therefore molecular weight, effects based on these polysaccharide blends were discussed in order to understand potential interactions. Tjuradi and Hartel (1995) evaluated the effects of corn syrup saccharides on sucrose crystal growth from solution. The different corn syrup fractions (degree of polymerization) showed differences in their effectiveness to reduce crystal growth when the solution were compared at a constant supersaturation. Fractions of higher molecular weight showed a stronger inhibitory effect on sucrose crystal growth. However, when the results were expressed in terms of average molar addition levels of each fraction, there was no difference in inhibition due to chain length of the saccharides. In later work, Gabarra and Hartel (1998) found that even if added at lower average molar addition, corn syrup fractions of higher molecular weight ( $M_n$ , number-average molecular weight) were more effective at reducing sucrose crystal growth. Comparable findings were published by Saleki-Gerhardt & Zografi (1994), who compared two disaccharides lactose, trehalose and the trisaccharide raffinose on their effect on sucrose crystallization in at low moisture levels (<1%). Here too, the molecule with the highest molecular weight (raffinose) showed the strongest inhibitory effect on the crystallization of amorphous sucrose. In both publications, the variation in the inhibitory effect could not be explained solely by an increase in  $T_g$  and subsequent reduction in molecular mobility. Gabarra and Hartel (1998) explained the additional inhibitory effect by effects during the crystal growth; corn syrup saccharides are assumed to adsorb at the crystal lattice where molecules of higher molecular weight

might counter-diffuse from the crystal surface at a slow rate, thus impeding the incorporation of sucrose growth units into the lattice.

#### **2.4.4.3.4 Viscosity / Molecular Mobility**

Viscosity as a specific influence on crystal growth rate is hard to separate from other factors such as temperature, supersaturation and impurities as all these parameters affect the viscosity of the matrix. In fact, it is widely misconstrued that bulk viscosity is the limiting factor influencing crystal growth. Rather, it is the molecular mobility of the molecules that influences crystallization, and this mobility is not always related to bulk viscosity. However, as concentration increases and temperature decreases the diffusivity of the matrix decreases, thus molecular mobility is reduced. However, generally speaking, an increase in viscosity inhibits crystal growth rate, especially in ranges when mass transfer mechanism is the rate limiting factor (van Hook, 1961). Finally, when a system reaches very high viscosities, any molecular mobility ceases and crystallization rate becomes zero. This effect is usually described as the glassy state (Hartel, 2001).

#### **2.4.5 Arrhenius Equation**

The Arrhenius equation in its basic form is a widely used mathematical equation expressing the rate of a reaction as a function of the temperature. Usually, the Arrhenius equation is best seen as an empirical relationship that describes kinetic data very well (Connors, 1990). According to the Arrhenius equation rate constant  $k$  can be expressed as:

$$k = A \exp\left\{-\frac{E_a}{RT}\right\} \quad (2.20)$$

where  $T$  is the absolute temperature (K),  $R$  is the universal gas constant,  $A$  is the pre exponential factor and  $E_a$  is the activation energy. The equation is used to model temperature variation of diffusion

coefficients, population of crystal vacancies, creep rates, and many other thermally induced reactions (Connors, 1990). Due to the temperature dependence of crystallization processes (nucleation and growth) variations of the Arrhenius equation are used to express the relationship between (a) temperature and nucleation in the classical nucleation equation (Equation 2.6) and (b) temperature and crystal growth, when both processes are modeled to mass transfer and diffusion. There is no simple or generally accepted method of expressing the rate of growth of a crystal, since it has a complex dependence on temperature, supersaturation, size, habit, and so on. However, for carefully defined conditions (e.g., constant supersaturation) crystal growth rates may be expressed as (Hartel, 2001)

$$k_G = A_g \exp \left\{ -\frac{E_g}{RT} \right\} \quad (2.21)$$

where  $A_g$  is a frequency factor,  $E_g$  is the activation energy for growth,  $R$  is the universal gas constant, and  $T$  is temperature. Activation energy can be found from the exponential relationship between  $k_G$  (or growth rate at constant supersaturation) and inverse temperature.

Roos (1995) found that the difference between true and reaction rate constants calculated by Arrhenius equation is relatively small for various food applications, and occurred within a relatively small temperature range above  $T_g$ . Additionally, in practice rates of diffusion-limited reactions have been determined for foods above  $T_g$  and the rates have followed the Arrhenius-type temperature dependence (Roos, 1995).

#### 2.4.6 William-Landel-Ferry Equation

The William-Landel-Ferry (WLF) theory assumes that the free volume of a polymer is directly related to the temperature above  $T_g$ , so that at higher temperatures the system has greater mobility and the relaxation time decreases (Levine & Slade, 1988). It has been suggested that the WLF equation applies above the glass transition temperature in any glass-forming polymer, oligomer or monomer (Levine & Slade, 1988). The kinetics of relaxation processes in a diffusion limited, glass forming system involves distinct temperature ranges. Depending on the range, Arrhenius or WLF theories have been used to describe the system. Arrhenius kinetics are supposed to apply in the glassy state at temperatures below  $T_g$ , where low molecular mobility is found, as well as in the liquid state above the solubility or melting curves. WLF kinetics apply in the rubbery state, between the  $T_g$  and the solubility curves, where molecular mobility and diffusion increase (Levine & Slade, 1988). Figure 2.8 show the regions where each equation should be used depending on the state of system. However, the classification of type of equation applicable to a certain temperature range remains controversial (Lomellini, 1992). Although Arrhenius type equations expressing viscosity as a function of temperature are less accurate for amorphous concentrated solutions than the WLF model, many empirical equations used to describe experimental viscosity-temperature data both for aqueous solutions and supercooled sugar melts are found in literature (Mathlouthi, Cholli, & Koenig, 1986). A detailed comparison between the two models is often difficult for various reasons:

- (i) If the polymer can crystallize, it is practically impossible to carry out rheological measurements at temperatures between the glass transition temperature  $T_g$  and crystallization temperature  $T_c$ .
- (ii) Sometimes the transition from WLF to Arrhenius behavior could be very smooth and with small effects (Berry & Fox, 2006).

The original form of the WLF equation is shown in equation 2.22:

$$\log_{10} \alpha_t = \frac{-C_1(T - T_s)}{C_2 + (T - T_s)} \quad (2.22)$$

where,  $\alpha_t$  is the ratio between relaxation phenomena at temperature  $T$  and the reference temperature  $T_s$ , and  $C_1$  and  $C_2$  are constants (Williams, Landel, & Ferry, 1955). Crystallization data, such as crystallization rates, can also be fitted with the WLF equation modified so that  $\alpha_t$  is the ratio of crystallization rate at temperature  $T$  and the reference temperature  $T_s$ ,  $T_g$  respectively (Roos & Karel, 1991a). This modification relates the rate of crystallization as an index of internal molecular mobility. The theory suggest, that above  $T_g$ , the rate of crystallization is related to viscosity and relaxation times of mechanical properties (Roos, 1995).

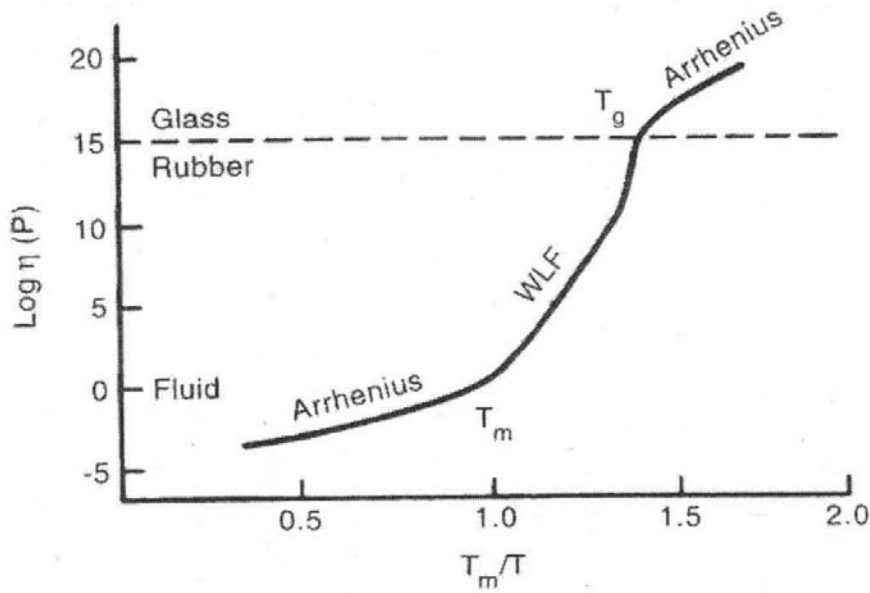


Figure 2.9 Application of the Arrhenius and Williams-Landel-Ferry (WLF) kinetics in different physical states. The glass transition temperature ( $T_g$ ) and melting temperature ( $T_m$ ) are shown on the graph. The diagram represents viscosity ( $\eta$ ) as a function of reduced temperature ( $T_m/T$ ). (Levine & Slade, 1988).



#### 2.4.6.1 WLF Coefficients

Williams et al. (1955) proposed constant coefficients for the WLF equation, derived from multiple experiments with various polymers. These coefficients are known to give a good description of the relaxation relationships of sugars to temperature above  $T_g$  (Roos & Karel, 1991a, 1991b). However, it has been suggested by Peleg (1992) and the original authors, Williams et al. (1955), that the use of these universal values is limited due to variability in measuring  $T_g$ , the difficulty of making measurements near  $T_g$ , and variations between physical and chemical properties of the averaged polymers. Roos&Karel (1991a) studied the crystallization times for both amorphous lactose and sucrose using universal values for  $C_1$  and  $C_2$ . In both cases, the deviation from the data increased with increasing temperature so that their crystallization data did not fit well using the universal constants. This is in agreement with the suggestion of Peleg (1992) that the WLF model should only be used in the original form with variable coefficients, at a temperature above  $T_g$ .

#### 2.4.7 Hoffmann-Lauritzen Growth Equation

The crystallization process of polymers does not always obey chemical rate equations. Polymers can crystallize through a variety of regimes, which are defined by two rates, the rate of nucleation and the rate of growth. As shown in Figure 2.6, both processes have different maxima over the temperature range between  $T_g$  and  $T_m$ . According to the Lauritzen-Hoffmann growth theory the kinetics of polymer crystallization can be described by two ultimate rates. On one hand side is the secondary nucleation, which is defined as the addition of a monomer to an already existing crystalline structure. As with heterogeneous nucleation, the energy required for nuclei formation is reduced by existing surfaces (Equation 2.19). On the other side is growth as defined in section 2.4.4. These rates can be expressed by three different regimes in the Lauritzen-Hoffman growth theory:

Regime I: At small super cooling,  $\Delta T = T_m - T$  the lateral growth rate  $g$  is significantly higher than secondary nucleation rate  $i_s$  ( $g \gg i_s$ ) and as a consequence a crystalline monolayer is formed on the substrate. Here growth is the rate limiting step (RDS) and the linear growth rate can be expressed as:

$$G = b_o i_s L \quad (2.23)$$

Where  $b_o$  is the thickness and  $L$  is the length of the crystalline polymer lamellae.

Regime II: moderate supercooling causes Regime II kinetics. The nucleation rate  $i_s$  becomes either comparable or higher than the lateral growth rate  $g$  ( $g \leq i_s$ ), and the rate of diffusion controlled growth could be expressed as:

$$G = b_o \sqrt{i_s g} \quad (2.24)$$

Regime III: lastly depicts the scenario when lateral growth is inconsequential to the overall rate, since the nucleation of multiple sites causes  $g \ll i_s$ . This means the growth can be modeled by the same equation than in Regime I.

The three types of growth kinetics according to regime I, II and III are shown in Figure 2.10

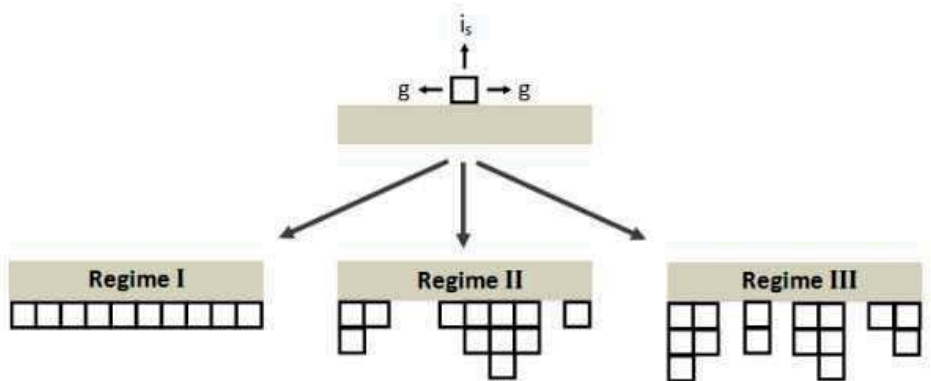


Figure 2.10 Classification of growth kinetics according to Hoffman and Lauritzen (Ohneiser, 2011).

The resulting crystallization rate as a function of temperature can be expressed according to Lauritzen and Hoffman (1973) as:

$$\left(\frac{1}{t_{1/2}}\right) = \left(\frac{1}{t_{1/2}}\right)_0 \exp\left(\frac{-U}{R(T - T_\infty)}\right) \exp\left(\frac{-K}{T \Delta T f}\right) \quad (2.25)$$

where  $T$  is the crystallization temperature,  $R$  is the universal gas constant,  $\Delta T = T_m^\circ - T$  is the supercooling,  $f = 2T/(T + T_m^\circ)$  is a correction factor accounting for the reduction in the latent heat of fusion as the temperature is decreased and  $T_m^\circ$  is the equilibrium melting point.  $(1/t_{1/2})_0$  is the pre-exponential factor that includes all terms independent of temperature,  $U$  is the activation energy or the transport of crystallizing units across the phase boundary,  $T_\infty$  is the temperature below such transport ceases, and  $K$  is a nucleation term. In the Lauritzen-Hoffman equation,  $T_\infty$  is usually taken to be  $T_g - 30\text{K}$ . The factor  $(1/t_{1/2})_0$  is known to show a weak, linear temperature dependency, which is usually negligible.

The general growth rate as a function of temperature according to Equation 2.25 is shown in Figure 2.11:

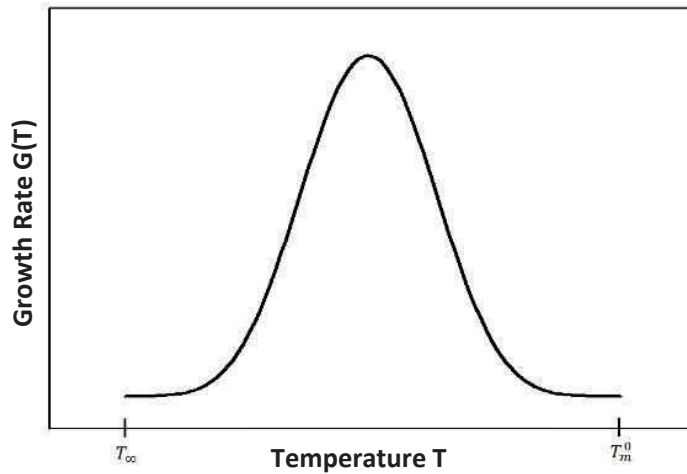


Figure 2.11 Growth rate as a function of temperature according to the Hoffman-Lauritzen equation.

The work of Kedward et al. (1998) showed good fits of Hoffman-Lauritzen like expression to the crystallization rates of amorphous sucrose. Based on these results, the data for isothermal crystallization rates of this work were applied to the HL equation in order obtain the quality of the fit to the Hoffman-Lauritzen model and furthermore approximate crystallization rates over a temperature range (above 110°C) that could not be investigated experimentally. The emphasis of this application was to compare approximate temperature and rate of maximum crystallization as a function of  $T_g$  and  $T_m$  with respect to the type of syrup used in the formulation.

### 3. Materials and Methods

The objective of this research is to investigate crystallization kinetics and behavior of amorphous sugar matrices composed of sucrose, corn syrup, and water. The experiments focus on induction times, time to crystallize the sample to both 50% and 100% and the glass transition temperature, temperature of maximum crystallization and solubility temperature of the samples with respect to different types of corn syrups. The sugar glasses were held at varying temperatures to promote nucleation and crystallization.

#### 3.1 Experimental Formulations

The sugar glasses were made with a mixture of corn syrup (ADM, Decatur, IL), fine granulated sugar (United Sugars, Crookston, MN), and deionized water (building supply). Six formulations with three different dextrose equivalent (DE) corn syrups (26DE, 42DE, and 62DE) at two different sucrose to corn syrup ratios were prepared. The amount of corn syrup was either 14% or 22% on a dry weight basis. Detailed information about the sugar and syrups used are shown in Table 3.1 and 3.2.

Fine Granulated Sugar		United Sugars Corp.	
Batch		K15050	
Moisture [%]		0.023	
Ash [%]		0.012	
Sucrose content		≥99,9%	
Invert on sugar		< 0,04%	

Table 3.1 Analysis of sugar used in all experiments, all % data on a w/w dry basis

Corn Syrup	ADM	ADM	ADM
Dextrose Equivalent	26	41.9	62.4
Baume	41.9	42.8	43.8
Dry solids [%]	77.7	80.4	83.8
DP1:	4.9	17.4	35.4
DP2:	7.7	13.4	7.8
DP3:	11.4	12.1	11.5
DP4+:	75.9	57.1	75.10

Table 3.2 Technical data of corn syrup used in all formulations, % data on a w/w dry basis

14% Corn syrup	Sugar	Water	Corn syrup		
			26 DE	42 DE	62 DE
Weight [g]	21.50	5.00	4.5	4.35	4.17
Ratio [%] dry (w/w)	86	-	14	14	14

22% Corn syrup	Sugar	Water	Corn syrup		
			26 DE	42 DE	62 DE
Weight [g]	21.50	5.00	7.07	6.84	6.6
Ratio [%] dry (w/w)	78	-	22	22	22

Table 3.3 Formulation of sugar glasses on a w/w dry basis before cooking. Each formulation contains sucrose and one type of corn syrup.

### 3.2 Cooking Procedure of Sugar Syrup

Every formulation was prepared using the same method. Sugar and corn syrup were weighted in a 30mL beaker (Corning Incorporated, Corning, USA), then 5mL of deionized water was added. The mixture was stirred slowly with a glass stick to ensure a homogenous mixture of the components before heating. The mixture was placed on a Corning PC-420 Stirrer Hot-Plate (Corning Incorporated, Corning, NY) with temperature set to 310°C. The syrup was heated without stirring to minimize initial nucleation. The samples were cooked until the solution reached target temperatures ( $T_x$ ) of 135°C, 140°C, 145°C and 150°C for 42 DE corn syrup. The effect of different boiling point elevation due to different DE corn syrups increased with amount of corn syrup in the formulation - solutions with 22% corn syrup were heated to

slightly different temperatures. The solutions containing 26DE corn syrup were heated to a slightly lower boiling temperature ( $T_x$  minus  $\sim 1.^\circ\text{C}$ ), whereas solution containing 62DE was heated to a slightly higher boiling temperature ( $T_x$  plus  $\sim 1.5^\circ\text{C}$ ). The temperatures were measured at the bottom center of the beaker using an electric thermometer (TP3001, China).

### 3.3 Sugar Glass Preparation

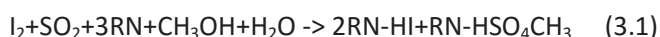
After reaching the target cooking temperature the solution was poured into pre-cooled aluminum pans ( $\varnothing$  65mm). Before usage, the aluminum pans were stored in a freezer and kept on an ice pack while being filled. After the solutions were poured into the pans, they were immediately transferred into a freezer to achieve high cooling rates. This was done to minimize initial nucleation within the glasses by lowering the temperature of the samples below the glass transition temperature as fast as possible. The glasses were stored at  $-18^\circ\text{C}$  for 1,5h to ensure a sample temperature below  $-14^\circ\text{C}$  for 1h.

After the glasses cooled, the pans were taken out of the freezer and transferred into a desiccator and stored over dessicant (Drierite, Xenia, OH) for 20min. The desiccator was used to ensure adjustment of the glasses to room temperature (RT) in a dry environment, to prevent water absorption of the hygroscopic glasses during the adjustment. If not stored properly, the absorption of water from the glass was seen in the outer lattice of the glass with increased stickiness. The temperature of the glass was monitored using a digital infrared thermometer (1310, TES, China). When the glass reached RT, it was taken out of the pan, wrapped in waxed paper and gently pulverized into a fine glass powder using a hammer. The powder was immediately transferred into  $\text{N}_2$  pre-flushed plastic vials to avoid any moisture uptake from the environment. The vial was transferred into a  $\text{N}_2$  purged glove bag. While working with the samples, the glove bag was constantly purged to ensure a  $\text{N}_2$  saturated, dry environment avoiding any moisture uptake by the pulverized samples. The humidity within the glove bag was monitored with a digital hygrometer (VWR, Radnor, PA) and kept below 5% at all times.

### 3.4 Moisture Content

The moisture content of the glass samples have a strong effect on the crystallization kinetics of the amorphous glasses. For this reason, the samples were stored and processed under controlled conditions throughout the whole sample preparation and during the experiments. To enable accurate and comparable conditions for the experiments the moisture content of the samples was determined as precisely as possible to select suitable samples for further analysis. All samples (26DE, 42DE, 62DE) cooked to same target temperature had to fit a small range of moisture content ( $\pm < 0.12\%$ ) for each of the cooking temperatures. Samples exceeding this range were discarded. For both ratios of syrup, formulations containing 42DE syrup were cooked to the different temperatures in duplicates and the water content from these samples were defined as the target moisture content for the other DE syrup formulations.

A Karl Fischer Aquametry instrument (795 KFT Titrino, Metrohm Ltd., Herisau, Switzerland) and a stand (Metrohm 703 Ti stand) with an automatic pump for the Karl Fischer reagent were used to measure the moisture content of the sugar glass samples. The titrant used was a one-component, pyridine-free Karl Fischer reagent containing sulfur dioxide and iodine (Hydranal Composite 5, Riedel de Haën, Sigma-Aldrich, Co., St Louis, MO). The technique involved titration of the Karl Fischer reagent into a 150mL reaction vessel containing the sample pre-dissolved in a solvent. The solvent was a 4:3 ratio of Formamide (Fisher scientific, Fair Lawn, NJ) and Karl Fischer grade methanol (low water content 0.006%) solution. The solution was used to completely dissolve the sugar glass and release the incorporated water. A platinum electrode was immersed in the solvent to measure the conductivity of the solution. In the presence of water,  $\text{SO}_2$  is oxidized by  $\text{I}_2$  according to the following reaction:





When the Karl Fischer reagent depleted the water, an excess of iodine depolarized the electrode to give the titration endpoint. According to the equation 3.1, the Karl Fischer reagent reacts with water on a volume basis. The apparatus was first calibrated with triplicates of sodium tartrate dehydrate (HYDRANAL<sup>®</sup> CRM Sodium Tartrate Dehydrate, Sigma Aldrich, St.Louis, MO). The calibration determines the average strength of the Karl Fischer reagent, or amount of Karl Fischer reagent necessary to titrate the sodium tartrate dehydrate, which contains a defined amount of water ( ~15,66 % w/w). For each calibration, approximately 0.125g of the sodium tartrate dehydrate were filled into the titration vessel and then dissolved for 60 seconds in the tempered solvent (50°C). The average of these 3 values was divided by 15.66 to obtain the adjustment factor:

$$\text{Adjustment factor} = 15.66 / \text{average moisture measures of sodium tartrate dehydrate} \quad (3.2)$$

This adjustment factor was used to calculate the actual water content of each sample.

For each sugar glass replicate, approximately 0.15g of each sample were weighed into a glass vial in a controlled N<sub>2</sub> environment. The vial was used to transfer the sample to the apparatus, avoiding any water uptake of the highly hygroscopic pulverized sugar glass through the environment. The vial was weighed and tared and the glass powder was poured into the titration vessel as quickly as possible. Before the titration was started, each sample was dissolved for 120 seconds in the stirred, tempered solvent (50°C). The actual water content was the given value multiplied by the adjustment factor. Three to four replicates were analyzed for each sample, with the moisture content taken as the average.

### 3.5 Non-isothermal Determination of Glass Transition Temperature $T_g$ , Crystallization Temperature $T_c$ and Solubility Temperature $T_m$ .

A differential scanning calorimeter (DSC 8500, Perkin Elmer Corporation, Wilton, CT) was used to determine glass transition temperature ( $T_g$ ), crystallization temperature ( $T_c$ ), and solubility temperature ( $T_m$ ) of the sugar glasses. The DSC was connected to a refrigeration system and used the Pyris software program (Version 11, Perkin-Elmer, Inc., Shelton, CT). For calibration, the onset melting temperature of Indium (156,60 °C) was used along with its latent heat of melting (28.45J/g). Baseline correction was done using runs with an empty furnace from 0-200°C at a heating rate of 40°C/min. Curvature of the baseline was less than 0,6 J/200°C and slope was adjusted to less than  $\Delta$  5J/200°C at any time. In a saturated N<sub>2</sub> environment (< 5% humidity), 20,5g ( $\pm$ 0.3g) of the pulverized sample were placed in each of two tared, O-ring sealed, large volume stainless steel DSC pans (Perkin Elmer, Inc., Shelton, CT) and then sealed with a Universal Crimper Press (Perkin-Elmer, Inc., Shelton, CT). Pieces of glass splinters in the pans were removed and the pulverized glass was distributed uniformly at the bottom of the sample pan to obtain an even interface between sample and pan. The sample pan was then placed in the DSC. The heating and cooling rate were 5°C/min and 40°C/min, respectively. The sample was heated through a first heating cycle to eliminate the effects of sample thermal history, with  $T_g$ ,  $T_c$  and  $T_m$  obtained from the second heating scan. Each run was performed in duplicates. The profile chosen was :

- 1) Hold at 0°C for 1 minute
- 2) Heat from 0 to 60°C at 5°C/min
- 3) Hold at 60°C for 1min
- 4) Cool from 60°C to 0°C at 40°C/min
- 5) Hold at 0°C for 1 min
- 6) Heat from 0°C to 200°C at 5°C/min

All DSC experiments, isothermally and nonisothermally for each type of glass (DE/ syrup ratio/ cooking temperature), were performed the same day as the sample was made. This was done to increase accuracy and to minimize the effect of aging of the sugar glasses. Each sample was produced and

analyzed in duplicates at two independent days with differences in the moisture of  $< \pm 0.1\%$  (w/w)

between samples of the same type. A typical DSC scan curve from 0°C-200°C is shown in Figure 3.1:

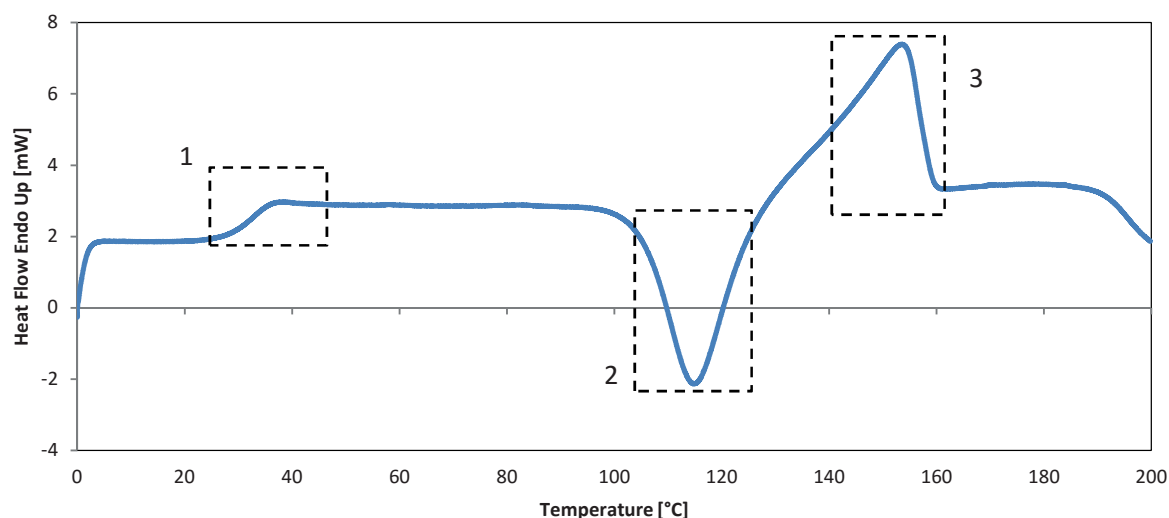


Figure 3.1 Schematic representation of a differential scanning calorimeter (DSC) thermogram for amorphous sugar glass cooked to 150°C, 14% w/w 42DE syrup dry basis.

The glass transition temperature was determined graphically using the Pyris software. The scan shows the x axis ranging from 0 - 200°C. First the scan shows the glass transition (1), visible as an endothermic step in the curve. The molecular arrangements of the former brittle glass changes into a rubber - like state increasing the mobility of molecules. With increasing temperature the mobility of the molecules increases and the sample starts to crystallize. Crystallization releases heat as the entropy decreases due to formation of ordered crystalline structures, the difference in the entropy must be exported from the system through heat. This is seen as an exotherm peak in the scan (2). The trace leaves the baseline when nucleation starts and reaches a maximum (maximum crystal growth) after which the exothermic peak starts to decrease, as crystallization slows down. The heat flow curve for the crystallization flattens out after all crystallizable material is fully crystallized. As the temperature rises further, the solubility of the solute also increases, and thus, the crystals start to dissolve in the remaining water contained in the samples. The heat flow curve increases steadily, reaching a maximum (maximum deviation from the baseline), after which it starts to decrease, as the remaining crystalline amount in the pan decreases (3).

The heat flow curve flattens out when all of the solids are dissolved and is a result of the heat capacities of the system. Crystallization temperature as well as solubility temperature was determined as the peak value of each of the heat flow curves (Mohan, Lorenz, & Myerson, 2002)

### **3.6 Isothermal Determination of Crystallization Characteristics**

A differential scanning calorimeter (DSC 8500, Perkin Elmer Corporation, Wilton, CT) was used to follow the crystallization of the sugar glass at a constant temperature over time. The same calibration was used as described in Section 3.5. The baseline was recorded with an empty sample pan at 100°C over 30 minutes and adjusted to a minimal slope of less than  $\Delta 0.2\text{J} / 30\text{min}$ . The same baseline calibration was used for all isothermal runs. In a saturated N<sub>2</sub> environment (< 5% humidity), 13g ( $\pm 0.3\text{g}$ ) of the pulverized sample were placed in each of 9 tared, standard aluminum DSC pans (Perkin Elmer, Inc., Shelton, CT) and sealed with a Crimper Press (Perkin-Elmer, Inc., Shelton, CT). The pans were placed in a dessicator over a dessicant (Drierite, Xenia, OH) during the day of analysis. Each sample was analyzed within one day and crystallized at various isothermal holding temperatures. Duplicate or triplicate measurements were made at each chosen temperature. The time for each run depended on type of syrup used, ratio of syrup to sucrose, moisture content of sample as well as temperature of crystallization.

The isothermal crystallization temperatures were chosen at 80°C/85°C, 90°C, 100°C, 110°C, for the 14% corn syrup samples and 90°C, 100°C and 110°C for the 22% corn syrup samples (Table 3.3). Samples of the highest syrup concentration were crystallized at 85°C instead of 80°C to avoid crystallization times of more than one hour. The applied DSC program was:

- 1) Hold for 1min at 0°C
- 2) Temperature ramped up from 0°C to target crystallization temperature ( $T_{xc}$ ) with heating rate of 400°C/min
- 3) Hold at crystallization temperature ( $T_{xc}$ ) for x min

26DE /42DE /62DE - 14% (w/w) syrup				
Cooking temp [°C]				
Holding temp [°C]	135	140	145	150
80	2-3x	2-3x	2-3x	N/A
85	N/A	N/A	N/A	2-3x
90	2-3x	2-3x	2-3x	2-3x
100	2-3x	2-3x	2-3x	2-3x
110	2-3x	2-3x	2-3x	2-3x

26DE /42DE /62DE - 22% (w/w) syrup			
Cooking temp [°C]			
Holding temp [°C]	140	145	150
90	2-3x	2-3x	2-3x
100	2-3x	2-3x	2-3x
110	2-3x	2-3x	2-3x

Table 3.4 Matrix plan of isothermal differential scanning calorimeter (DSC) experiments using three different types of syrup with varying dextrose equivalent (DE) cooked to 4 different temperatures.

In order to characterize the crystallization processes, isothermal DSC curves were analyzed for different crystallization parameters. A typical curve with corresponding analysis is shown in Figure 3.2:

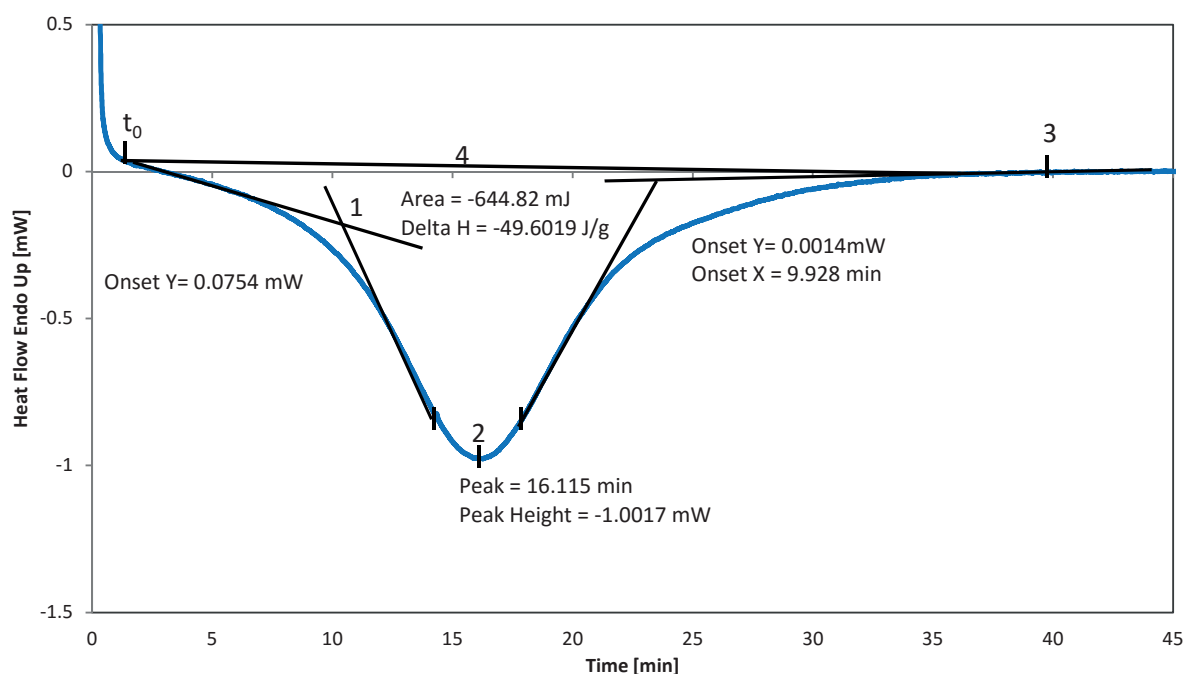


Figure 3.2 Pyris (v. 11) analysis of isothermal crystallization curve (42DE, 22% syrup, 3.8% moisture, 90°C) for the determination of onset, peak height, time until peak, time until end of crystallization and peak area.

Pyris software was used to analyze the isothermal scans and parameters describing the crystallization.

The parameters analyzed from each scan were:

- Onset time of crystallization,  $t_{on}$  [min], (if definable): This was determined using the Pyris Software. Two tangents were aligned to the baseline and the onset area of the peak. The point of intersection was defined as the onset of the curve. (1)
- Time until peak of exotherm,  $t_{peak}$  [min]: defined as  $\Delta t$  between induction time  $t_0$  and the peak of the crystallization exotherm. (2)
- Peak height,  $h_{peak}$  [mJ]: taken as the height of the exotherm peak to the basis. Equals the maximum amount of energy released during the crystallization process. (2)
- Time until end of crystallization,  $t_{end}$ : defined as time  $t$  when the trace comes back to the baseline. (3)
- Area [mJ]: Taking either  $t_0$  or the end of the induction period as time zero, the peaks were integrated with respect to time. (4)
- Enthalpy  $H$  [J/g]: The enthalpy was calculated with the Pyris software using both the integrated peaks as well as the sample weight. (4)

The crystallization peaks were integrated in respect to time. The degree of crystallinity [ $\Theta(t)$ ] was plotted against time for each peak,  $\Theta(t) = 0\%$  was the end of induction time or  $t_0$  and  $\Theta(t) = 100\%$  was the end of the exotherm, when the trace had returned to the baseline and crystallization was complete.

Analyzed data from the integrated peaks:

- Crystallization halftime values  $t_{1/2}$ : these halftime values were determined with integrated peaks, halftime  $t_{1/2}$  was defined as  $\Theta(t) = 50\%$  (4)
- Rate of crystallization  $1/t_{1/2}$ : reciprocal crystallization halftime values

### 3.7 Data Analysis

To determine significant differences in the data, an analysis of variance was conducted with ANOVA using a 95% confidence interval (SPSS v.20.0, IBM, New York, NY). This analysis was performed on data for moisture,  $T_g$ ,  $T_c$ , solubility temperature  $T_m$ , crystallization half times, and growth rate using a comparison of moisture content, crystallization temperature and formulation. SPSS was also used for non-linear regression using the Levenberg-Marquard method to analyze crystallization rate with the Arrhenius equation. Microsoft Excel (Version 2007 SP3, Microsoft Corp., Redmond, WA) was used to generate linear regression models for  $T_g$  and  $R_T$  as a function of molecular mass of and moisture content. The solver function of Microsoft excel was utilized to analyze data of crystallization rates with the WLF equation as well as the Hoffman-Lauritzen equation using nonlinear optimization.

## 4. Results and discussion

In this work, 6 different formulations of sugar glasses made with three different dextrose equivalent syrups (26DE, 42DE, 62DE) in two different ratios 14/86 and 22/78 w/w on a dry basis were investigated. Experiments were conducted non-isothermally to investigate glass transition temperature, temperature of maximum crystal growth and solubility temperature of the matrices. Subsequent isothermal crystallization experiments were performed to investigate crystallization kinetics of the amorphous sugar glasses, both using DSC. Due to the importance of moisture content, all samples were prepared to 5 different moisture levels, and the variation in moisture content between samples of same level was kept to a minimum. The focus of this work was to investigate variations in the effect of corn syrup of different DE on the crystallization of amorphous sucrose in amorphous sugar – corn syrup systems.

### 4.1 Moisture content

In order to achieve different moisture level, formulations containing 14% w/w corn syrup (26DE, 42DE, 62DE) were cooked to four different temperatures (135°, 140°, 145°, 150°C), while formulations with 22% w/w corn syrup (26DE, 42DE, 62DE) were cooked to three different cooking temperatures (140°, 145°, 150°C). The moisture levels for each type of corn syrup had to be similar, in order to obtain comparable data solely focusing on the effect of syrup on crystallization kinetics, thus minimizing unwanted effects based on variations in the water content of the samples.

To define the target moisture range for each cooking temperature, formulations containing 42DE syrup (14% and 22%) were cooked to each of the temperatures (135, 140, 145, 150°C) and the obtained moisture contents at each temperature were defined as the target moisture content.

These target moisture contents were partly reproducible, samples of any type of syrup cooked to the same temperature were roughly in the same moisture range, but showed variations up to 0.6 %H<sub>2</sub>O (14% syrup) and up to 1,5 %H<sub>2</sub>O (22% syrup). Due to the acceptance of only a narrow range of acceptable



moisture content ( $\pm 0.1\%$  of target moisture content), some samples were prepared up to septuplicates (n=7) in order to select samples that fit the target moisture content reasonably well. Samples not fitting the target moisture content were discarded.

It was likely, that the variation of the moisture content was caused by errors in the temperature measurement of the boiling mixture. Since the boiling matrix was not stirred, mixing was simply based on convection of the highly viscous matrix. This experimental setup caused different temperatures zones within the beaker as well as upward and downward currents of different temperatures during the cooking process. Even though the electronic thermometer was placed in the exact center of the beaker in order to ensure most accurate and reproducible measurement, it was inevitable that the measured temperature varied from the “real” temperature of the mixture.

The deviation from target values did not show any relationship to the type of syrup for formulations of 14% syrup, but are more likely to be randomly distributed.

Samples containing 22% syrup, however, showed a relationship between deviation from target moisture level (higher / lower) and the type of syrup used. At equal cooking temperatures, a relationship between type of syrup and deviation of moisture content was observable. This was most likely due to boiling point elevation  $T_{bp}$ .

$T_{bp}$  depends on the property of the solute and concentration according to Equation 4.1 (Eisenberg & Crothers, 1979):

$$\left[ \frac{\partial T_{bp}}{\partial c_B} \right]_p = \frac{RT_{bp}^2 v_a}{\Delta H_{vap} M_B} \quad (4.1)$$

where  $c_B$  is the concentration of the solute (polysaccharides),  $R$  is the universal gas constant,  $T_{bp}$  is the boiling temperature of the pure solvent (water),  $v_a$  is the partial molar volume of the mixture,  $\Delta H_{vap}$  is the heat of vaporization of the solvent, and  $M_B$  is the gram molecular weight of the solute.

Boiling point is inversely related to the molecular weight of the solute. Based on the colligative effect, corn syrups with different dextrose equivalent (DE) values have different boiling point elevation curves caused by their inherent differences in average molecular weight. High-DE corn syrups, such as 63 DE, contain a higher amount of low-molecular-weight saccharides, thus have a higher boiling point elevation than lower-DE corn syrups.

However, two corn syrups with the same DE may also have slightly different boiling point elevations if their saccharide profiles are significantly different (Hartel, Ergun, & Vogel, 2011). The average molecular weight of 62DE corn syrup ( $M_w = 295 \text{ g/mol}$ ) is lower than the molecular weight of sucrose, thus addition of 62DE syrup leads to an increase in the boiling point of the mixture whereas 42DE and 26DE corn syrups have a higher average molecular weight than sucrose resulting in a lower boiling point than sucrose.

Subsequently, when cooked to the same temperature, samples with a higher boiling point (62 DE) should have a higher level of moisture content and vice versa, samples with a lower boiling point should have a lower level of moisture content. This effect is expected to increase with the concentration of corn syrup in the mixture as the mole fraction of the corn syrups increases. As formulations with 42DE were chosen as the default sample for all cooking temperatures, it was expected that samples of the same cooking temperature containing 26DE would contain less water and samples containing 62DE would contain more water than samples prepared with 42DE corn syrup.

As mentioned previously, boiling point elevation and corresponding variation in moisture content were evidenced for samples made with 22% corn syrup. Samples cooked to the same temperature showed significantly different moisture contents ( $\pm 1.5\%$ ). This effect, however, was not observable for samples prepared with 14% corn syrup.

For this reason, cooking temperatures of 22% samples were adjusted to compensate for this effect.

Solutions containing 26DE corn syrup were heated to a slightly lower boiling temperature

( $T_x$  minus  $\sim 1.^\circ\text{C}$ ), whereas solutions containing 62DE were heated to a slightly higher boiling temperature ( $T_x$  plus  $\sim 1.5^\circ\text{C}$ ), 42DE syrup samples were heated to each of the target temperatures. Experimental moisture contents for samples of 14%/22% corn syrup are shown in Appendix A1. The data shows that the selected samples made with 14% corn syrup, had no significant difference ( $p < 0.04$ ) of moisture content between the three different types of corn syrup at any moisture level. The average moisture content ranged within a small variation of  $< 0.1\%$ . Within the group of samples of 22% syrup, selected samples showed the same high comparability between types of syrups at the same level of moisture content ( $\pm < 0.1\%$ ).

The comparability between both syrup concentrations (14% and 22%) was equally high ( $< 0.2\%$  moisture) and the difference not significant ( $p > 0.04$ ). Moisture contents of the amorphous sugar glasses are plotted as a function of cooking temperature in Figure 4.1:

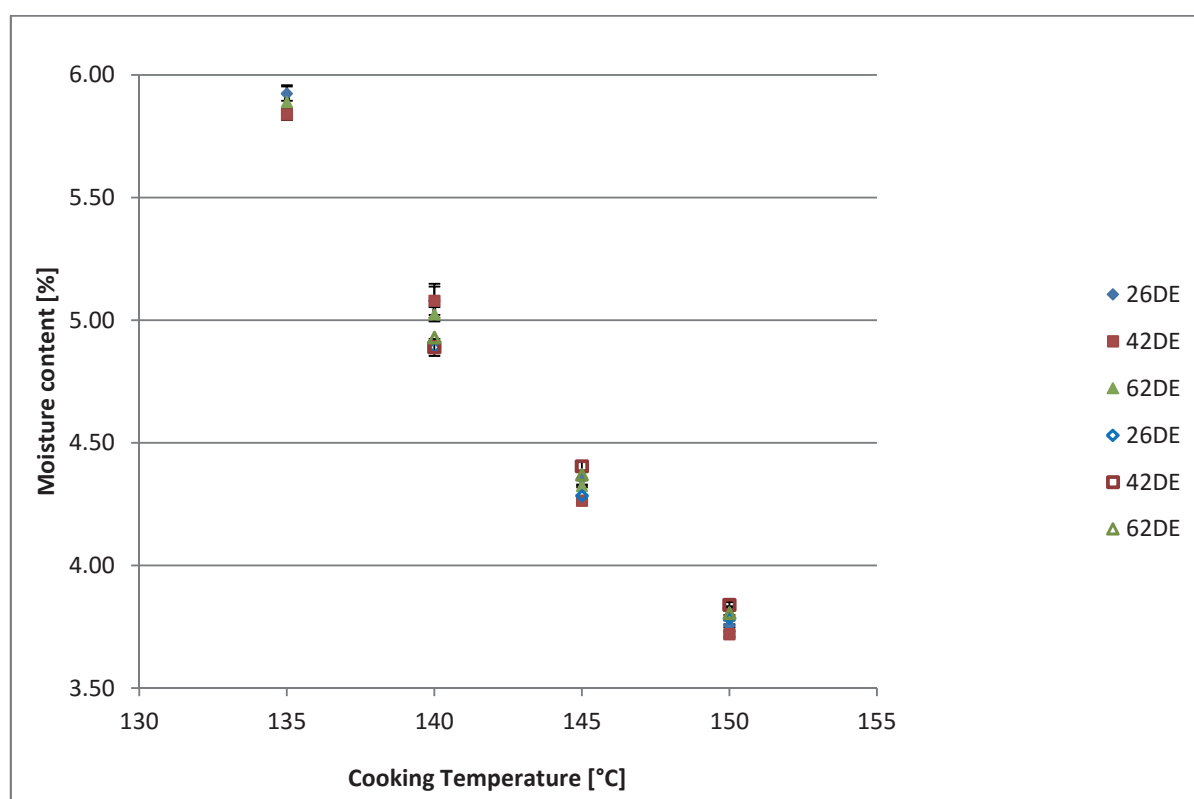


Figure 4.1 Moisture content (%) of sugar glasses made with sucrose and 14 & 22 % w/w corn syrup on a dry basis (26DE, 42DE, 62DE). Solid symbols represent samples containing 14% corn syrup, outlined symbols represent samples containing 22% corn syrup.

## 4.2 Non-isothermal DSC

### 4.2.1 Glass Transition Temperature

The glass transition temperature ( $T_g$ ) for the six formulations under 4 cooking temperatures was analyzed in measurement duplicates. Each sample was prepared in a replicate of two. The  $T_g$  of the sugar glasses containing 14%/22% corn syrup are listed in Appendix A2. Mean repeatability of the samples was found to be less than 1°C between replicates of each sample. The  $T_g$  values showed a low standard deviation and high comparability. Literature values for  $T_g$  of comparable formulations showed a higher variability at similar moisture contents (Chen, Nowakowski, Green, & Hartel, 2015; Levenson & Hartel, 2005). The differences in the variability of literature values might have been caused by a higher variation of the samples' moisture content, where a broader range of moisture content was accepted. The higher variability in the initial moisture content is likely to cause a higher variability in the  $T_g$  of the glasses.

All steps in the storage and preparation of the sugar glass samples of this work were performed in a controlled environment (saturated  $N_2$  environment, < 5% humidity) decreasing the likelihood of variability of the moisture contents. Experimental  $T_g$  values at similar moisture level and syrup concentration do not fully agree with values obtained for comparable systems (63DE, 14% syrup, 3.8% & 4.9% moisture) (Chen et al., 2015). Values of this work range roughly 3°C above literature values; however a direct comparison is not advisable, due to the usage of a different corn syrup in this work. As previously described, not only the DE of the syrup but the exact polysaccharide profile show a significant effect on  $T_g$ . Hence, two syrups of same DE but varying polysaccharide profile are likely to cause different  $T_g$  values, explaining different values under comparable experimental conditions.

#### 4.2.1.1 Effect of Moisture Content

Figure 4.2 shows  $T_g$  for the formulations with 14% corn syrup plotted as a function of moisture content.

The error bars represent the combined standard deviation of means for preparation ( $n=2$ ) and analytical replicates ( $n=2$ ).

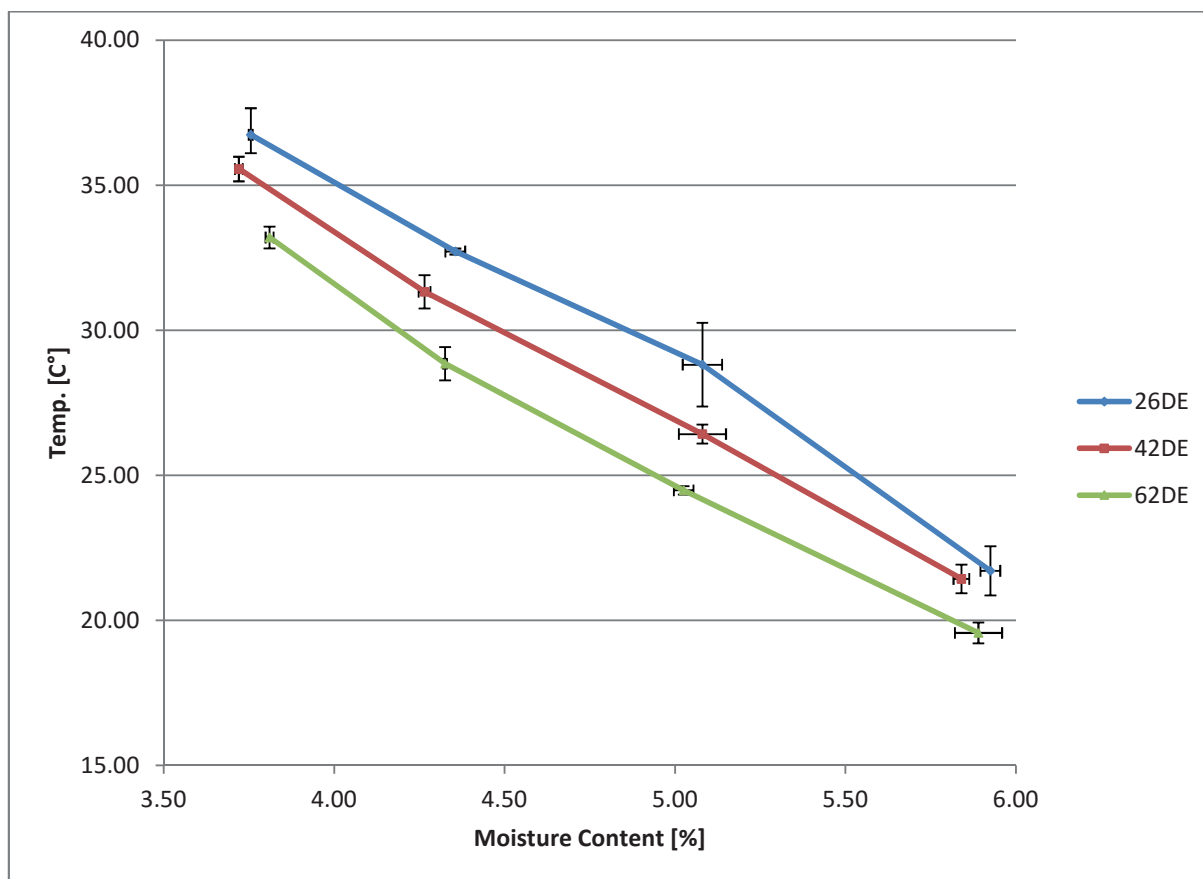


Figure 4.2 Glass transition temperature ( $T_g$ ) for amorphous sugar matrices composed of 14% corn syrup (26DE, 42DE, or 62DE).

Below,  $T_g$  of samples containing 22% syrup are plotted as a function of moisture content (Figure 4.3.).

The error bars represent the standard deviation for the two preparation replicates, each analyzed in measurement duplicates.

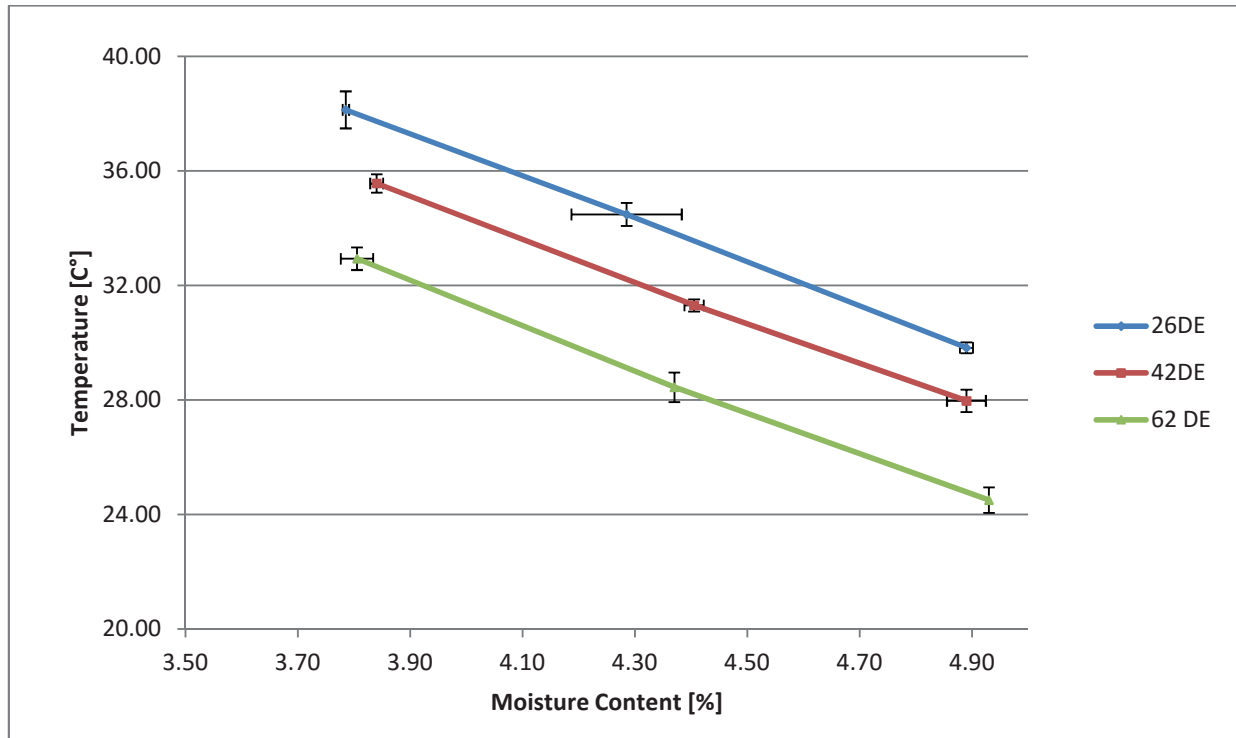


Figure 4.3 Glass transition temperature ( $T_g$ ) for amorphous sugar matrices composed of 22% corn syrup (26DE, 42DE, or 62DE) as a function of moisture content.

Both plots (Figure 4.2 and 4.3) show the inverse correlation between the water content of the sample and the  $T_g$ .  $T_g$  decreased significantly with increasing moisture content of the samples ( $p < 0.05$ ). Samples containing 22% corn syrup (Figure 4.3) showed an almost linear relationship between the moisture contents and  $T_g$  for all three formulations, and followed the prediction of water as plasticizer, hence a parameter affecting  $T_g$  (Hartel, 2001).

The strong effect of water present in the sample on molecular mobility and  $T_g$  was observable at both levels of syrup. Taking experimental values into account, approximation (4.2) could be established:

$$\frac{\partial T_g}{\partial u} \sim -7.5 \quad (4.2)$$

where,  $T_g$  is the change in the glass transition temperature [°C], and  $u$  is the gravimetric water content.

An increase in the moisture content by 1% altered the samples'  $T_g$  by roughly 7.5°C, illustrating the strong influence of water on the  $T_g$  in amorphous sugar glasses of this type.

#### 4.2.1.2 Effect of Composition

##### *Effect of Dextrose Equivalent*

Figure 4.3 and 4.4 show the inverse relationship between DE ( $M_w$ ) and  $T_g$ .  $T_g$  increased significantly with decreasing DE of the syrup ( $p < 0.05$ ). Only at the moisture level of 5.9% did values for 42DE and 26DE formulations fall below the significance level of 95% ( $p < 0.05$ ). The difference of  $T_g$  between the types of syrup came to roughly  $\Delta 3^\circ\text{C}$  at both levels of corn syrup and remained relatively constant over the experimental range of moisture content.

If approximated as a binary system, the equation by Gordon and Taylor (Equation 2.2) could be applied, stating that the  $T_g$  of the glass is a function of the MW of each of the components. To investigate if there is a significant relationship between average MW of the experimental samples and the  $T_g$ , glass transition temperatures were plotted over average MW of the glass. In order to determine the average molecular mass of the glasses,  $MW_n$  values of the syrups (Table 4.1) (as supplied by ADM) were used to calculate the average molecular mass of the glasses on a dry solid basis:

Average molecular weight [g/mol]	Sucrose	26DE	42DE	62DE
100%	342	790	481	298
14% / 86 % ratio	-	405	361	335
22% / 78 % ratio	-	440	373	332

Table 4.1 Average molecular weight (dry) of experimental formulations with 14% and 22% corn syrup w/w on a dry basis.

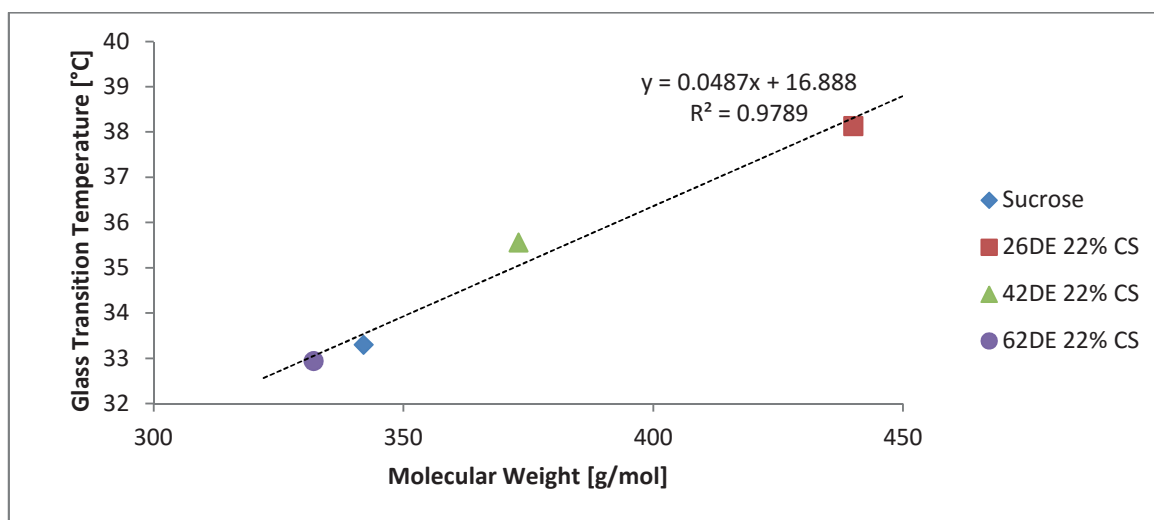


Figure 4.4 Glass transition temperature of sugar glasses with 22% (w/w on a dry basis) corn syrup (CS) (26DE, 42DE, 62DE) at ~3.8% moisture content. Data for pure sucrose obtained from Sun et al. (3.66% moisture content) (1996).

Figure 4.4 shows a fairly good linear fit ( $R^2 = 0.9789$ ) of experimental glass transition temperature as a function of molecular weight for samples of 22% corn syrup and 3.8% moisture content. This result is in agreement with the Gordon & Taylor equation and literature (Gabarra & Hartel, 1998; Roos & Karel, 1991b). Gabarra & Hartel (1998) found a linear relationship between the  $T_g$  of sucrose–corn syrup mixtures and the average molecular weight of the corn syrup components at moisture levels <1%.

#### *Effect of Corn Syrup Ratio*

According to Herrington & Branfield (1984), sugar glasses containing 14-30% DE corn syrup showed negligible differences in glass transition temperatures between samples. This is in contradiction to the findings of Gabarra & Hartel (1998). Nowakowski & Hartel (2002) studied the effect of different DE corn syrup (43DE and 43 DE High maltose) on the  $T_g$  of amorphous sugar glasses, where the effect of increasing  $T_g$  due to higher ratios of corn syrup was observable only over a small range of moisture content.

In order to compare  $T_g$  values of different ratios (14% to 22% ) of syrup (26DE, 42DE), experimental  $T_g$  values were plotted as a function of moisture content (Figure 4.5):



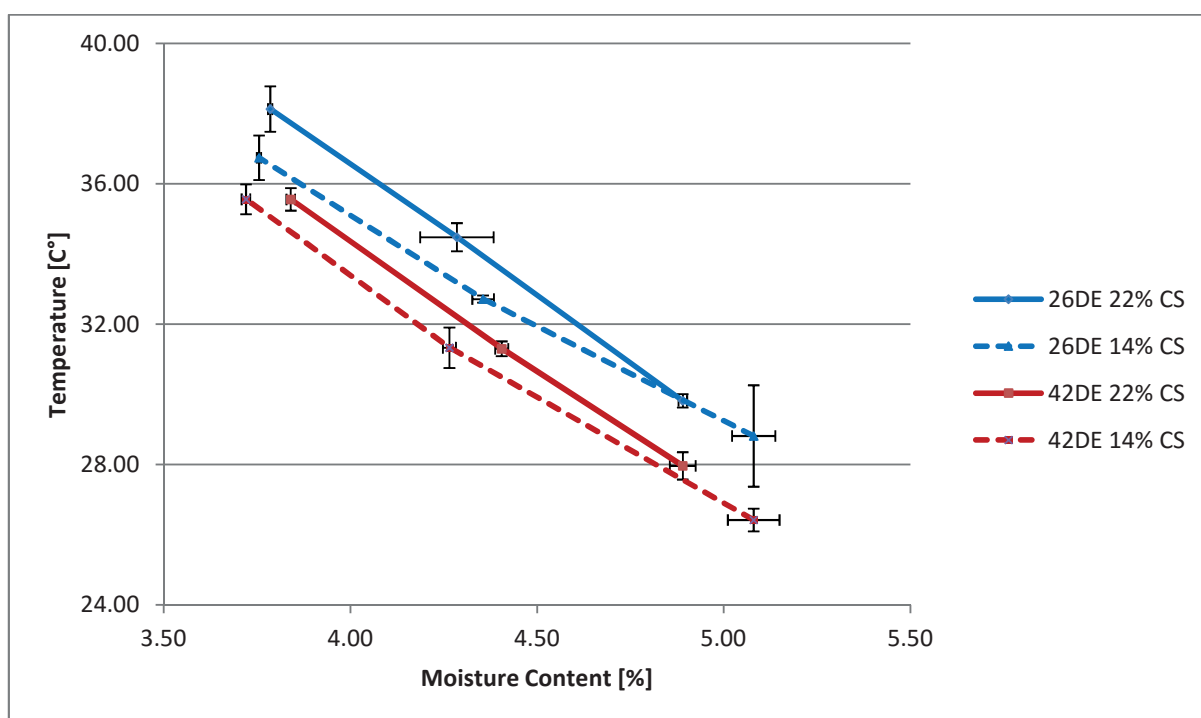


Figure 4.5 Glass transition temperature ( $T_g$ ) for amorphous sugar matrices as a function of moisture content for formulations containing 14 and 22% (w/w dry basis) corn syrup (CS) (26DE, 42DE).

Samples of 14% and 22% corn syrup show a small variation in their water contents, which should be considered in this comparison. However, formulations of 26DE show a significant difference of  $T_g$  between two levels of corn syrup over the observed range of moisture content ( $p > 0.05$ ). The  $T_g$  increased with MW of the matrix, thus samples of higher ratio of syrup (22%, 42DE and 62DE) showed higher glass transition temperature than the samples of lower syrup ratio (14%).

Though a difference in  $T_g$  between 14% and 22% corn syrup samples is obvious, significance is only given ( $p > 0.05$ ) at the lowest moisture content. This is in agreement with literature where a difference in  $T_g$  in respect to CS MW was more distinct at low moisture contents ( $< 5\%$ ) (Gabarra & Hartel, 1998; Nowakowski & Hartel, 2002). Samples containing 62DE syrup (not shown) showed no alteration in  $T_g$  due to the negligible difference of MW between 14% and 22% syrup formulations ( $\Delta 3$  g/mol) (Table 4.1).

As mentioned previously, alteration of  $T_g$  in those systems is a function of the MW of the corn syrup used. It follows that if increased by the same w/w ratio, syrup of higher MW should show a stronger

effect on  $T_g$ . This effect can be seen in Figure 4.5, where the same weight increase of syrup between 26DE and 42DE syrup, caused bigger increase in  $T_g$  for formulations containing 26DE corn syrup.

## **4.2.2 Crystallization Temperature**

The temperature of the maximum rate of crystallization ( $T_c$ ) for formulations of 14% or 22% corn syrup (26DE, 42DE, 62DE) at 4 different moisture levels was analyzed non-isothermally using DSC. Each sample was prepared in duplicate. The obtained values for  $T_c$  and the ratio  $T_c - T_g / T_m - T_g$  are shown in Appendix A3.

### **4.2.2.1 Effect of Moisture Content**

The temperature of maximum crystallization rate derived from non-isothermal DSC experiments increased significantly with decreasing water content of the samples ( $p < 0.05$ ). Figure 4.6 and data in Appendix A3 show that the temperature of maximum crystal growth (14% syrup) correlated in an almost inverse linear manner to the water content of the samples. Only 22% corn syrup of 26DE showed an effect of water content below the statistical significance ( $p > 0.05$ ). Nonetheless, temperature of maximum crystal growth decreased with increasing water content in every formulation .

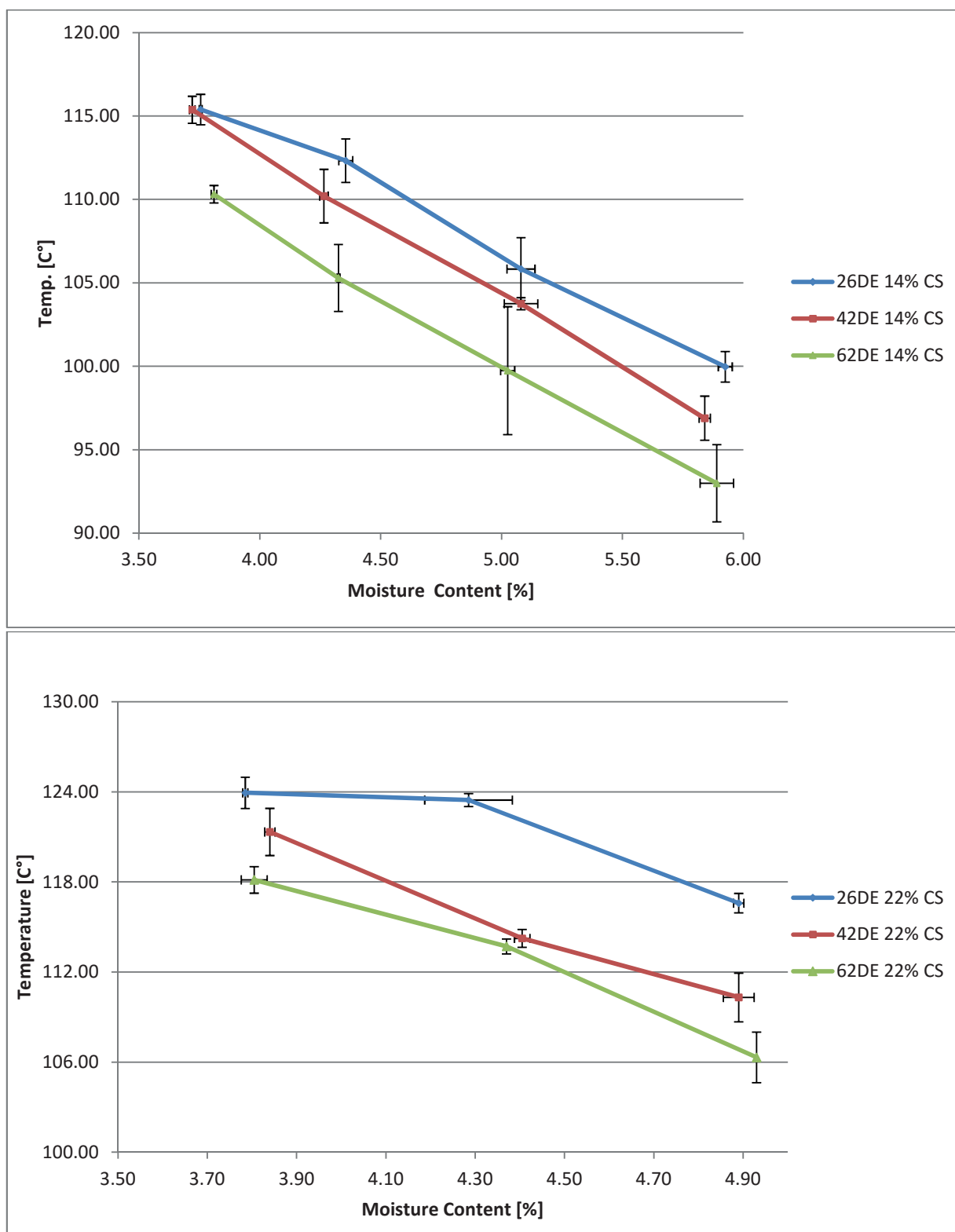


Figure 4.6 Temperature of maximum crystallization rate ( $T_c$ ) of sugar glasses composed of 14%/22% corn syrup (CS) (26DE, 42DE, 62DE) as a function of moisture content.

The observed inverse correlation between  $T_c$  and water content of the sample can be explained by the relationship of  $T_c$  to  $T_g$  and  $T_m$  (Saleki-Gerhardt & Zografi, 1994). The correlation between  $T_c$ ,  $T_g$  and  $T_m$  is given in Equation 4.3:

$$T_c = k (T_m - T_g) + T_g \quad (4.3)$$

Where,  $T_c$  is the temperature of maximum crystal growth,  $T_g$  is the glass transition temperature and  $T_m$  is the solubility temperature,  $k$  is a constant. The constant  $k$  represents the ratio between  $T_g$  and  $T_m$  at which the temperature of maximum growth is found. With increasing water content the plasticizing effect of water increases, thus molecular mobility increases, resulting in a decrease of the glass transition temperature (Hartel, 2001) (Equation 4.1). Variations of  $T_g$  simultaneously affect  $T_c$  according to the relationship shown in Equation 4.3.

Saleki-Gerhardt & Zografi (1994) found  $k$  to be 0.5, at the midpoint between  $T_g$  and  $T_m$  for amorphous sucrose at different moisture levels (0%- 3.1%). Kedward et al. (1998) found this ratio to be between 0.5 and 0.53 for freeze dried sucrose of constant moisture content (0.92 %).

Experiments in this work showed that this constant ranges from 0.57-0.63 for formulations with 14% corn syrup w/w on a dry basis and 0.66-0.73 for samples containing 22% corn syrup w/w dry. This circumstance is discussed later.

#### **4.2.2.2 Effect of Composition**

##### *Effect of Dextrose Equivalent:*

The experimental data showed a significant compositional effect on the temperature of maximum crystallization ( $p < 0.05$ ). Experimental  $T_c$  values increased with decreasing DE of the syrup and increasing molecular weight of the glass.

At the lowest moisture level, however, no significant compositional effect on the temperature of maximum crystallization rate was observed.

Alterations in  $T_c$  correlate to both  $T_m$  and  $T_g$ . The increase in the molecular mass of the system, hence the increase in DP or decrease in DE of the syrup causes an increase in the glass transition temperature (Roos, 1995). As  $T_c$  relates to  $T_g$  (Equation 4.3),  $T_c$  is similarly affected by this parameter.

#### *Effect of Corn Syrup Ratio*

The same effect applies when the ratio of syrup is increased from 14% to 22% w/w. The  $T_c$  increased significantly ( $\Delta T_c \sim 4\text{-}11^\circ\text{C}$ ) due to the increased amount of corn syrup (26DE, 42DE, 62DE) correlating to variation of the  $T_g$  as a function of MW. This relationship however, does not apply to the  $T_g$  values of 62DE syrup samples. The glass transition temperature of 62DE syrup samples did not increase significantly with increased amount of syrup (from 14% to 22%) due to the negligible change in the MW of the glass. However, the temperature of maximum crystallization significantly alters with increased amount of 62DE syrup even though the average molecular weight of the sample did not change substantially. This might indicate that in certain cases,  $T_c$  in amorphous sugar glasses might not be solely based on (i) the glass transition temperature or (ii) the overall molecular weight of the system. Other factors such as very weak, relatively weak or strong specific interactions of these systems were suggested for such systems (Gabarra & Hartel, 1998; Lu & Weiss, 1992; Saleki-Gerhardt & Zografi, 1994) and are discussed further in Section 5.1.

### **4.2.3 Solubility Temperature**

The solubility temperature  $T_m$ , also called saturation temperature, is the temperature at which the solution reaches the saturation concentration. Samples were prepared and evaluated in duplicates for each cooking temperature and formulation, with results listed in Appendix A4.

#### **4.2.3.1 Effect of Moisture Content**

Experimental results indicate an almost linear correlation between water content of the samples and solubility temperature (Fig. 4.7). Solubility temperature increases significantly ( $p > 0.05$ ) as water content decreases. The obtained results agreed well with values found in literature (Bubník, Kadlec, Urban, & Bruhns, 1995; Chen et al., 2015; Woodroof, Junk, & Pancoast, 1973).

#### **4.2.3.2 Effects of Composition**

##### *Effect of Ratio of Corn Syrup*

The increase in the ratio of corn syrup caused a significant ( $p > 0.05$ ) decrease in solubility temperature (Figure 4.7) due to the competition between sucrose and corn syrup components for hydrogen bonding sites with water molecules (Mullin, 2001). The results are in agreement with published data (Tjuradi & Hartel, 1995) and (Chen et al., 2015).

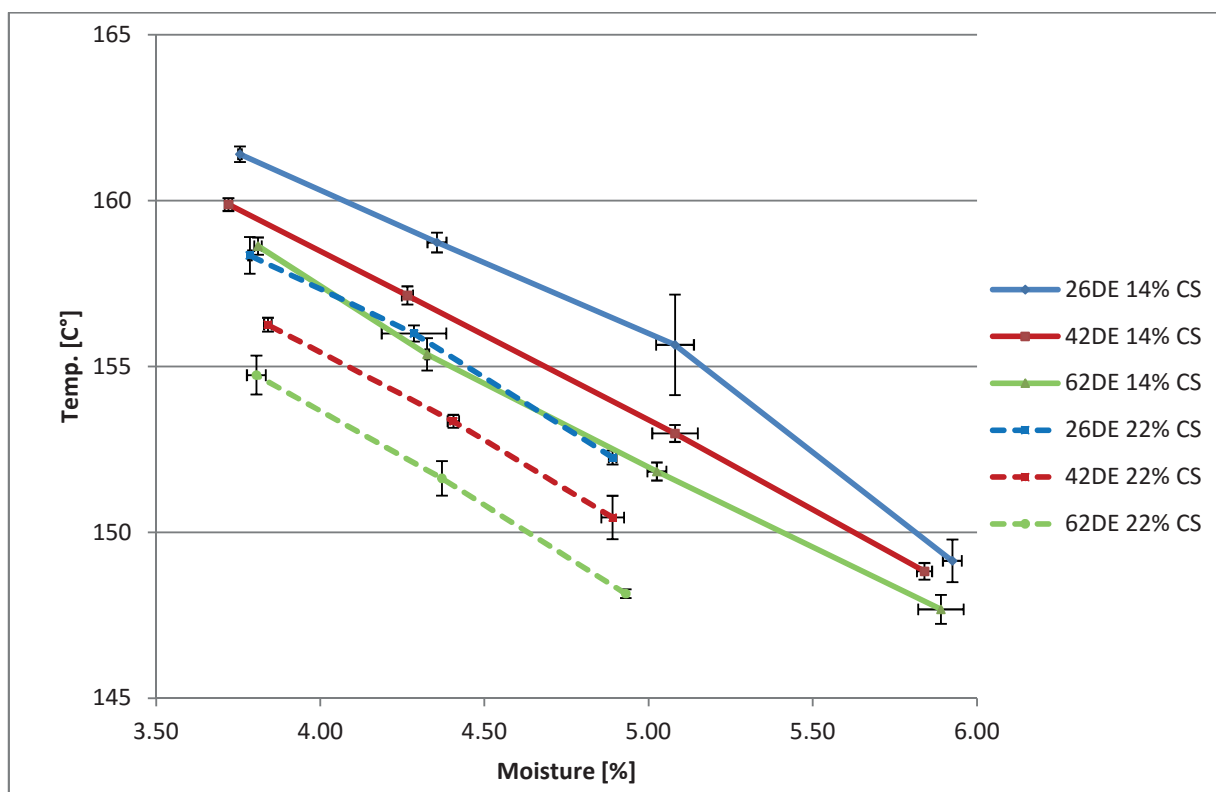


Figure 4.7 Solubility temperature ( $T_m$ ) as a function of moisture content for sucrose glasses composed of 14% and 22% (w/w on dry basis) corn syrup (CS) (26DE, 42DE, 62DE).

#### *Effect of Dextrose Equivalent:*

In general, the decrease in dextrose equivalent of syrup caused an increase in solubility temperature ( $p < 0.05$ ). Syrups were added on a weight basis, hence syrup with high DE and low DP added a higher number of competing molecules to the matrix. The higher number of molecules showed the same effect on sucrose solubility as an increase in syrup (from 14% to 22%) due to the increased amount of molecules competing with sucrose for hydrogen bonding sites, resulting in a decrease of sucrose solubility in the formulation. These results agree well with findings in literature (Tjuradi & Hartel, 1995), where the same effect was found for 42DE syrup fractions of different DP.

#### 4.2.4 Relationship between Temperature of Maximum Crystallization Rate $T_c$ , Glass Transition Temperature $T_g$ and Solubility Temperature $T_m$

The relationship between  $T_g$ ,  $T_c$  and  $T_m$  for amorphous/crystalline systems has been described previously (Okui, 1990; Saleki-Gerhardt & Zografi, 1994; Kedward et al., 1998).

The relationship of  $T_c$  to  $T_g$  and  $T_m$  was previously expressed as the constant  $k$  (Eq. 4.3). The expression as ratio  $R_{Tc}$  is used in this section:

$$R_{Tc} = \frac{T_{(c)} - T_g}{T_m - T_g} \quad (4.4)$$

Saleki-Gerhardt & Zografi found the ratio  $R_{Tc}$  to be 0.5, with  $T_c$  located at the midpoint between  $T_g$  and  $T_m$  for amorphous sucrose at different moisture levels (0%- 3.1%) whereas Kedward et al. (1998) found  $R_{Tc}$  values of 0.5 to 0.55 for freeze dried sucrose at a constant moisture content (0.92 %). These values for  $R_{Tc}$  at the midpoint between  $T_g$  and  $T_m$  were obtained from pure amorphous sucrose or lactose. However, values for combined systems of di, tri, or polysaccharides and amorphous sucrose, showed  $R_{Tc}$  to be much higher than 0.5 or the midpoint between  $T_g$  and  $T_m$  (Gabarra & Hartel, 1998; Saleki-Gerhardt & Zografi, 1994).

The ratio of  $T_c$  to  $T_g$  &  $T_m$  for the experimental sugar glasses are listed in Appendix A4 and are plotted for different formulations as a function of moisture content in Figure 4.8.



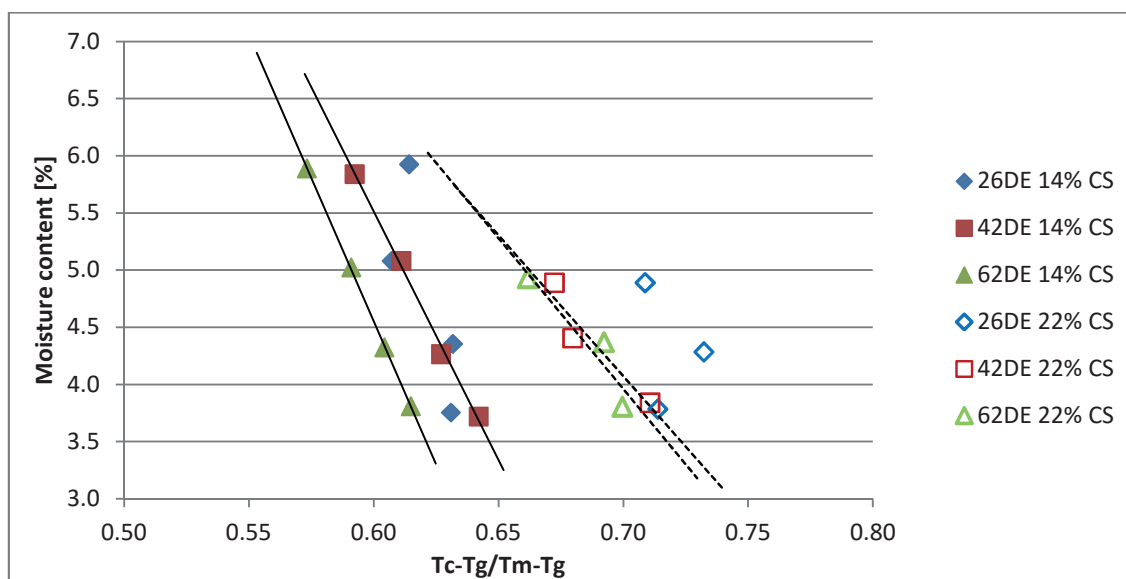


Figure 4.8 Ratio of temperature of maximum crystal growth  $T_c$  vs.  $(T_m/T_g)$  as function of moisture content [%] at either 14%/22% (w/w on dry basis) corn syrup (CS) level. Solid symbols represent samples containing 14% corn syrup, outlined symbols represent samples containing 22% corn syrup.

Any deviation in the values for  $R_{T_c}$  from 0.5, the midpoint between  $T_g$  and  $T_m$ , might indicate that  $T_c$  is not only related to  $T_g$  but other factors or parameters beyond molecular mobility and free volume (Saleki-Gerhardt & Zografi, 1994).

#### *Effect of Dextrose Equivalent:*

A distinct differential between  $R_{T_c}$  values for formulations of 62DE and 42DE syrup at a 14% syrup level was observable, indicating that 42DE samples need higher temperatures to crystallize at maximum rate, although variations of  $T_g$  between the compared types of syrups are relativized by the term  $(T_m - T_g)$ . The assumption follows that other effects beyond  $T_g$  cause differences in the inhibitory effect of the types of syrup on the crystallization of sucrose. However, no significant increase of  $R_{T_c}$  with alteration of DE from 42DE to 26DE was apparent. Samples with higher level of corn syrup did not show a significant difference of  $R_{T_c}$  between the types of DE either.

### *Effect of Corn Syrup Ratio*

$R_{T_c}$  increased significantly when the corn syrup level was increased from 14% to 22%, indicating that with higher ratio of CS polysaccharides, the temperature of maximum crystal growth shifted to higher temperatures and closer to  $T_m$ .

### *Effect of moisture content:*

$R_{T_c}$  decreased with increasing water content of the samples (42DE, 62DE 14% and 22% corn syrup). These observations correspond to results from literature (Kedward et al., 2000). The alteration in  $R_{T_c}$  is explained by changes in  $T_m$  and  $T_g$ , which in turn are explained by differences in moisture content. The ratio of  $T_m - T_g$  in this work stays mostly constant, while the value for  $T_c - T_g$  increases with decreasing moisture content. This trend seemed to be caused by the stronger effect of water on values of  $T_c$  than for  $T_g$  and supports the hypothesis that effects beyond  $T_g$  have an influence on  $T_c$ . Those effects could show higher alteration with respect to water content of the sample. A significant effect of water on the  $R_{T_c}$  of 26DE corn syrup samples was indefinite.

## **4.3 Isothermal DSC**

All isothermal DSC experiments were conducted using the same samples as described for the non-isothermal DSC experiments. Each sample was held at an initial temperature low enough to ensure no crystallization and then ramped up quickly (400°C/min) to the final isothermal holding temperature (80, 85, 90, 100, 110°C). The sample was held until the crystallization was completed and the trace came back to the baseline. During this time the crystallization of each sample was observed.

### 4.3.1 Crystallization from the Amorphous State

Previous experiments on growth rate and isothermal crystallization kinetics have been conducted using DSC to investigate crystallization kinetics of various amorphous disaccharides (Lactose, Sucrose) (Kedward et al., 1998; Saleki-Gerhardt & Zografi, 1994). In these experiments, the materials all exhibited a maximum growth rate with increasing holding temperatures, after which the rate of crystallization decreased.

Above 110°C holding temperature, some of the samples of this work crystallized so fast, that the remaining water boiled readily, thus making the analysis of the sample impracticable. It was not possible to reach higher crystallization temperatures without severe distortions on the thermograms and grossly incorrect analysis.

As a result, 110°C was chosen as the upper temperature limit for isothermal DSC experiments in combination with standard aluminum pans. Due to the experimental limitation, it was not possible to exceed the temperature of maximum crystallization rate. Subsequently, the corresponding crystallization rates unlike in the literature experiments, continually increased with increasing temperature over the experimental temperature range.

For the study of crystallization kinetics, the samples were held at 80, 85, 90, 100, 110°C. The temperature range was chosen due to previous work on comparable systems (Chen et al., 2015; Levenson & Hartel, 2005). Samples with the lowest water content crystallized the slowest and would have caused very long analytical runs on the DSC if crystallized at 80°C; hence, 85°C was chosen as the lowest temperature for crystallization.

### 4.3.2 Parameters of Isothermal Crystallization

Every isothermal run was analyzed using the Pyris software (Pyris 11, Perkin Elmer Corporation, Wilton, CT) to obtain results from the isothermal crystallization scans. Beside the crucial parameter, crystallization halftime  $t_{1/2}$  and its reciprocal value crystallization rate  $1/t_{1/2}$  numerous other values and parameters were determined from the isothermal scans (Section 3.6). However, due to the complexity of such an amount of data, crystallization halftime values were used for further analysis of the isothermal crystallization kinetics.

For all isothermal scans in this work, onset of crystallization was defined when the trace left the baseline. Correspondent to that was the end of crystallization defined when the trace came back to the baseline. During the analysis of isothermal DSC data, it was necessary to consider the transient response of the system. The final isothermal holding temperature required considerable time to reach equilibrium when it was ramped from the initial temperature at a rate of 400°C/min. This time period (response time or time lag) is different from the induction period of the sample. A fully crystallized sample was analyzed using the same temperature program at each temperature to define the response time. This time was defined when the trace decreases from the end of the heating step and forms a flat baseline. This time was usually around 20 seconds and defined as  $t_0$  (Appendix A6).

Most of the samples started to crystallize quickly at the chosen temperatures so that no distinct onset of crystallization could be defined. The induction period could be so short that crystallization might have started before thermal equilibrium was reached, resulting in an inaccuracy in the initial data points.

Samples with higher concentration and lower crystallization temperatures crystallized slower.

Correspondent traces are shown in Figure 4.9. In the scans of slowly crystallizing samples a certain lag was observed before the exotherm started, albeit the transition from the baseline to the peak was not distinct and hard to define. Further description is presented in Section 4.3.2.

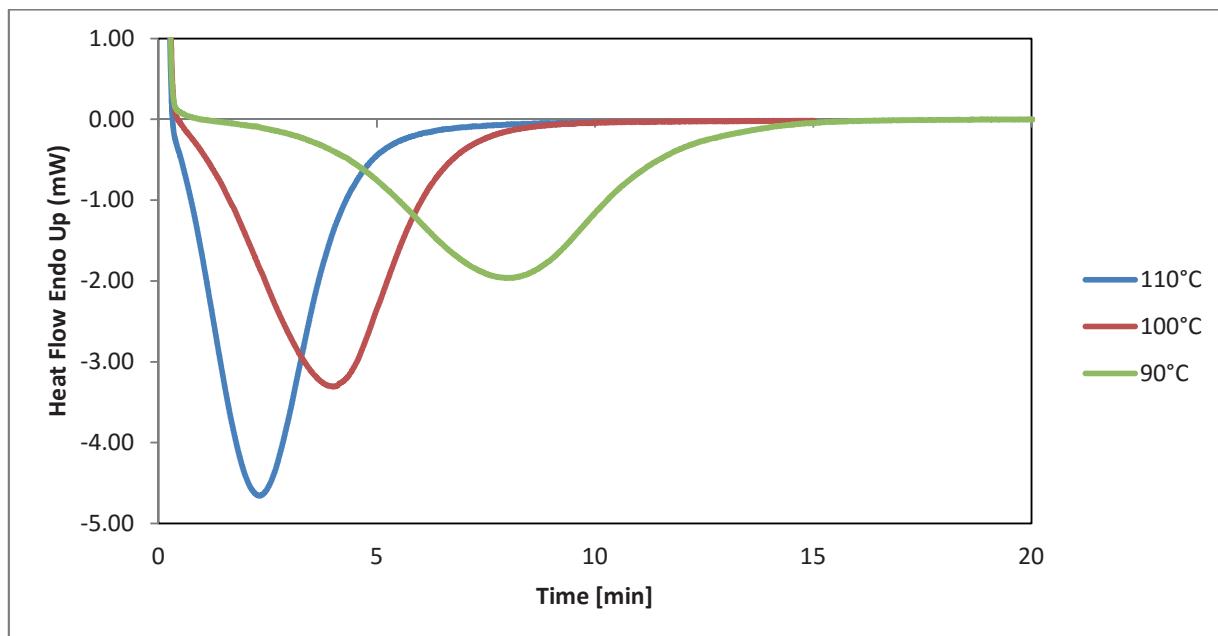


Figure 4.9: Combined scans of 42DE samples with the same moisture content (4.3 %) crystallized at 3 different crystallization temperatures (110°, 100°, 90°C).

### 4.3.2 Experimental Difficulties

As mentioned in Section 4.3.1, some of the samples differ from classic isothermal curves in terms of baseline slope and onset of crystallization. Samples in literature of pure sucrose or lactose show a flat baseline and a distinct onset of the crystallization peak (Kedward et al., 1998). Most of the samples started to crystallize quickly at the chosen temperatures, thus no distinct onset of crystallization could be defined. Samples with higher concentration and at lower crystallization temperatures crystallized more slowly. Here, an onset-like behavior was observed. The onset is usually defined as the most probable time from the beginning of isothermal crystallization to the point at which a stable nucleus starts to grow (Kedward et al., 1998). All scans with an visible onset-like behavior showed a slight negative slope of the baseline before the onset of the exothermic peak, as a result the baseline was not totally flat before the crystallization exotherm started. Often the onset trace transitioned into the crystallization peak in an

uncertain manner. The cause of the negative slope of the baseline remains unclear, a typical scan of such behavior is shown in Figure 4.10.

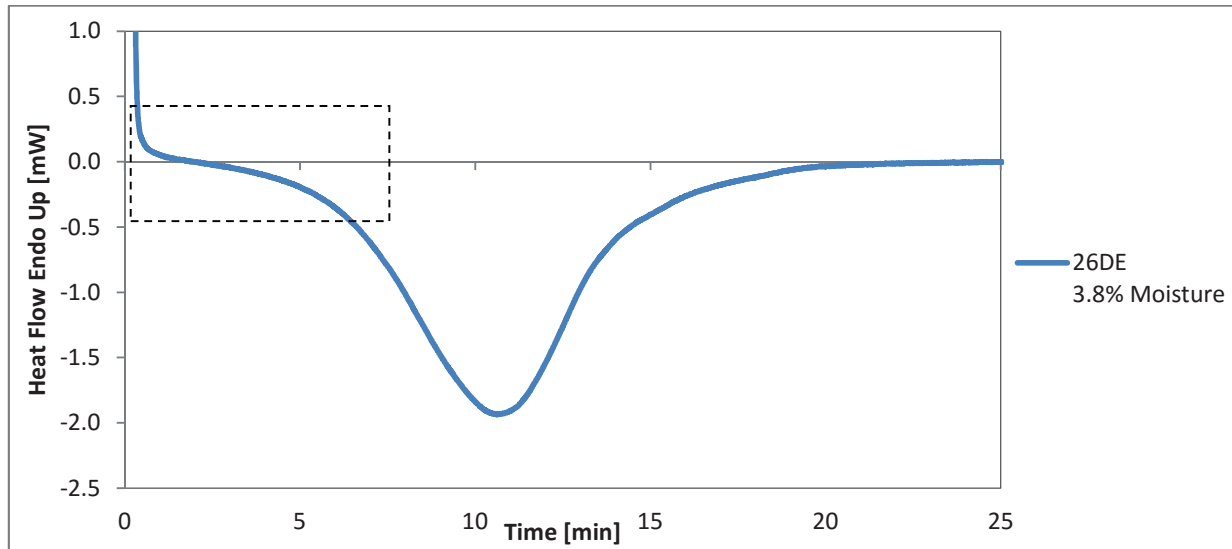


Figure 4.10: Isothermal DSC trace of amorphous sugar glass containing 26DE syrup and 3.8% moisture at 90°C over 20 minutes. The indistinct onset can be seen between min. 1 and min. 8 (dotted rectangle).

There has been a long debate about the form of the experimental baseline before, during and after isothermal crystallization when recorded with a DSC, and several procedures have been proposed in order to establish it correctly. Hay (1971) proposed the use of the projection of the horizontal line from a point after the crystallization exotherm has finished to a point at the beginning of the DSC trace just at  $t_0$ . Scott and Ramachandrarao (1977) adopted the drawing of a straight line between the local maxima/minima before and after the exothermic curve. This local maximum in the scans equals  $t_0$  as obtained from the run with a fully crystallized sample. Therefore the proposition of Scott and Ramachandrarao was adopted and response time  $t_0$  was used as  $\Theta(t) = 0\%$  for the integration of all scans.

### 4.3.3 Crystallization Kinetics (Crystallization Half Times)

Based on both the high amount of data derived from isothermal analysis, and the usability to investigate the relationship between DE and crystallization, only isothermal crystallization halftimes  $t_{1/2}$  and their reciprocal values, crystallization rates  $1/t_{1/2}$  or are discussed in the following sections.

Peaks of isothermal crystallization were integrated with respect to time, and the degree of crystallinity  $[\Theta(t)]$  was plotted against time for each peak.  $\Theta(t) = 0\%$  was the end of induction time or  $t_0$  and  $\Theta(t) = 100\%$  was the end of the exotherm, when the trace had returned to the baseline and crystallization was complete. This data was used to obtain crystallization halftime  $t_{1/2}$ , defined as the time  $t$  when 50% of the crystallizable amorphous sucrose had crystallized.

A typical isothermal DSC trace and the related integrated trace are shown in Figure 4.11. Corresponding experimental crystallization halftimes are shown in Appendix A5.

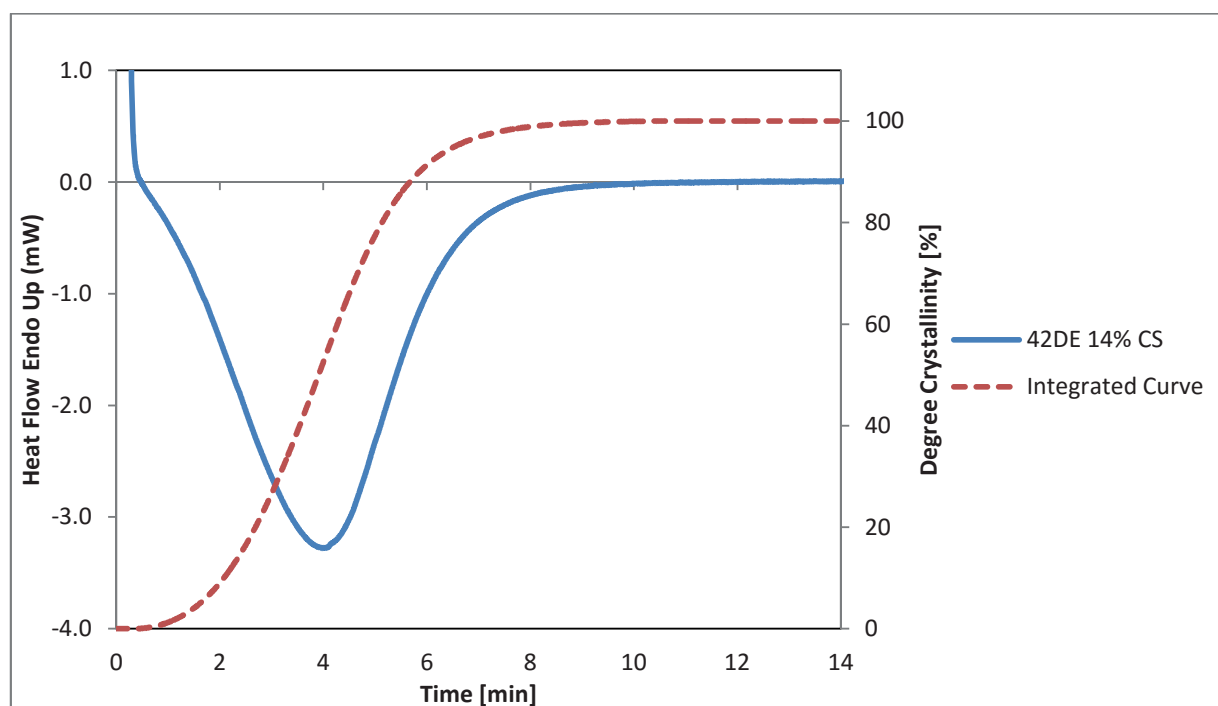


Figure 4.11 Isothermal DSC trace for amorphous sugar glass containing 42DE corn syrup (CS) and 3.8% moisture, crystallized at 100°C (solid line). The integrated isothermal DSC trace is shown by the dotted line.

As previously described, the temperature of 110°C was the limiting upper temperature since the crystallization of some samples were so fast that water from the matrix was separated and started to boil. This effect could be seen in the scans by a jagged trace, especially after the maximum growth was exceeded. The effect increased with increasing holding temperature, thus 110°C was the highest holding temperature possible in this work.



#### 4.3.3.1 Effect of Crystallization Temperature

Experimental data indicate that the holding temperature has a significant ( $p > 0.05$ ) influence on the crystallization halftime. However, samples of high moisture content failed to show a statistically significant effect of holding temperature on the crystallization halftime ( $p < 0.05$ ). This could be explained by the plasticizing effect of water, which, at higher levels, mitigated the inhibitory forces acting against the crystallization, thus making the system less sensitive to temperature. To underline the effects of crystallization temperature, crystallization halftimes were plotted as a function of crystallization temperature (Figure 4.12; 4.13).

In general, crystallization halftime continuously decreased with increasing crystallization temperature. However, a minimum or crystallization halftime or a maximum crystallization rate could not be determined as the experimental maximum crystallization temperature ( $110^{\circ}\text{C}$ ) did not exceed the temperature of maximum crystallization. These results correspond well with literature (Chen et al., 2015) for samples with same level of syrup (42DE ; 14% and 22% w/w) and comparable moisture contents ( 3.77%; 4.63%). The initial increase in temperature above  $T_g$  resulted in increasing molecular mobility, thus increasing the growth rate and decreasing crystallization halftimes. After a temperature of maximum crystallization rate is exceeded, crystallization rates decrease due to the increase in solubility of the solvent caused by holding temperatures closer to the solubility temperature  $T_m$ .

The overall relationship between holding temperature and crystallization rate found in these experiments corresponded well with literature (Chen et al., 2015; Gabarra & Hartel, 1998; Kedward et al., 1998) and showed that temperature was very influential on crystal growth in these systems.

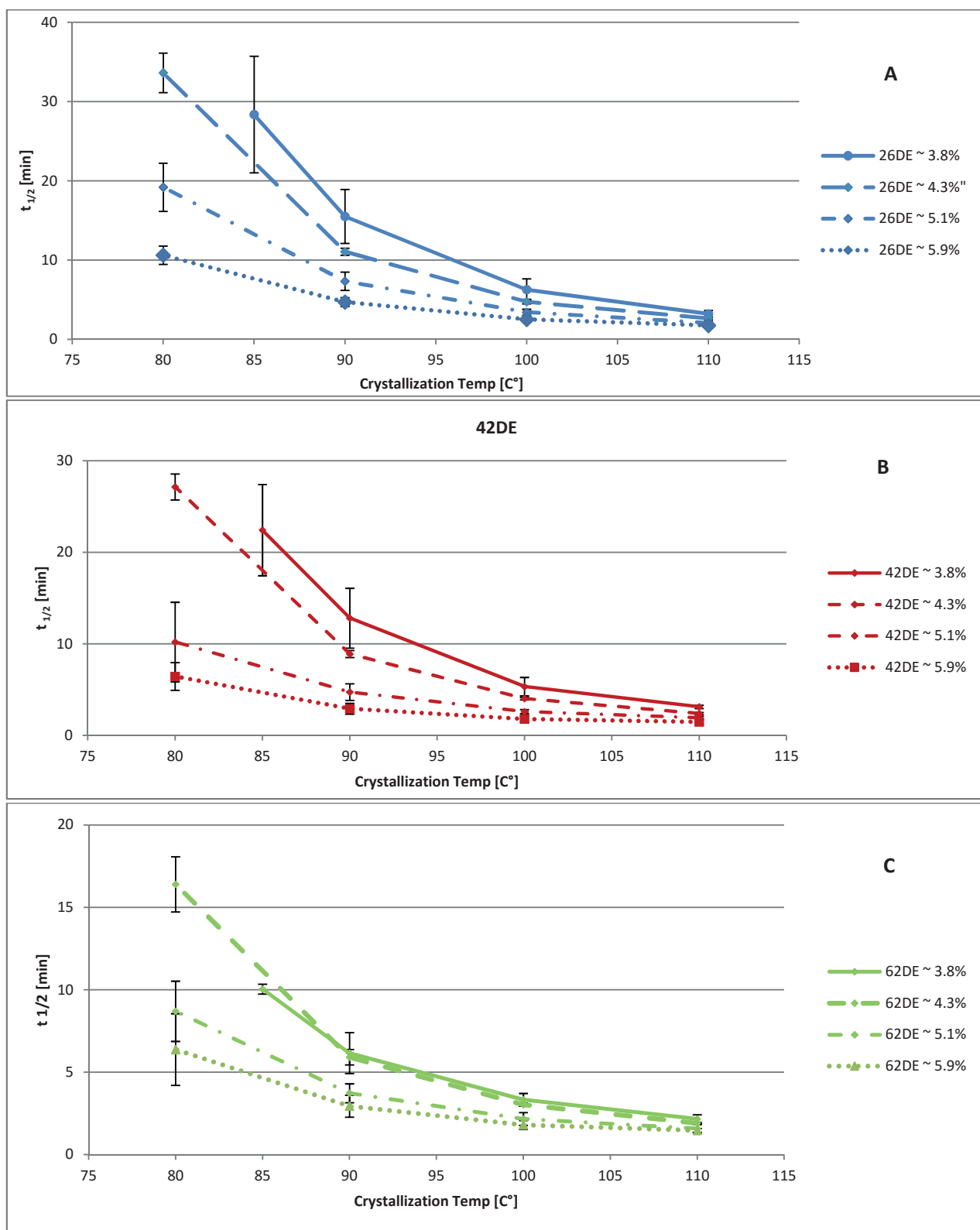


Figure 4.12 Crystallization half times as a function of crystallization temperature for samples containing 14% w/w corn syrup (26DE, 42DE, 62DE)(a-c) at different moisture levels (%).

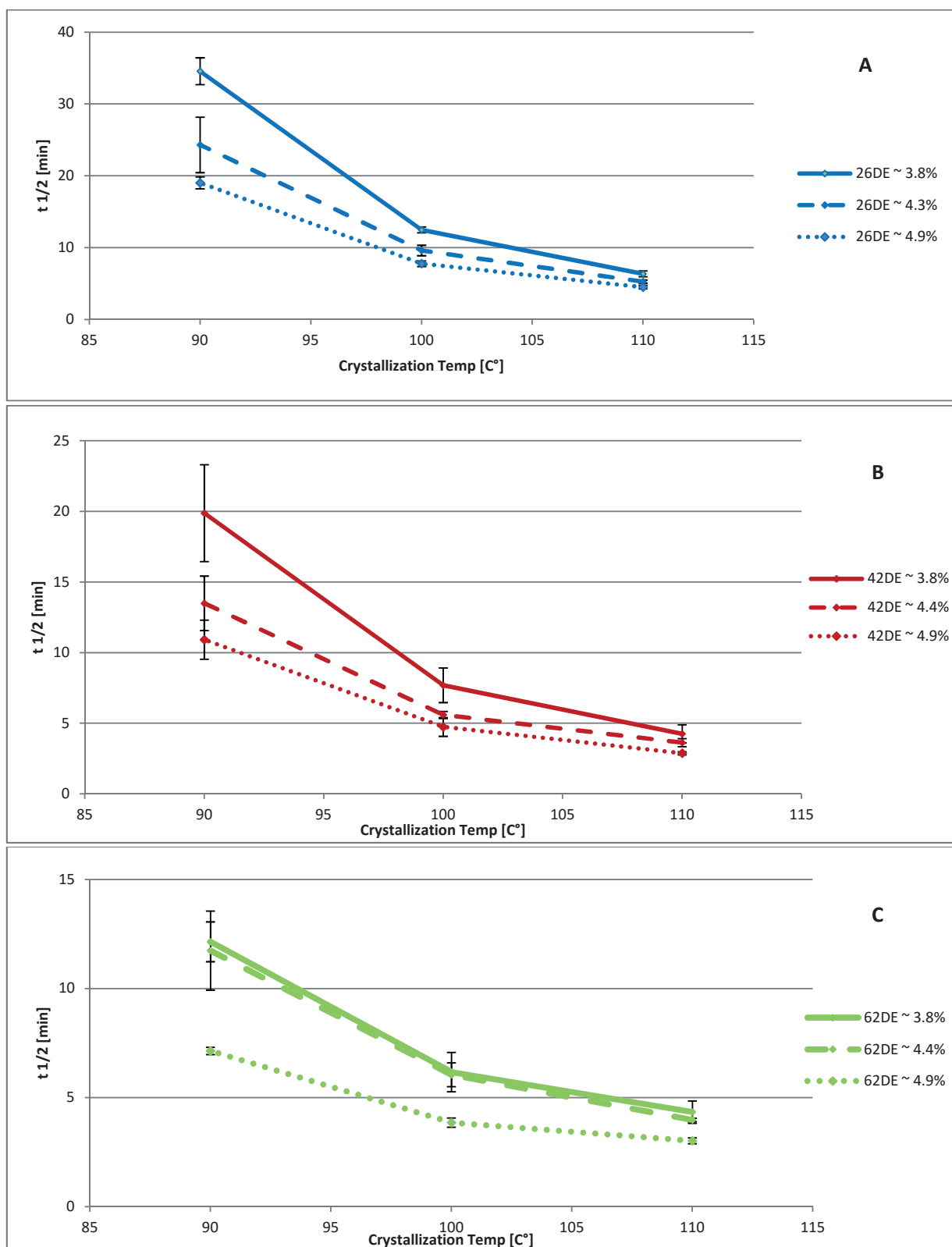


Figure 4.13 Crystallization half times as a function of crystallization temperature for samples containing 22% w/w corn syrup (26DE, 42DE, 62DE)(a-c) at different moisture levels (%).

#### 4.3.3.2 Effect of Moisture Content

Figure 4.12 and 4.13 illustrate the correlation between moisture content and crystallization half times. Samples of the same syrup but different water content showed significantly different crystallization half times ( $p > 0.05$ ) when crystallized at 80° or 90°C. However, samples crystallized at 100°C and 110°C showed no significant effect of moisture ( $p < 0.05$ ) on crystallization halftimes. This decrease in the effect of other parameters (moisture, DE, syrup concentration) was also observed when higher crystallization temperatures were applied.

The decreasing effect of moisture content on the crystallization halftimes at high crystallization temperatures could be explained by two effects: (a) high temperatures increased the molecular mobility to an extent that other effects (moisture, DE, amount syrup) became progressively negligible, (b) samples crystallized so fast that the ratio between halftime values and their standard deviation decreased, thus lowering the statistical significance of those effects. The governing effect of high crystallization temperatures on other inhibitory effects agreed with findings in literature (Myerson, 1993).

The second deviation from the overall trend concerned samples of 62DE corn syrup. Within this group of samples, the effect of water on the crystallization halftimes was absent between samples of higher moisture content. Samples containing 5.1% moisture did not crystallize faster than samples with 5.9% moisture content. It seemed that this step in moisture content did not affect the crystallization kinetics in any way. This phenomenon remained unclear as data for  $T_g$ ,  $T_c$  and  $T_m$  from nonisothermal experiments show significant differences between these two formulations.

However, the majority of crystallization rates  $1/t_{1/2}$  increased with increasing moisture content without reaching a maximum over the range of holding temperatures. These observations agree with results by Chen et al. (2015). Crystallization rates of samples with comparable moisture contents and syrup levels followed a similar trend when they were crystallized at the same temperature levels.

### 4.3.3.3 Effect of Composition

#### *Effect of Dextrose Equivalent*

In general, dextrose equivalent of corn syrup altered the crystallization halftimes of the amorphous sugar glasses significantly ( $p < 0.05$ ). Experimental crystallization halftime values were plotted over crystallization temperatures to compare the effect of DE on the crystallization kinetics at constant moisture levels (Figure 4.14 and 4.15). The corresponding crystallization halftime values are listed in Appendix A6.

The effect of DE on the crystallization halftime decreased in two ways below the statistical significance level: (i) with increasing crystallization temperature, (ii) with increasing moisture content of the samples. Hence, samples at low temperatures (80°-90°C) with low moisture content (3.8-4.3%) showed the strongest effect of DE on the crystallization (Figure 4.14 solid lines). The decrease in the effect of DE due to the parameters water content and temperature was previously described and explained in the section 4.3.2.1 and 4.3.2.2 .

However, a distinct correlation between DE and the crystallization halftimes was apparent with the crystallization halftimes increasing with decreasing DE. Halftime values correlated to the degree of polymerization, thus the MW of the amorphous sucrose matrices. Glasses of higher molecular weight crystallized slower than those of lesser molecular weight. This correlation did not change with the ratio of syrup in the formulation (Figure 4.15). The differences of crystallization rates between the types of syrups increased at the 22% syrup level. This difference in crystallization rate, however, corresponds to the overall increase in the inhibitory effect due to higher amount of syrup in the matrix. .

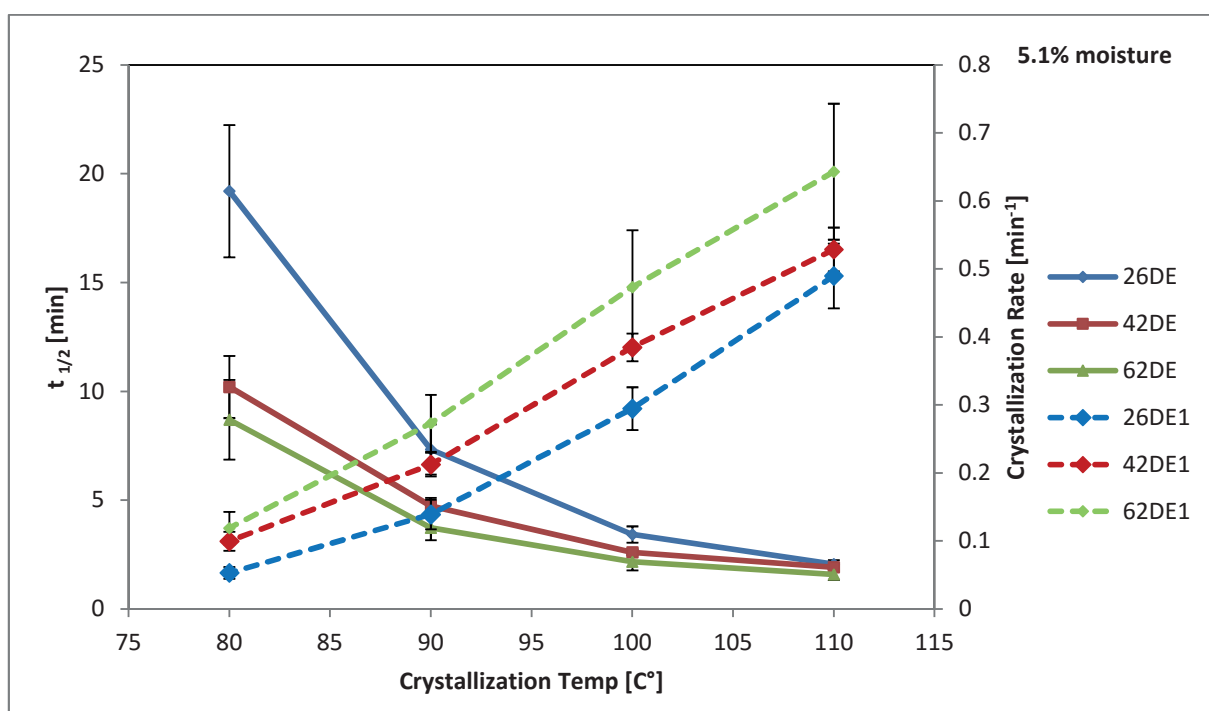
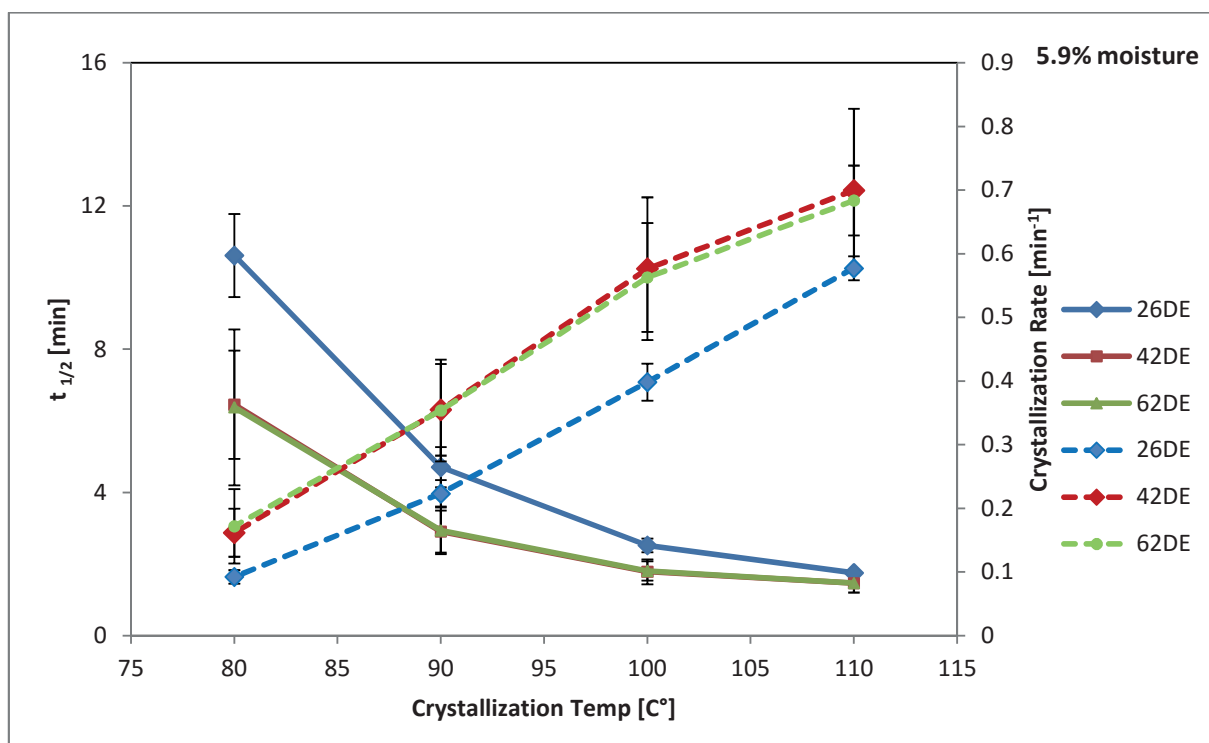


Figure 4.14 (cont`d)

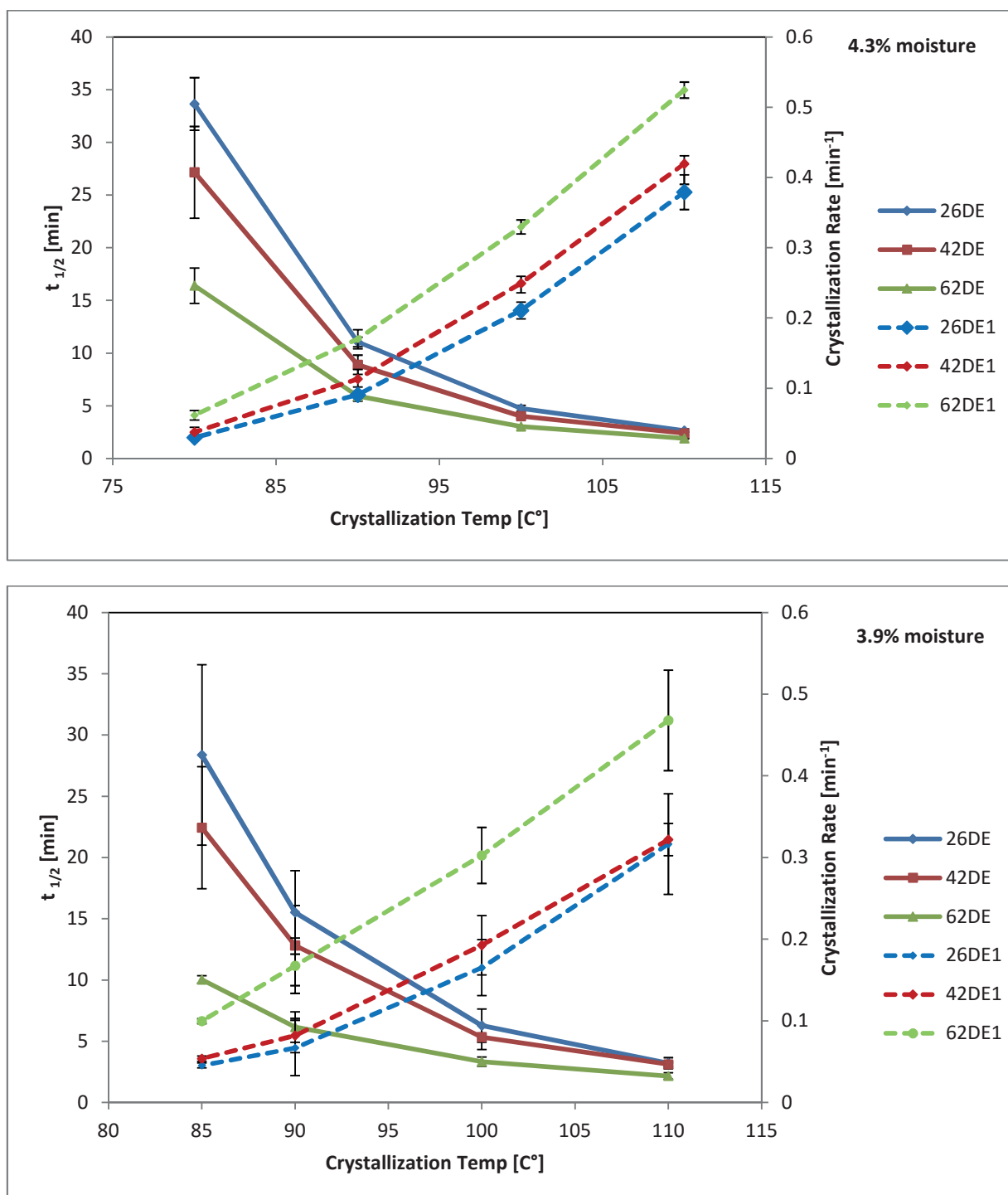


Figure 4.14 Crystallization half-times as a function of crystallization temperature in order to compare the effect of DE at different crystallization temperatures [C°] and moisture levels [%] for samples containing 14% corn syrup. Solid lines represent crystallization half-times, dotted lines represent crystallization rates [min<sup>-1</sup>].

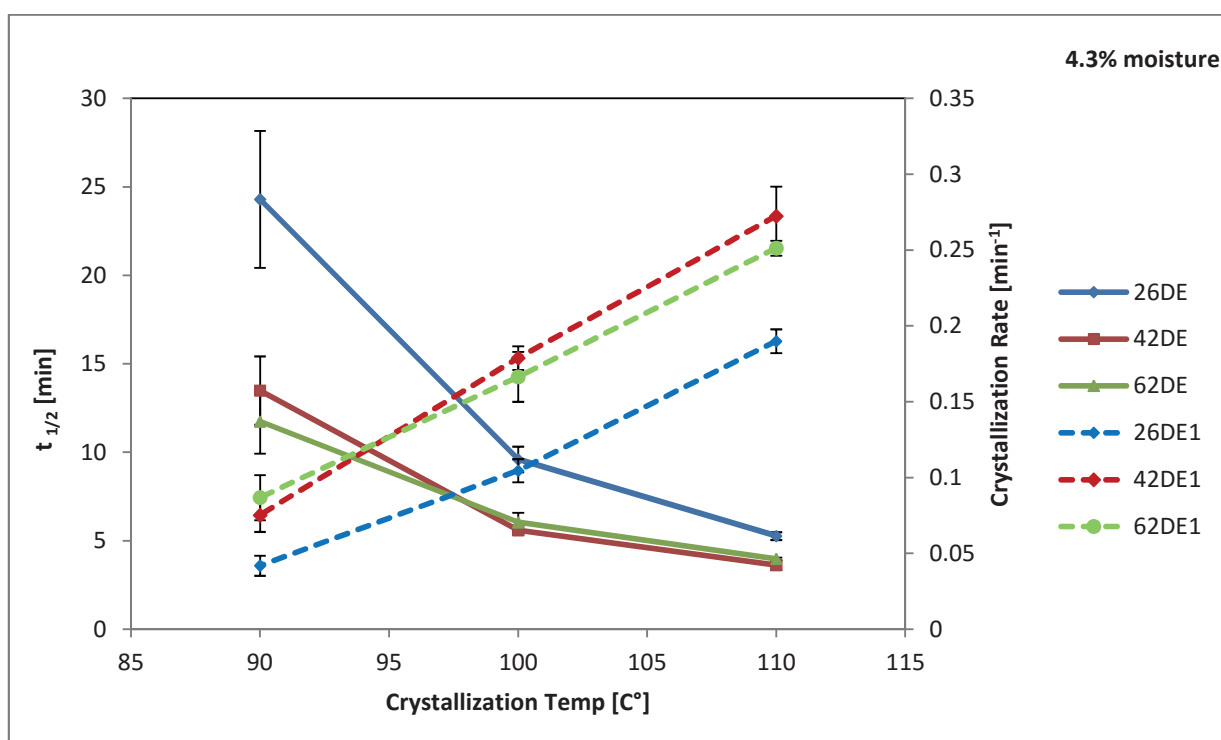
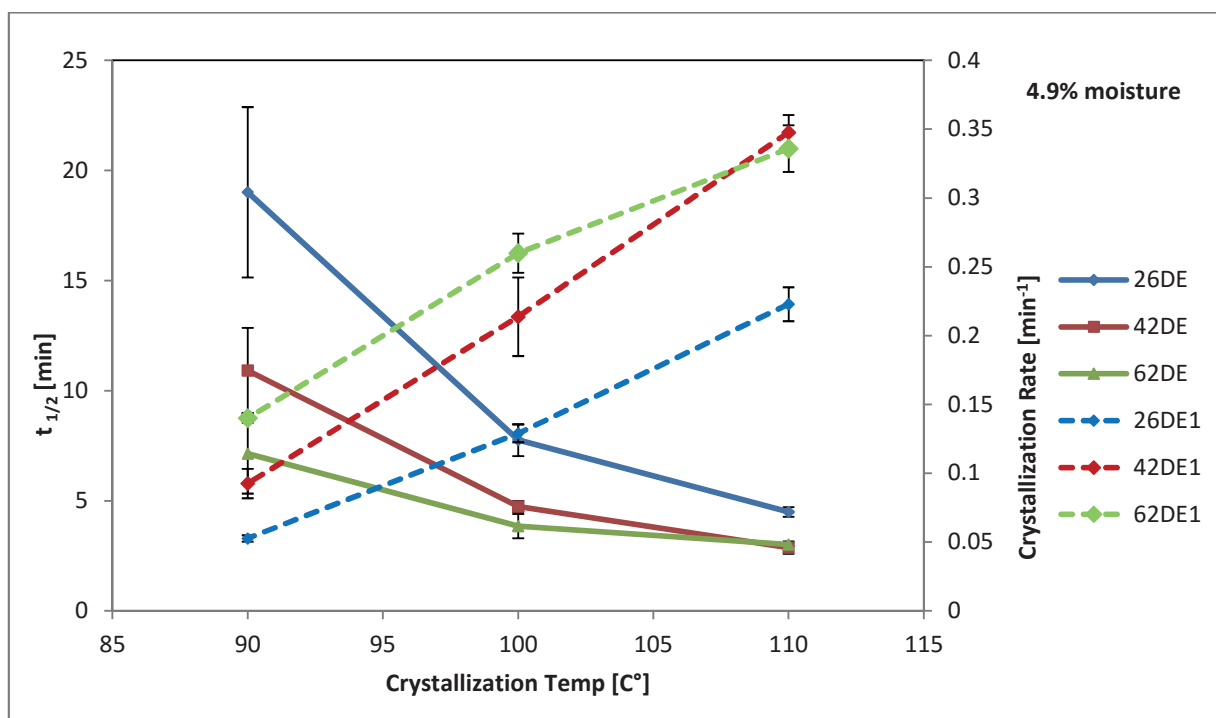


Figure 4.15 (cont`d)



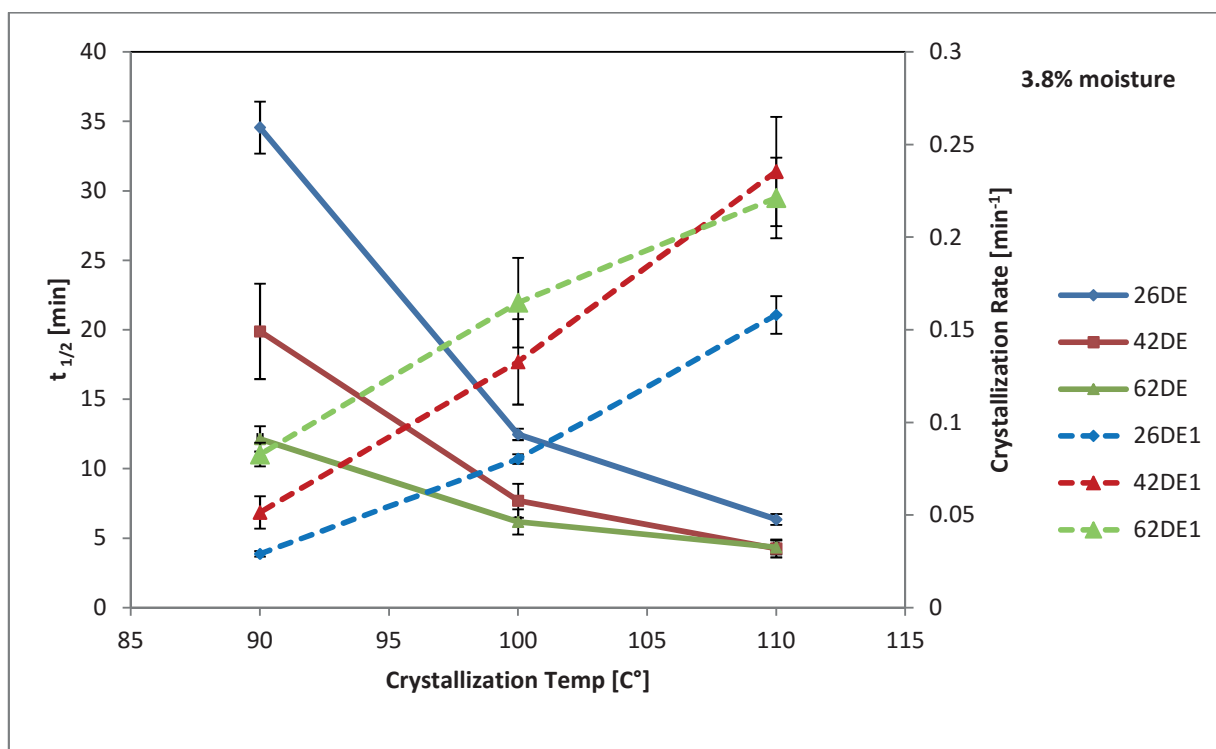


Figure 4.15 Crystallization half-times and rates as a function of crystallization temperatures [°C] at different moisture levels[%] for samples consisting of 22% corn syrup. Solid lines represent crystallization half-times, dotted lines represent crystallization rates [ $\text{min}^{-1}$ ].

#### *Effect of Corn Syrup Ratio*

Crystallization half-times increased significantly with increasing level of syrup ( $p < 0.05$ ) in samples of the same moisture content. Again, molecular weight of the glass showed a correlation to crystallization kinetics, with glasses of higher molecular weight crystallizing slower than glasses of lesser molecular weight. The effect of corn syrup ratio on the crystallization rate was apparent over the whole moisture range observed.

## 4.4 Factors on Crystallization Deviations between Syrups

Section 4.3.2.3 showed a significant difference in the crystallization rate between samples of the same formulation but different type of syrup. In general, the inhibitory effect of corn syrup on the sucrose crystallization can be explained by different approaches: (i) corn syrup saccharides (monosaccharides, glucose, fructose, and glucose polymers) adsorb onto the crystal lattice structure. This mechanism was proposed for crystallization of sucrose in solutions (Bamberger et al., 1980; Hartel, 2001). (ii) The addition of corn syrup may increase the viscosity of the system, lowering the mobility of the molecules and thus increasing the energy required for crystallization (Levenson & Hartel, 2005). (iii) Corn syrup polysaccharides may also interact with sucrose molecules by hydrogen bonding, thereby affecting both, translational and rotational diffusion. More energy would be needed for the sucrose molecules to diffuse through bulk solution for nucleation and growth to occur (Levenson & Hartel, 2005). As samples were crystallized at the same constant temperature  $T_x$  the difference between crystallization temperature  $T_x$  and glass transition temperature  $T_g$  should be investigated as the driving force for the differences in the crystallization rate observed. The level of moisture was selected at which the formulations of different DE showed the most significant difference on crystallization and the values were plotted as a function of  $T_x - T_g$  in Figure 4.16.

The plot shows that the values for crystallization halftimes follow quite commonly a negative logarithmic or exponential trend. The differences in  $t_{1/2}$  between the types of syrup decreased considerably when plotted as a function of  $T - T_g$ , so that crystallization rate can be related to molecular mobility, free volume and  $T_g$ . Due to the rather small range of experimental holding temperature, these values were fitted to Arrhenius equation, the Williams-Landel-Ferry equation and the Lauritzen-Hoffman equation to investigate the potential effect of  $T_g$  on the crystallization of the samples in greater detail.

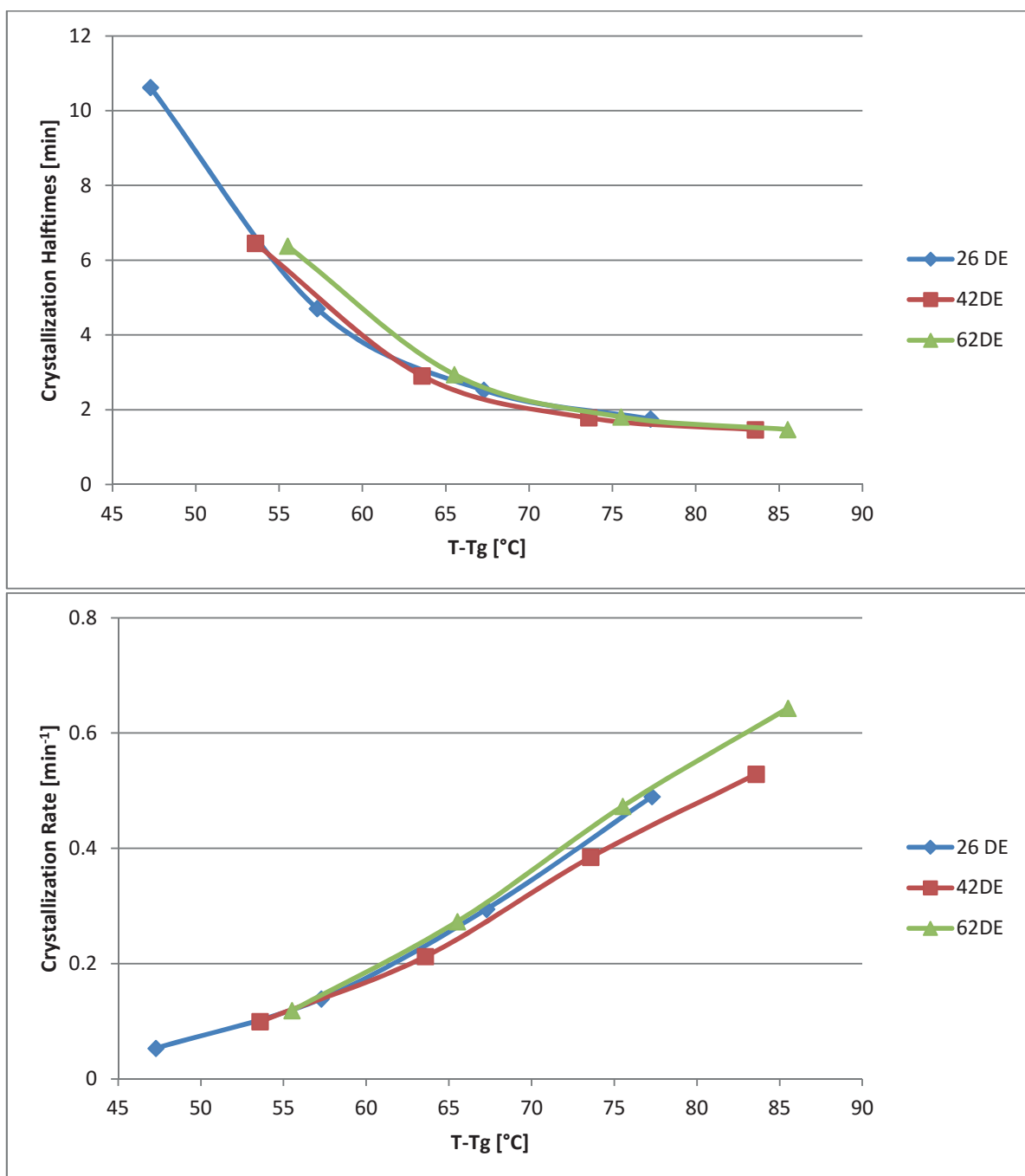


Figure 4.16 Crystallization halftime values and rates plotted as a function of  $T - T_g$  for samples of 4.3% moisture and 14% (w/w dry basis) corn syrup.

### 4.3.1 Arrhenius Equation

The activation energy for crystallization in an amorphous system can be evaluated by the Arrhenius-type equation (Hartel, 2001):

$$k_G = A_g \exp \left\{ -\frac{E_g}{RT} \right\} \quad (2.21)$$

where  $A_g$  is a frequency factor,  $E_g$  is the activation energy for growth,  $R$  is the universal gas constant, and  $T$  is temperature. Activation energy can be found from the exponential relationship between  $k_G$  (or growth rate at constant supersaturation) and inverse temperature. The measured crystallization rates were plotted with the Arrhenius fit in Figure 4.17 for amorphous sugar matrices containing 26DE, 42DE and 62DE corn syrups and crystallization rate [ $\text{min}^{-1}$ ] values were plotted as a function of the reciprocal of temperature. SPSS Statistics (Version 20, IBM, NY) was used with nonlinear Levenberg-Marquard optimization until  $\Delta\text{SSD}$  was less than  $1 \times 10^{-8}$  in order to determine the values of  $A_g$  and  $E_g$  from the observed crystallization data at different temperatures and moisture contents. The equation fits the data reasonably well, confirming that  $E_g$  controls the crystallization in this range. The activation energies found from the exponential term are shown in Table 4.2 for amorphous sugar matrices containing different levels of different DE corn syrups at varying moisture contents.

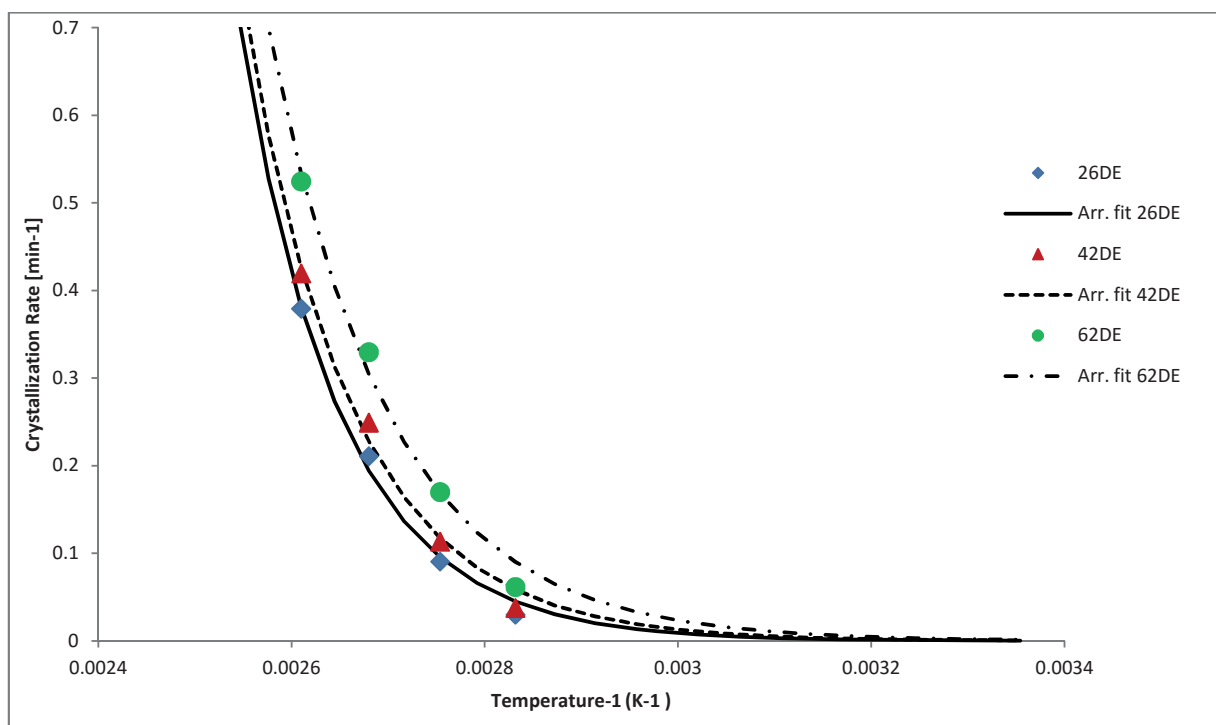


Figure 4.17 Arrhenius equation fit to crystallization rate data for amorphous sugar matrices with 14% corn syrup (w/w dry basis) at a 4.3% moisture level.

Sugar Glass 14% Corn Syrup						
Moisture Content [%]	26DE		42DE		62DE	
	$E_G$ [kJ/mol]	Standard error	$E_G$ [kJ/mol]	Standard error	$E_G$ [kJ/mol]	Standard error
5.9	57.57 <sup>a</sup>	7.23	45.35 <sup>a</sup>	9.55	42.91 <sup>a</sup>	8.60
5.1	71.79 <sup>a</sup>	6.59	53.90 <sup>a</sup>	7.48	52.64 <sup>a</sup>	7.96
4.3	80.59 <sup>a</sup>	6.91	74.58 <sup>a</sup>	7.81	66.79 <sup>a</sup>	7.04
3.8	81.06 <sup>a</sup>	5.59	74.67 <sup>a</sup>	7.20	61.98 <sup>a</sup>	5.84

Sugar Glass 22% Corn Syrup						
Moisture Content [%]	26DE		42DE		62DE	
	$E_G$ [kJ/mol]	Standard error	$E_G$ [kJ/mol]	Standard error	$E_G$ [kJ/mol]	Standard error
4.9	75.05 <sup>a</sup>	9.93	68.72 <sup>a</sup>	10.32	45.17 <sup>a</sup>	11.59
4.3	79.41 <sup>a</sup>	9.17	64.71 <sup>a</sup>	13.85	57.23 <sup>a</sup>	6.89
3.8	86.21 <sup>a</sup>	9.38	78.61 <sup>a</sup>	11.25	50.03 <sup>a</sup>	12.54

Table 4.2 Activation energy for crystal growth of amorphous sugar matrices composed of either 14% or 22% corn syrup (26DE, 42DE, 62DE) at different moisture levels. <sup>a</sup> values with the same superscript are not significantly different at the 95% confidence interval.

The values for both samples of 14% and 22% syrup show differences in the activation energy for growth between the types of syrup used. Although not statistically significant ( $p < 0.05$ ), the activation energy for growth increases with increasing MW of polysaccharides from the syrup. This trend is apparent over all levels of moisture and syrup. Since the comparison of the activation energy is conducted at the same holding temperature, it cannot be ruled out that the trend of the values is based on variation in  $T_g$  between the different syrup formulations. However, the fit showed that crystallization rate follows Arrhenius behavior and is related to the activation energy  $E_g$ . In highly viscous systems, the molecular mobility is low, and the energy of diffusion, expressed in the term  $\Delta G'/kT$ , dominates the classical nucleation equation (Hartel, 2001). As the fit to the Arrhenius equation could be conducted simultaneously with the mathematically similar  $\Delta G'/kT$  term of the classic nucleation equation,  $E_g$  and Gibbs free energy of molecular diffusion  $\Delta G'$  could be put in the relation. Taking the statistical insignificance into account, this then would imply that the kinetic barrier to diffusion in the experimental crystallization process is likely to be related to the DE of corn syrup used.

#### 4.4.2 Williams-Landel-Ferry (WLF) Kinetics

The Williams-Landel Ferry equation has been used to model kinetics of various polymer systems above the glass transition temperature according to their internal molecular mobility.

$$\log_{10} \alpha_t = \frac{-C_1(T - T_s)}{C_2 + (T - T_s)} \quad (4.6)$$

In equation 4.6,  $\alpha_t$  is the ratio between relaxation phenomena at temperature  $T$  and the reference temperature  $T_s$ , and  $C_1$  and  $C_2$  are constants. The equation was used to fit the crystallization halftimes for the sugar glasses containing different corn syrups at different moisture contents. The WLF equation was published using “universal” values for both  $C_1$  (17.4) and  $C_2$  (51.6) (Williams et al., 1955). These universal values might be inaccurate due to the variability in  $T_g$ , difficult measurements near  $T_g$ , and variations

between averaged polymers (Peleg, 1992). Peleg advises the use of a reference temperature with variable constants and within the experimental range. Roos et al. (1991) used Arrhenius and WLF equation to determine the time dependence of crystallization. The modified WLF equation used was:

$$\log(t_{1/2}) = \log t_{T_g} + \frac{-C_1(T - T_g)}{C_2 + (T - T_g)} \quad (4.7)$$

where  $t_{1/2}$  is the crystallization halftime and  $t_{T_g}$  is the crystallization halftime at  $T_g$ .  $t_{T_g}$  is determined by solving Equation 4.6 for all experimental points, and the average time obtained for each set of samples was used as  $t_{T_g}$  (Roos & Karel, 1991a). The experimental crystallization time data was fit using the  $T_g$  and the respective crystallization temperature for each glass at a specific moisture content. The solver function in Excel, with nonlinear optimization was used to find the best fit values for  $C_1$  and  $C_2$  for each formulation. The values for  $C_1$  and  $C_2$  are shown in Table 4.3 and values for  $C_1$  are reasonably close to the universally proposed constants. Values for constant  $C_2$  however do not fit the proposed “universal” value. The deviation from “universal” values is not unusual and was previously described by Levenson & Hartel (2005) and Peleg (1992). The values  $C_1$  and  $C_2$  showed no relationship to the DE of syrups, amount of syrup or moisture content. The WLF approximation, however, fit reasonably well with the observed crystallization halftimes; therefore, the analysis show that crystallization from low moisture amorphous matrices obeys the WLF equation and the suggestion applies that above  $T_g$  the rate of crystallization is related to viscosity and relaxation times of mechanical properties (Roos, 1995).

<b>Sugar Glass 14% Corn Syrup</b>						
Moisture Content [%]	<b>26DE</b>		<b>42DE</b>		<b>62DE</b>	
	$C_1$	$C_2$	$C_1$	$C_2$	$C_1$	$C_2$
5.9	13.05	15.48	11.60	14.00	11.84	14.22
5.1	12.52	14.94	11.58	14.00	12.05	14.41
4.3	13.65	15.99	13.61	15.86	13.05	15.32
3.8	13.57	15.92	13.06	15.38	11.39	13.76

<b>Sugar Glass 22% Corn Syrup</b>						
Moisture Content [%]	<b>26DE</b>		<b>42DE</b>		<b>62DE</b>	
	$C_1$	$C_2$	$C_1$	$C_2$	$C_1$	$C_2$
4.9	14.08	16.55	13.81	16.16	10.96	13.45
4.3	13.58	16.06	13.01	15.39	11.92	14.43
3.8	13.67	16.14	13.48	15.81	10.76	13.31

Table 4.3 WLF values for constants  $C_1$  and  $C_2$  for crystallization halftimes of amorphous sugar matrices composed of 14% / 22% corn syrup with different DE using crystallization temperatures  $T$  of 80, 85, 90, 100, 110°C and  $T_g$  of each formulation.

Using the method of Roos & Karel (1991a) the data for the crystallization halftimes and WLF approximation were plotted over  $T-T_g$  for each formulation using the calculated values  $C_1$  and  $C_2$  (Figure 4.18). The data is shown at temperature values of  $(T-T_g)$  because the WLF equation represents the relationship of the driving force of the temperature differential above  $T_g$ .

The WLF equation fits reasonably well with the experimental crystallization halftimes; therefore, the analysis shows that crystallization rate from low moisture amorphous matrices of sucrose and corn syrup obeys the WLF equation. The theory suggests that above  $T_g$ , the rate of crystallization is related to viscosity and relaxation times of mechanical properties (Roos, 1995).

The particular WLF fits for the different DE samples seemed to be fairly close to each other and, as previously mentioned, no distinct trend for the constants  $C_1$  and  $C_2$ , with respect to the different types of corn syrup was found. These findings suggest that the differential  $T-T_g$  is the governing factor accountable for the differences seen in crystallization kinetics between the types of syrup.



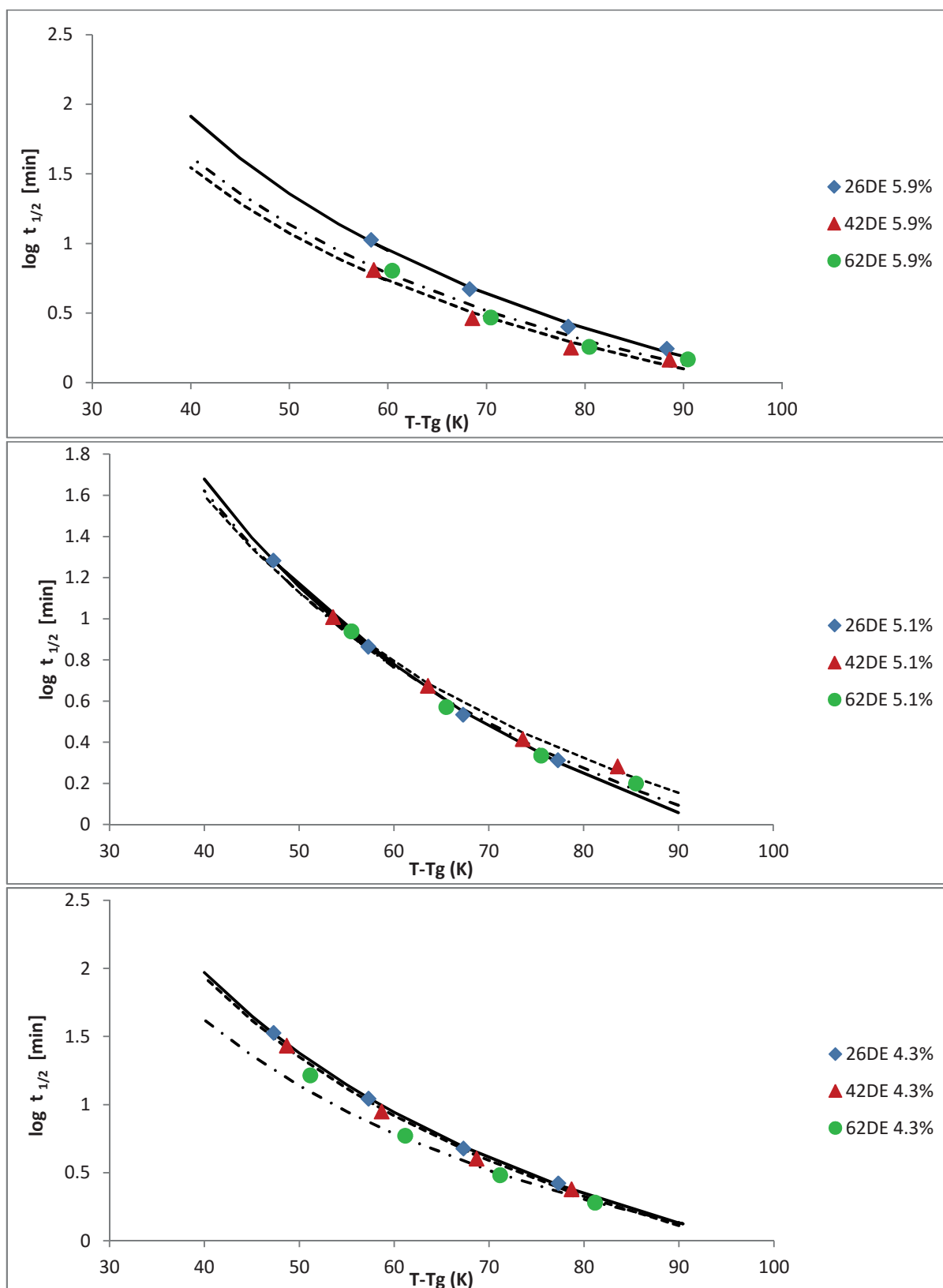


Figure 4.18 Williams-Landel Ferry (WLF) fit to crystallization halftime data for amorphous sugar matrices composed of 14% / 22% corn syrup with different DE at different moisture levels. WLF fit represented for: 26DE as solid line, 42DE as dotted line, 62DE as dot-dashed line.

#### 4.4.2 Hoffman-Lauritzen Kinetics

As described previously, the applied holding temperatures represented only a limited temperature range between  $T_g$  and  $T_m$  and samples did not exceed a temperature of maximum crystallization rate within this range. In order to investigate the difference in the crystallization caused by varying DE of syrup, the Lauritzen Hoffman like expression was used, which describes the overall rate of crystallization as a function of temperature (Lauritzen & Hoffman, 1973):

$$\left(1/t_{1/2}\right) = (1/t_{1/2})_0 \exp\left(\frac{-U}{R(T - T_\infty)}\right) \exp\left(\frac{-K}{T \Delta T f}\right) \quad (2.25)$$

where  $T$  is the crystallization temperature,  $R$  is the universal gas constant,  $\Delta T = T_m^\circ - T$  is the supercooling,  $f = 2T/(T + T_m^\circ)$  is a correction factor accounting for the reduction in the latent heat of fusion as the temperature is decreased and  $T_m^\circ$  is the equilibrium melting point.  $(1/t_{1/2})_0$  is the pre-exponential factor that includes all terms independent of temperature,  $U$  is the activation energy or the transport of crystallizing units across the phase boundary,  $T_\infty$  is the temperature below where such transport ceases, and  $K$  is a nucleation term. In the Lauritzen-Hoffman equation,  $T_\infty$  is usually taken to be  $T_g - 30K$ . In the original Hoffman-Lauritzen equation, the nucleation term was directly related to surface energies of the folded polymer. This is inappropriate for small molecular materials. However, it is hypothesized that a similar equation containing surface energy and heat of fusion terms would apply here, although the exact relationship to  $K$  is unknown (Kedward et al., 1998). The 4 unknown parameters  $U$ ,  $T_\infty$ ,  $K$  and  $(1/t_{1/2})_0$  were obtained using a nonlinear least squares fitting routine. These values were compared to values calculated using the method of Marsh and Blanshard (1988), which were identical with those obtained by nonlinear least squares fitting.

The values for  $T_m$  and  $T_g$  were taken from non-isothermal crystallization experiments. The calculated activation energy for the transport of crystallizing units across the boundary phase,  $U$ , is fairly constant (

$\pm 200$  J) and accounts for 7.200 J/mol. This activation energy slightly increases from 14% to 22% syrup in the formulation. Kedward et al. (1998) found this parameter to be 4500 J/mol for pure amorphous sucrose at a 0.94% moisture level. It appears that sucrose molecules need significantly more energy to cross the boundary phase in matrices containing polysaccharides from corn syrup, offering a magnitude of about 1.5 in comparison to pure amorphous sucrose. A Hoffman-Lauritzen like fit was calculated for the samples of different DE syrup as well as different levels of syrup and moisture content. A corresponding Hoffman-Lauritzen like plot for 3 formulations (26DE, 42DE, 62DE) as a function of crystallization temperature (K) is shown in Figure 4.19.

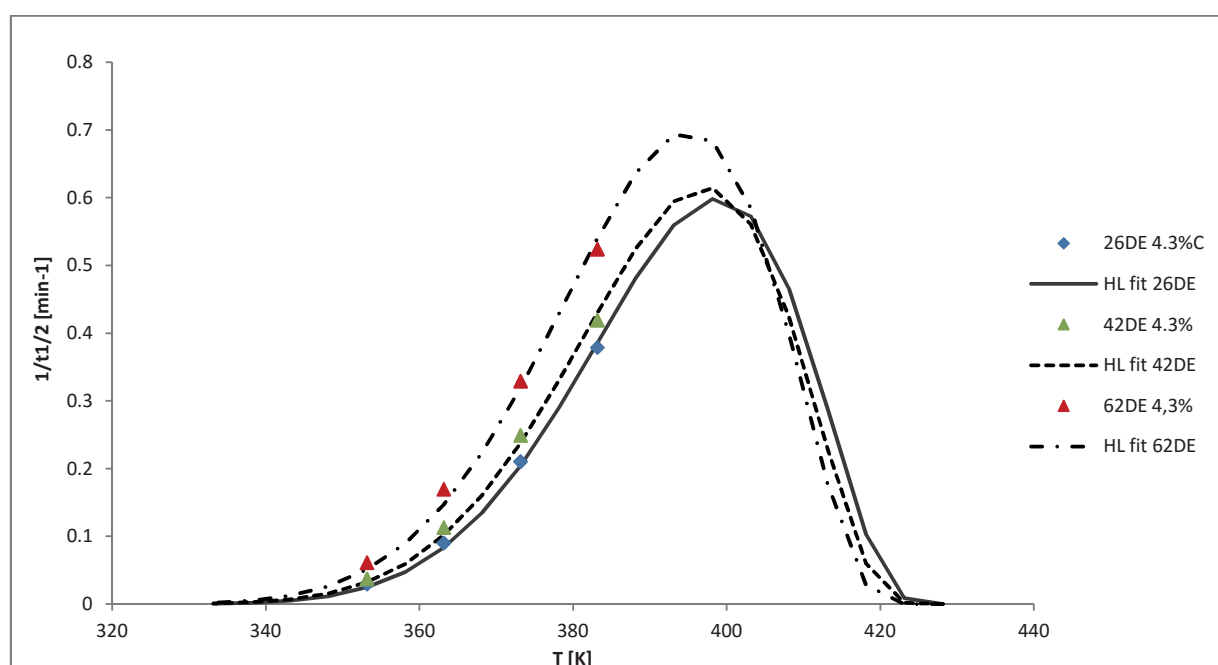


Figure 4.19 Experimental crystallization rate and Hoffman-Lauritzen like fit as a function of crystallization temperature for amorphous sugar glasses made with 14% (w/w dry basis) corn syrups (26DE, 42DE, 62DE) at a moisture level of 4.3%.

The Hoffman-Lauritzen approximation fits reasonably well with the observed crystallization rate data and shows a shift for both the temperature of maximum crystallization  $T_c$  and a deviation in the maximum crystallization rate. Both parameters correlate with the DE of the syrup used and the overall molecular weight of the glasses. Glasses with low DE syrup showed a higher maximum crystallization rate at a lower  $T_c$ . The trend of  $T_c$  with respect to DE from the Hoffman Lauritzen like fit agrees well with the

experimental  $T_c$  values obtained from non-isothermal DSC experiments (Section 4.2.2). However, the differences between these parameters were smaller between samples of 26DE and 42DE syrup.

To investigate the effect of  $T-T_g$  on the crystallization kinetics, the same fit and data was plotted as a function of  $T-T_g$  or  $T-T_g/T_m-T_g$ , respectively (Kedward et al., 1998)(Figure 4.20).

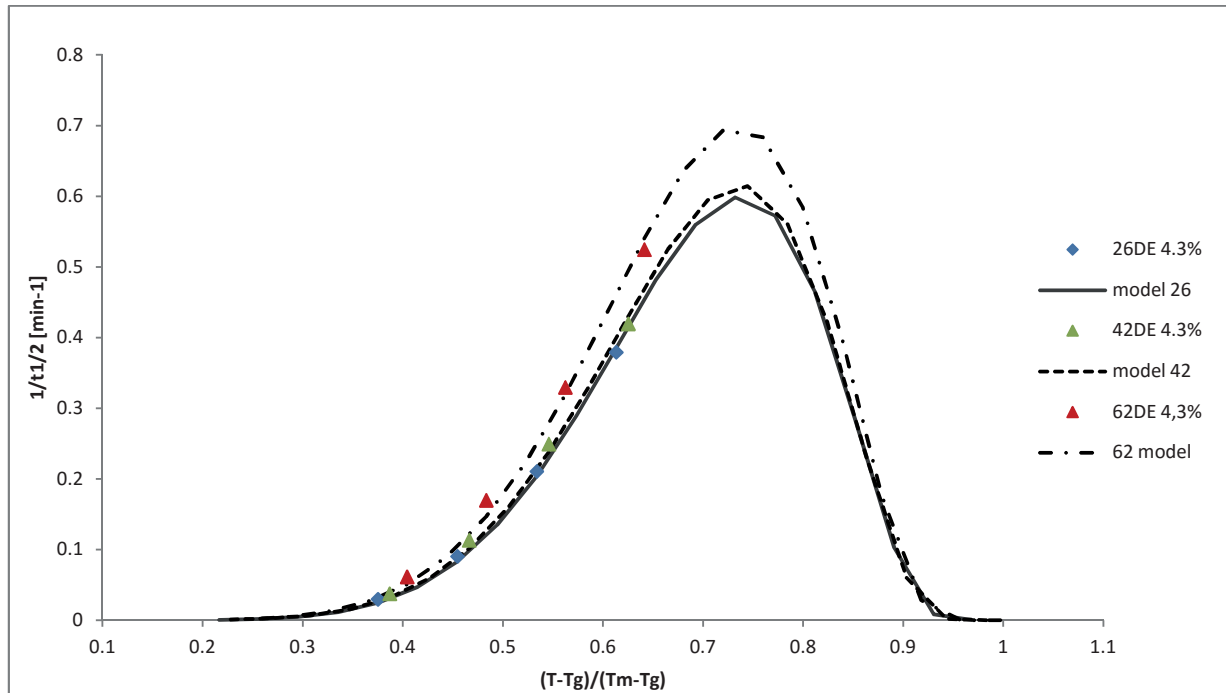


Figure 4.20 Experimental crystallization rate and Hoffman-Lauritzen like fit as a function of  $T-T_g/T_m-T_g$  for amorphous sugar glasses made with 14% (w/w dry basis) corn syrups (26DE, 42DE, 62DE) at a moisture level of 4.3%.

Again, the Hoffman-Lauritzen like approximation fit the experimental data reasonably well.

Figure 4.20 shows that if the Hoffman-Lauritzen like fit and the experimental data were plotted as a function of  $T-T_g/T_m-T_g$ , any shift in the temperature of maximum crystallization became negligible.

However, the rate of maximum crystallization differed still between the DE of the syrup in the formulation, mainly between 62DE syrup and 42DE/26DE syrup. In the comparison between Figure 4.19 and 4.20, the assumption follows that  $T-T_g$  is governing factor accountable for the differences seen in crystallization kinetics between the types of syrup at lower temperatures.

However, if the system approaches the temperature of maximum crystallization rate, differences in the crystallization rate between the types of syrup are observable, and this differential did not fully correlate with  $T-T_g$ . This effect is observable for the three types of syrup at any of the experimental moisture levels. The result from this fit underlined the assumption that effects other than  $T_g$  might influence crystallization directly.

As previously described, higher holding temperatures could not be applied without severe distortions of the thermograms in this experimental setup. To investigate the interactions of different effects on crystallization more precisely, approximated rates of maximum crystallization should be verified with experimental data, by crystallizing the samples over a wider range of temperature closer to  $T_m$ .

## 5. Conclusion and Recommendation

### 5.1 Conclusion

State behavior and crystallization kinetics of amorphous sugar glass consisting of sucrose, water and three different types of corn syrup (26DE, 42DE, 62DE) at two syrup levels (14% and 22%) were studied under varied experimental conditions. Experiments were conducted non-isothermally to investigate glass transition temperature, temperature of maximum crystal growth and solubility temperature of the matrices. Subsequent isothermal crystallization experiments were performed to investigate crystallization kinetics of the amorphous sugar glasses, both using DSC.

The observed glass transition temperature increased with both the MW of the glass and the decrease in moisture content of the glass. The differences in  $T_g$  between the types of syrup were significant and remained fairly constant over the observed moisture range. Samples of the same syrup but at higher concentration showed a significant increase  $T_g$  at low moisture content, which correlated with the molecular weight of the glasses and agreed with the finding of  $T_g$  as a function of MW (Gabarra & Hartel, 1998). The temperature of maximum crystallization rate was found to show the same relationship to moisture, and decreased with increasing moisture content. Differences in temperature of maximum crystallization were significant between the DE of syrup at a 14% level, but insignificant at a 22% syrup level. The temperatures of maximum crystallization were found to be above the midpoint between  $T_g$  and  $T_m$ .  $T_c$  increased significantly with the amount of syrup in the glass. However, a direct correlation to Mw of the glass could not be confirmed. Solubility temperatures of the crystallized samples followed the same relationship - values decreased with increasing amount of water in the sample. Moreover, the solubility temperature decreased with increasing mol% of the corn syrup polysaccharides due to competition between corn syrup saccharides and sucrose for hydrogen bonding sites with water molecules (Mullin, 2001).

Results from the isothermal crystallization kinetic experiments suggested that the sucrose crystallization rates were highly related to temperature, moisture content, corn syrup to sucrose ratio and DE of syrup used. Moisture content of samples and temperature influenced sucrose crystallization rates, with an increase in temperature and moisture content giving higher crystallization rates; however a maximum in crystallization rate was not found due to experimental limitations avoiding holding temperatures above 110°C.

Crystallization rates were also dependent on the corn syrup to sucrose ratio, with higher addition level of corn syrup resulting in a greater reduction in growth rates. This indicates that amorphous sugar matrices containing higher amount of sucrose needed substantially more time to crystallize.

Emphasis of this work was put on the question whether different DE syrups show variations in their effect on the crystallization kinetics of sucrose. The difference between DE and crystallization rate as a function of temperature was substantiated by experimental results. Crystallization rate was found to increase with decrease in DE of the syrup. The overall difference in the inhibitory effect on the crystallization rate between the DE of syrup decreased with higher holding temperatures as well as increase in moisture content.

The difference between DE and crystallization rate diminished distinctly when plotted as a function of  $T - T_g$ . Subsequently, the crystallization data was fitted to different crystallization models, also in order to clarify whether  $T_g$  is accountable for differences in crystallization rates.

The WLF equation was deployed based on the suggestion that the WLF equation applies to crystallization processes above the glass transition temperature in any glass-forming polymer, oligomer or monomer (Slade et al., 1993). Here, WLF kinetics are applicable in the rubbery state, between the  $T_g$  and the solubility curves, where molecular mobility and diffusion increase (Slade et al., 1993). The WLF equation fit the experimental crystallization data reasonably well, and the  $C_1$  and  $C_2$  constants were calculated.

However, no trend with respect to DE of syrup used was observable in the calculated values for these two constants.

To investigate potential differences in the activation energy for crystal growth in the amorphous sugar matrices, the Arrhenius equation was applied as a function of temperature. The crystallization data fit the Arrhenius equation quite well. Calculated values for activation energy followed a clear trend increasing with decreasing DE and increasing MW of the glass. This trend was apparent at every level of moisture content as well as sucrose to corn syrup ratio.

In addition, experimental data was used in a Hoffman-Lauritzen like fit, because this model offered good approximation for isothermal crystallization data of sucrose (Kedward et al., 1998). The experimental crystallization rates fit the Hoffman-Lauritzen like expression well. Plotted as a function of  $T_g$  and  $T_m$ , the HL like fits showed differences in the approximated maximum crystallization rates of different types of syrup. The differences generally followed the same trend with highest values for the lowest DE syrup and vice versa.

Values for  $T_c$  from non-isothermal DSC experiments were significantly higher than values calculated from the midpoint of  $T_g$  and  $T_m$ .  $T_c$  increased to a greater extent than glass transition temperature ( $T_g$ ) and this difference was greater with increasing addition of syrup. This finding agreed well with literature (Gabarra & Hartel, 1998; Saleki-Gerhardt & Zografis, 1994) and initiates the conclusion that crystallization processes are not only affected by  $T_g$  and its differential  $T-T_g$ .

The experimental systems in this work were sugar glasses of low moisture content and high viscosity. In such systems, the theory suggests that above  $T_g$  the rate of crystallization is related to viscosity and relaxation times of mechanical properties (Roos, 1995). It is assumed that the free volume of a polymer is directly related to the temperature above  $T_g$ , so that at higher temperatures the system has greater mobility and relaxation time decreases, thus taking the temperature differential  $T-T_g$  as the driving force for crystallization above  $T_g$  (Roos, 1995; Slade et al., 1993).



As mentioned previously, crystallization rate differed significantly between the types of syrup used as a function of holding temperature. This difference in crystallization rates decreased by two factors, (a) increasing moisture content, (b) increasing crystallization temperature.

However, if plotted as function of  $T-T_g$ , most of the crystallization rates of different DE syrups were fairly similar. It is assumable that the driving factor  $T-T_g$  is sufficient to explain major differences in the crystallization rate.  $T_g$  of a corn syrup-sucrose system, in return, was found to be a linear function of the MW of the polymers added (Gabarra & Hartel, 1998).

However, crystallization rates as a function of  $T-T_g$  still showed differences with respect to the types of syrup used.

A Hoffmann-Lauritzen like fit was calculated, which underlined this differential, especially at higher temperatures close to  $T_c$  max, where formulations of different DE had varying crystallization rates. Even though these values were partially obtained from a model (Hoffman-Lauritzen) it stands to reason that  $T-T_g$  is not the only effect accountable for a difference in crystallization rate; thus, crystallization rate differences cannot be explained only by variability of  $T_g$ . In addition,  $T_c$  obtained from non-isothermal experiments showed a deviation from the general relationship to  $T_g$ , supporting this theory.

These findings are in agreement with literature, Gabarra & Hartel (1998) and Saleki-Gerhardt & Zografi (1994) assumed that the effect of polysaccharide additives on crystallization of amorphous sucrose was not just linked to an increase in  $T_g$  but also involved a specific inhibition such as molecular charge or steric hindrance effects.

Subsequently, it might be useful to assume two different factors, (i) the effect on molecular mobility through an effect on  $T_g$  and (ii) an inhibitory effect that cannot be explained by  $T_g$  in order to explain differences in crystallization rate between the DE of syrup used in the formulation, at both, comparable moisture content and same crystallization temperature,

While (i) is not unusual and corresponds with the overall theory, the inhibitory effect (ii), which cannot be explained by  $T_g$ , should be investigated to address possible mechanisms of different DE syrups in respect to their effect on the inhibition of sucrose crystallization.

As crystallization involves nucleation and growth, both processes should be considered separately to conclude if potential interactions occur during nucleation, growth, or both.

To start off with, it should be clarified if, and what type of nucleation occurs in the experimental systems.

The two types of mechanism by which amorphous sucrose may crystallize after gaining enough mobility (e.g., by heating in the DSC) are: (A) heterogeneous primary nucleation followed by crystal growth (Saleki-Gerhardt & Zografi, 1994); or (B) growth of existing nuclei (with no nuclei formed). The second mechanism has been suggested by several authors, with the explanation that freeze-drying often produces a solid with higher degree of short-range order as compared to rapidly cooled melt (Gabarra & Hartel, 1998; Mathlouthi et al., 1986). The experimental system in this work, however, is a rapidly cooled melt and with respect to findings from others (Levenson & Hartel, 2005), heterogeneous primary nucleation is assumed to be the type of nucleation occurring in these types of amorphous glasses.

With the investigation of possible interactions or effects of corn syrup polysaccharides on sucrose nucleation rates, one must first separate any solubility effects. In order to determine the true effect of corn syrup, for example, on the nucleation process, nucleation rates must be compared at equivalent supersaturation. Because added on the same weight basis, the three different corn syrups caused variations in sucrose solubility (Section 4.2.3) as a result of different molar% of corn syrup saccharides in the final formulations. Those sugars compete with sucrose for hydrogen bonding site of water molecules, thus change the solubility and supersaturation of sucrose. The system of lower supersaturation would nucleate more slowly than the one with higher supersaturation. Due to the observed effect, it would not

be possible to ascertain whether the type of corn syrup had an inhibition effect on nucleation separate from the effect of supersaturation (Hartel, 2001).

However, making the supposition that the inhibitory effect of corn syrup, which cannot be explained by  $T_g$ , is not only an expression of varying supersaturation of sucrose, Saleki-Gerhardt and Zografi (1994) proposed interactions of corn syrup fractions on the molecular level. The possibility was addressed that the additives accumulate at the solid-particle interface as an adsorbed layer during mixing and cooking in an amount sufficient to inhibit any nucleation that might be initiated on the surface of the particle, or that steric hindrance for mass transport is playing a role.

However, suggested by Gabarra & Hartel (1998), not only nucleation but growth of crystals might be affected by the inhibitory effects explained in (ii). Crystal growth of existing nuclei from solution involves several different steps (Hartel & Shastri, 1991). Two events may be important in crystallization of amorphous sucrose: (1) bulk mass transfer of sucrose units to the crystal surface, (2) surface diffusion of the sugar molecules to an appropriate lattice incorporation site, and (3) incorporation of the growth unit into the crystal lattice. The surface and bulk diffusion of sucrose molecules is probably inhibited by the high viscosity – low molecular mobility of the system caused by the presence of high MW components. In order to explain the inhibitory effect on crystal growth that could not be explained by  $T_g$ , molecular interaction at the crystal lattice should be discussed. The incorporation of sucrose molecules into the lattice may be inhibited by the slow displacement of molecules larger than sucrose present on or near crystallizing surfaces. Smaller saccharides could also affect this step as they might fit more easily on the crystallizing surface than high MW saccharides (Gabarra & Hartel, 1998). The high effectiveness of low DE corn syrup in inhibiting the crystallization of sucrose may be due the combination of long-chain saccharides, which would slowly counter-diffuse from the crystallizing surface as well as short-chain saccharides, which probably interfere with the incorporation of sucrose molecules into the lattice.

To sum up, differences in the crystallization of highly viscous amorphous sugar-corn syrup systems with varying DE at constant crystallization temperatures were found. The difference of the inhibitory effect of the syrups used on the crystallization of amorphous sucrose could be explained by a combination of effects: (i) by the temperature differential  $T-T_g$ , which is considered the driving force for crystallization above  $T_g$  (Levenson & Hartel, 2005; Williams et al., 1955). This differential however is dependent on  $T_g$ , which, in turn, is a function of MW of corn syrup polysaccharides in amorphous sucrose blends (Gabarra & Hartel, 1998).

In accordance with Gabarra & Hartel (1998) and Saleki-Gerhardt & Zografi (1994) differences in crystallization that could not be related to  $T_g$  were found, and might be explained by (ii) effects beyond a general effect on molecular mobility and free volume. These effects could be considered to apply at both steps, nucleation and growth. Even though any inhibition effect of the types of syrup on nucleation could not be examined separately from their effect on supersaturation, accumulation of corn syrup saccharides at solid-particle interface as a nucleation-inhibiting adsorbed layer is possible. Growth, on the other hand, might be affected by inhibitory effects of corn syrup saccharides on the diffusion and incorporation of sucrose units at the crystallizing surface. However, the mechanisms behind the inhibitory effects not explained by  $T_g$  remain theoretical and would need further work to be clarified.

## 5.2 Recommendations for Future Work

As the experiments were limited in their experimental execution, due to water evaporation from the crystallizing samples, it was not possible to approach higher temperatures than 110°C. For that reason, it was not possible to determine values for maximum crystallization rates experimentally and these values remained data that needed to be approximated by model fit. However, isothermally determined values for both temperature of maximum crystallization rate and maximum crystallization rate itself would enable an experimental confirmation of approximated data. This could be conducted in two ways: (i) by decreasing the moisture content of the samples to values around 1%, using the method of freeze drying. The residual amount of water in the sample might be low enough to avoid distortions in the thermograms. In further consequence, isothermal holding temperatures close to, or above  $T_c$ , would be possible and enable experimental determination of values for maximum crystallization rate. The other option could be: (ii) an increase in the moisture content of samples. Chen et al. (2015) showed that temperature of maximum crystallization decreased with the increasing moisture content of the samples. This too might allow the experimental determination of  $T_c$  and rate of maximum crystallization by using lower holding temperatures, resulting in lower crystallization rates. Lower crystallization rates in return might prevent water from evaporating from the crystallizing material. This would provide more information with a an increased accuracy concerning differences in sucrose crystallization in respect to DE and polysaccharide profile of syrup.

Further analysis with mono, di, tri and polysaccharides (glucose, maltose, maltotriose, maltotetrose) on a molar% as well as weight% basis, in combination with viscosity measurements might provide additional information to clarify the molecular interactions affecting sucrose crystallization in combined systems.

## 6. References

- Bamberger, M., Segall, S., & Lee, C. (1980). Factors affecting crystallization of sugars in multi-component systems. *34th PMCA Production Conference*.
- Berry, G., & Fox, T. G. (2006). The viscosity of polymers and their concentrated solutions. In *Fortschritte der Hochpolymeren-Forschung* (pp. 261–357). Springer Science & Business Media.
- Browne, C. A. (1912). *A handbook of sugar analysis: a practical and descriptive treatise for use in research, technical and control laboratories*. J. Wiley & sons.
- Bubník, Z., Kadlec, P., Urban, D., & Bruhns, M. (1995). Sugar technologists manual: Chemical and physical data for sugar manufacturers and users., *120*(6), 574–575.
- Chen, J. (2013). *State Behavior of Sucrose and Corn Syrup Mixtures or RTE Cereal Coatings*. Master Thesis; University of Wisconsin, Madison.
- Chen, J., Nowakowski, C., Green, D., & Hartel, R. W. (2015). State behavior and crystal growth kinetics of sucrose and corn syrup mixtures. *Journal of Food Engineering*, *161*, 1–7.
- Connors, K. A. (1990). *Chemical Kinetics: The Study of Reaction Rates in Solution*. John Wiley & Sons.
- Cown, J. M. G. (1975). Some general features of relations for oligomers and amorphous polymers. *European Polymer Journal*, *11*(4), 297–300.
- Dirksen, J. A., & Ring, T. A. (1991). Fundamentals of crystallization: Kinetic effects on particle size distributions and morphology. *Chemical Engineering Science*, *46*(10), 2389–2427.
- Dziedzic, S. Z., & Kearsley, M. W. (1984). Glucose syrups: science and technology.
- Dziedzic, S. Z., & Kearsley, M. W. (2012). *Handbook of Starch Hydrolysis Products and their Derivatives*. Springer Science & Business Media.
- Eisenberg, D. S., & Crothers, D. M. (1979). *Physical chemistry: with applications to the life sciences*. Benjamin/Cummings Pub. Co.
- Fennema, O. R. (1996). *Food Chemistry, Third Edition*. CRC Press.
- Fox, T. G., & Flory, P. J. (1950). Second-Order Transition Temperatures and Related Properties of Polystyrene. I. Influence of Molecular Weight. *Journal of Applied Physics*, *21*(6), 581.
- Gabarra, P., & Hartel, R. W. (1998). Corn Syrup Solids and Their Saccharide Fractions Affect Crystallization of Amorphous Sucrose. *Journal of Food Science*, *63*(3), 523–528.
- Greenberg, A. R., & Kusy, R. P. (1984). Quantitative evaluation of the Gibbs—DiMarzio theory of the glass transition. *Polymer*, *25*(7), 927–934.
- Hartel, R. W. (2001). *Crystallization in Foods*. Springer.

- Hartel, R. W. (2013a). Advances in food crystallization. *Annual Review of Food Science and Technology*, 4, 277–92.
- Hartel, R. W. (2013b). Advances in food crystallization. *Annual Review of Food Science and Technology*, 4, 277–92.
- Hartel, R. W., Ergun, R., & Vogel, S. (2011). Phase/State Transitions of Confectionery Sweeteners: Thermodynamic and Kinetic Aspects. *Comprehensive Reviews in Food Science and Food Safety*, 10(1), 17–32.
- Hartel, R. W., & Shastry, A. V. (1991). Sugar crystallization in food products. *Critical Reviews in Food Science and Nutrition*, 30(1), 49–112.
- Hay, J. N. (1971). Application of the modified avrami equations to polymer crystallisation kinetics. *British Polymer Journal*, 3(2), 74–82.
- Höhne, G., Hemminger, W., & Flammersheim, H.-J. (2003). *Differential Scanning Calorimetry*. Springer Science & Business Media.
- Kedward, C. J., Macnaughtan, W., Blanshard, J. M. V., & Mitchell, J. R. (1998). Crystallization kinetics of lactose and sucrose based on Isothermal Differential Scanning Calorimetry. *Journal of Food Science*, 63(2), 192–197.
- Kedward, C. J., MacNaughtan, W., & Mitchell, J. R. (2000). Crystallization Kinetics of Amorphous Lactose as a Function of Moisture Content Using Isothermal Differential Scanning Calorimetry. *Journal of Food Science*, 65(2), 324–328.
- Kelton, K., & Greer, A. L. (2010). *Nucleation in Condensed Matter: Applications in Materials and Biology*. Elsevier.
- Lauritzen, J. I., & Hoffman, J. D. (1973). Extension of theory of growth of chain-folded polymer crystals to large undercoolings. *Journal of Applied Physics*, 44(10), 4340.
- Levenson, D. A., & Hartel, R. W. (2005). Nucleation of amorphous sucrose–corn syrup mixtures. *Journal of Food Engineering*, 69(1), 9–15.
- Levine, H., & Slade, L. (1988). Water as a plasticizer: Physico-chemical aspects of low-moisture polymeric systems. *Water Science Reviews 3: , Volume 3: , 358*.
- Lomellini, P. (1992). Williams-Landel-Ferry versus Arrhenius behaviour: polystyrene melt viscoelasticity revised. *Polymer*, 33(23), 4983–4989.
- Lu, X., & Weiss, a. (1992). Relationship between the Glass Transition Temperature and the Interaction Parameter of Miscible Binary Polymer Blends. *Macromolecules*, 25, 3242–3246.
- Marsh, R. D. L., & Blanshard, J. M. V. (1988). The application of polymer crystal growth theory to the kinetics of formation of the B-amylose polymorph in a 50% wheat-starch gel. *Carbohydrate Polymers*, 9(4), 301–317.

- Mathlouthi, M., Cholli, A. L., & Koenig, J. L. (1986). Spectroscopic study of the structure of sucrose in the amorphous state and in aqueous solution. *Carbohydrate Research*, 147(1), 1–9.
- Mathlouthi, M., & Reiser, P. (2012). *Sucrose: Properties and Applications*. Springer Science & Business Media.
- Mohan, R., Lorenz, H., & Myerson, A. S. (2002). Solubility Measurement Using Differential Scanning Calorimetry. *Industrial & Engineering Chemistry Research*, 41(19), 4854–4862.
- Mullin, J. W. (2001). *Crystallization*. Butterworth-Heinemann.
- Myerson, A. S. (1993). *Handbook of industrial crystallization*.
- Nowakowski, C. M., & Hartel, R. W. (2002). Moisture Sorption of Amorphous Sugar Products. *Journal of Food Science*, 67(4), 1419–1425.
- Ohneiser, A. (2011). Kombination von Ultrallschallspektroskopie und Dilatometrie zur Analyse der Strukturbildung während der Kristallisation von Polymeren unter Druck. *Technische Universität Darmstadt*, (Ph.D. dissertation).
- Okui, N. (1990). Relationship between crystallization temperature and melting temperature in crystalline materials. *Journal of Materials Science*, 25(3), 1623–1631.
- Pantaraks, P. (2004). A study into the mechanism of crystal growth rate dispersion. *Suranee University of Technology*, (Ph.D. Dissertation).
- Peleg, M. (1992). On the use of the WLF model in polymers and foods. *Critical Reviews in Food Science and Nutrition*, 32(1), 59–66.
- Roos, Y. (1995). *Phase Transitions in Foods*. Academic Press.
- Roos, Y., & Drusch, S. (2015). *Phase Transitions in Foods*. Elsevier Science.
- Roos, Y., & Karel, M. (1991a). Plasticizing Effect of Water on Thermal Behavior and Crystallization of Amorphous Food Models. *Journal of Food Science*, 56(1), 38–43.
- Roos, Y., & Karel, M. (1991b). Water and molecular weight effects on glass transitions in amorphous carbohydrates and carbohydrate solutions. *Journal of Food Science*.
- Saleki-Gerhardt, a., & Zografi, G. (1994). Non-isothermal and isothermal crystallization of sucrose from the amorphous state. *Pharmaceutical Research*.
- Scott, M. ., & Ramachandrarao, P. (1977). The kinetics of crystallisation of an Fe<sub>80</sub>P<sub>13</sub>C<sub>7</sub> glass. *Materials Science and Engineering*, 29(2), 137–144.
- Slade, L., Levine, H., Ievolella, J., & Wang, M. (1993). The glassy state phenomenon in applications for the food industry: Application of the food polymer science approach to structure–function relationships of sucrose in cookie and cracker systems. *Journal of the Science of Food and Agriculture*, 63(2), 133–176.



- Sperling, L. H. (2005). *Introduction to Physical Polymer Science* (Vol. 207). Hoboken, NJ, USA: John Wiley & Sons, Inc.
- Sun, W. Q., Leopold, A. C., Crowe, L. M., & Crowe, J. H. (1996). Stability of dry liposomes in sugar glasses. *Biophysical Journal*, 70(4), 1769–76.
- Tjuradi, P., & Hartel, R. W. (1995). Corn Syrup Oligosaccharide Effects on Sucrose Crystallization, 60(6), 1353–1356.
- Van Hook, A. (1961). *Crystallization: Theory and Practice*. Reinhold Publishing Corporation.
- Van Hook, A. (1981). Growth of sucrose crystals. A review. *Sugar Technology Reviews*.
- Williams, M. L., Landel, R. F., & Ferry, J. D. (1955). The Temperature Dependence of Relaxation Mechanisms in Amorphous Polymers and Other Glass-forming Liquids. *Journal of the American Chemical Society*, 77(14), 3701–3707.
- Woodroof, J. G., Junk, W. R., & Pancoast, H. M. (1973). *Handbook of Sugars: For Processors, Chemists and Technologists*.

## Appendix

A1. Moisture contents of the sugar matrices consisting of sucrose, corn syrup and water, cooked to 4 / 3 different temperatures, containing 3 different types of corn syrup (26DE, 42DE, 62DE) at 2 different syrup concentrations.

<b>Sugar glass (14% corn syrup w/w dry)</b>			
Cooking Temperature [°C]	Moisture content [%]		
	<b>26DE</b>	<b>42DE</b>	<b>62DE</b>
135	5.93 ± 0.03 <sup>a</sup>	5.84 ± 0.02 <sup>a</sup>	5.89 ± 0.07 <sup>a</sup>
140	5.08 ± 0.06 <sup>b</sup>	5.08 ± 0.07 <sup>b</sup>	5.03 ± 0.03 <sup>c</sup>
145	4.36 ± 0.03 <sup>d</sup>	4.27 ± 0.02 <sup>d</sup>	4.33 ± 0.01 <sup>d</sup>
150	3.76 ± 0.01 <sup>e</sup>	3.72 ± 0.01 <sup>e</sup>	3.81 ± 0.01 <sup>e</sup>

<b>Sugar glass (22% corn syrup w/w dry)</b>			
Cooking Temperature [°C]	Moisture content [%]		
	<b>26DE</b>	<b>42DE</b>	<b>62DE</b>
140	4.89 ± 0.01 <sup>a</sup>	4.89 ± 0.03 <sup>a</sup>	4.93 ± <0.00 <sup>a</sup>
145	4.29 ± 0.10 <sup>b</sup>	4.41 ± 0.02 <sup>c</sup>	4.37 ± <0.00 <sup>b</sup>
150	3.79 ± 0.01 <sup>d</sup>	3.84 ± 0.01 <sup>d</sup>	3.81 ± 0.03 <sup>d</sup>

<sup>a-e</sup> Means with the same superscript are not significantly different at the 95% confidence interval (n=3)

A2. Glass transition temperature ( $T_g$ ) of sugar glasses composed of 14%/22% corn syrup (26DE, 42DE, 62DE) at 4/3 moisture levels

<b>Sugar Glass 14% CS w/w dry</b>			
Corn Syrup Moisture content [%]	26DE	42DE	62DE
5.9	$21.72 \pm 0.80^a$	$21.44 \pm 0.49^b$	$19.58 \pm 0.36^c$
5.1	$28.82 \pm 1.44^d$	$26.43 \pm 0.33^e$	$24.49 \pm 0.14^f$
4.3	$32.72 \pm 0.10^g$	$31.33 \pm 0.57^h$	$28.85 \pm 0.57^i$
3.8	$36.75 \pm 0.63^j$	$35.56 \pm 0.42^k$	$33.20 \pm 0.37^j$

<b>Sugar Glass 22% CS w/w dry</b>			
Corn Syrup Moisture content [%]	26DE	42DE	62DE
4.9	$29.83 \pm 0.19^k$	$27.97 \pm 0.39^l$	$24.51 \pm 0.45^f$
4.3	$34.48 \pm 0.40^m$	$31.31 \pm 0.21^h$	$28.45 \pm 0.51^i$
3.8	$38.13 \pm 0.56^n$	$35.56 \pm 0.32^k$	$32.94 \pm 0.39^j$

<sup>a-k</sup> Means with the same superscript are not significantly different at the 95% confidence interval (n=4)

A3. Temperature of maximum crystal growth ( $T_c$ ) and  $T_c$  ratio against  $T_m$  and  $T_g$  of sugar glasses composed of 14%/22% corn syrup (26DE, 42DE, 62DE) for 4 different moisture contents

<b>Sugar glass (14% corn syrup w/w dry)</b>						
Moisture Content [%]	<b>26DE</b>		<b>42DE</b>		<b>62DE</b>	
	$T_c$	$\frac{T_c - T_g}{T_m - T_g}$	$T_c$	$\frac{T_c - T_g}{T_m - T_g}$	$T_c$	$\frac{T_c - T_g}{T_m - T_g}$
5.9	$99.97 \pm 0.92^a$	0.61	$96.89 \pm 1.32^b$	0.59	$93.00 \pm 2.31^c$	0.57
5.1	$105.83 \pm 1.88^d$	0.61	$103.75 \pm 0.36^d$	0.61	$99.74 \pm 3.83^e$	0.59
4.3	$112.32 \pm 0.32^f$	0.63	$110.20 \pm 1.60^f$	0.63	$105.30 \pm 2.01^g$	0.6
3.8	$115.39 \pm 0.91^h$	0.63	$115.38 \pm 0.81^h$	0.64	$110.31 \pm 0.52^i$	0.61

<b>Sugar glass (22% corn syrup w/w dry)</b>						
Moisture Content [%]	<b>26DE</b>		<b>42DE</b>		<b>62DE</b>	
	$T_c$	$\frac{T_c - T_g}{T_m - T_g}$	$T_c$	$\frac{T_c - T_g}{T_m - T_g}$	$T_c$	$\frac{T_c - T_g}{T_m - T_g}$
4.9	$116.59 \pm 0.65^j$	0.71	$110.32 \pm 1.62^j$	0.67	$106.32 \pm 1.68^k$	0.66
4.3	$123.46 \pm 0.43^l$	0.73	$114.25 \pm 0.59^m$	0.68	$113.71 \pm 0.50^n$	0.69
3.8	$123.94 \pm 1.04^{o,l}$	0.71	$121.34 \pm 1.57^p$	0.71	$118.14 \pm 0.89^q$	0.7

<sup>a-q</sup> Means with the same superscript are not significantly different at the 95% confidence interval (n=4)

A4. Table Solubility temperature ( $T_m$ ) of sugar glasses composed of 14% and 22% corn syrup (26DE, 42DE, 62DE) for 4 different moisture contents.

<b>Sugar Glass 14% CS w/w dry</b>			
Corn Syrup Moisture content [%]	<b>26DE</b>	<b>42DE</b>	<b>62DE</b>
5.9	$149.14 \pm 0.65^a$	$148.82 \pm 0.25^a$	$147.68 \pm 0.44^b$
5.1	$155.65 \pm 1.52^c$	$152.98 \pm 0.26^d$	$151.13 \pm 0.27^e$
4.3	$158.74 \pm 0.74^f$	$157.14 \pm 0.28^g$	$155.37 \pm 0.49^h$
3.8	$164.40 \pm 0.24^i$	$159.88 \pm 0.20^j$	$3158.63 \pm 0.26^k$

<b>Sugar Glass 22% CS w/w dry</b>			
Corn Syrup Moisture content [%]	<b>26DE</b>	<b>42DE</b>	<b>62DE</b>
4.9	$152.26 \pm 0.21^l$	$150.45 \pm 0.66^m$	$148.15 \pm 0.13^n$
4.3	$155.99 \pm 0.25^o$	$153.35 \pm 0.19^p$	$151.63 \pm 0.52^q$
3.8	$158.35 \pm 0.56^r$	$156.26 \pm 0.21^s$	$154.74 \pm 0.59^t$

<sup>a-q</sup> Means with the same superscript are not significantly different at the 95% confidence interval (n=4)

A5. Experimental crystallization halftimes of amorphous sugar matrices composed of 14% / 22% corn syrup (26DE,42DE,62DE) with varying moisture contents at different crystallization temperatures

Sugar Glass 14% Corn Syrup												
Moisture Content [%]	80/85°C			90°C			100°C			110°C		
	26DE	42DE	62DE	26DE	42DE	62DE	26DE	42DE	62DE	26DE	42DE	62DE
5.9	10.61 ± 1.16 <sup>a</sup>	6.45 ± 1.51 <sup>b</sup>	6.38 ± 2.17 <sup>c</sup>	4.70 ± 0.56 <sup>d</sup>	2.91 ± 0.59 <sup>d,1</sup>	2.94 ± 0.66 <sup>d,2</sup>	2.52 ± 0.18 <sup>e,3</sup>	1.78 ± 0.35 <sup>e,5</sup>	1.807 ± 0.27 <sup>e,7</sup>	1.75 ± 0.06 <sup>f,8</sup>	1.46 ± 0.26 <sup>f,9</sup>	1.47 ± 0.12 <sup>f,10</sup>
5.1	19.20 ± 3.04 <sup>g</sup>	10.2 ± 1.42 <sup>h</sup>	8.70 ± 1.82 <sup>h</sup>	7.33 ± 1.15 <sup>i</sup>	4.73 ± 0.37 <sup>i,1</sup>	3.72 ± 0.57 <sup>i,2</sup>	3.42 ± 0.37 <sup>k,3</sup>	2.61 ± 0.13 <sup>k,5,6</sup>	2.17 ± 0.39 <sup>k,7</sup>	2.06 ± 0.19 <sup>k,8</sup>	1.92 ± 0.11 <sup>k,9</sup>	1.59 ± 0.25 <sup>k,10</sup>
4.3	33.64 ± 2.49 <sup>m</sup>	27.15 ± 4.35 <sup>n</sup>	16.40 ± 1.67 <sup>o</sup>	11.05 ± 0.44 <sup>p</sup>	8.89 ± 0.93 <sup>p</sup>	5.92 ± 0.47 <sup>q,2</sup>	4.75 ± 0.28 <sup>r,3,4</sup>	4.02 ± 0.21 <sup>r,5,6</sup>	3.04 ± 0.09 <sup>r,7</sup>	2.64 ± 0.17 <sup>s,8</sup>	2.39 ± 0.16 <sup>s,9</sup>	1.91 ± 0.04 <sup>s,10</sup>
3.8	28.37 ± 7.36 <sup>u</sup>	22.43 ± 4.98 <sup>v</sup>	10.04 ± 0.30 <sup>w</sup>	15.51 ± 3.40 <sup>x</sup>	12.81 ± 3.27 <sup>y</sup>	6.16 ± 1.24 <sup>z</sup>	6.28 ± 1.35 <sup>z,4</sup>	5.33 ± 1.00 <sup>z,6</sup>	3.33 ± 0.37 <sup>z,7</sup>	3.21 ± 0.45 <sup>z,8</sup>	3.11 ± 0.19 <sup>z,9</sup>	2.16 ± 0.26 <sup>z,10</sup>

Sugar Glass 22% Corn Syrup												
Moisture Content [%]	90°C			100°C			110°C					
	26DE	42DE	62DE	26DE	42DE	62DE	26DE	42DE	62DE	26DE	42DE	62DE
4.9	19.01 ± 0.83 <sup>a</sup>	10.92 ± 1.38 <sup>b</sup>	7.14 ± 0.17 <sup>c</sup>	7.76 ± 0.39 <sup>d</sup>	4.75 ± 0.66 <sup>e,u</sup>	3.86 ± 0.20 <sup>e</sup>	4.50 ± 0.25 <sup>f</sup>	2.88 ± 0.10 <sup>f,y</sup>	2.88 ± 0.10 <sup>f,y</sup>	2.88 ± 0.10 <sup>f,y</sup>	2.88 ± 0.10 <sup>f,y</sup>	3.02 ± 0.13 <sup>f,z</sup>
4.3	24.30 ± 3.86 <sup>g</sup>	13.50 ± 1.93 <sup>h</sup>	11.74 ± 1.81 <sup>i,v</sup>	9.6 ± 0.73 <sup>i</sup>	5.60 ± 0.25 <sup>k,u</sup>	6.05 ± 0.55 <sup>k,w</sup>	5.27 ± 0.22 <sup>L,x</sup>	3.63 ± 0.28 <sup>m,y</sup>	3.63 ± 0.28 <sup>m,y</sup>	3.63 ± 0.28 <sup>m,y</sup>	3.63 ± 0.28 <sup>m,y</sup>	3.98 ± 0.07 <sup>m,z</sup>
3.8	34.56 ± 1.87 <sup>n</sup>	19.88 ± 3.43 <sup>o</sup>	12.14 ± 0.91 <sup>p,v</sup>	12.47 ± 0.40 <sup>q</sup>	7.70 ± 1.23 <sup>f</sup>	6.17 ± 0.90 <sup>r,w</sup>	6.35 ± 0.40 <sup>s,x</sup>	4.26 ± 0.63 <sup>t,y</sup>	4.26 ± 0.63 <sup>t,y</sup>	4.26 ± 0.63 <sup>t,y</sup>	4.26 ± 0.63 <sup>t,y</sup>	4.33 ± 0.50 <sup>t,z</sup>

<sup>a&-10</sup> Means with the same superscript are not significantly different at the 95% confidence interval (n=4/5/6)

A6. Main response times  $t_0$ , determined from a fully crystallized sample under experimental conditions. The shown response times are approximate values, slight variations are based on the analysis of each crystallization curve.

Crystallization Temp [C°]	$t_0$ [min]
110	0.3
100	~ 0.4
90	~ 0.6
85	~ 0.8
80	~ 1